coatings

Review

Sustainable New Technology for the Improvement of Metallic Materials for Future Energy Applications

Patricia Jovičević-Klug [1,2,*] and Michael Rohwerder [1]

[1] Group of Corrosion, Department of Interface Chemistry and Surface Engineering, Max-Planck-Institute for Iron Research, Max-Planck-Str. 1, 40237 Düsseldorf, Germany; rohwerder@mpie.de
[2] Alexander von Humboldt PostDoc Research Fellow, Jean-Paul-Str. 12, 53173 Bonn, Germany
* Correspondence: p.jovicevic-klug@mpie.de

Abstract: The need for a more sustainable and accessible source of energy is increasing as human society advances. The use of different metallic materials and their challenges in current and future energy sectors are the primary focus of the first part of this review. Cryogenic treatment (CT), one of the possible solutions for an environmentally friendly, sustainable, and cost-effective technology for tailoring the properties of these materials, is the focus of second part of the review. CT was found to have great potential for the improvement of the properties of metallic materials and the extension of their service life. The focus of the review is on selected surface properties and corrosion resistance, which are under-researched and have great potential for future research and application of CT in the energy sector. Most research reports that CT improves corrosion resistance by up to 90%. This is based on the unique oxide formation that can provide corrosion protection and extend the life of metallic materials by up to three times. However, more research should be conducted on the surface resistance and corrosion resistance of metallic materials in future studies to provide standards for the application of CT in the energy sector.

Keywords: energy sector; renewable energy; fusion; metallic materials; cryogenic treatment; surface; interface; corrosion

Citation: Jovičević-Klug, P.; Rohwerder, M. Sustainable New Technology for the Improvement of Metallic Materials for Future Energy Applications. *Coatings* **2023**, *13*, 1822. https://doi.org/10.3390/coatings13111822

Academic Editor: Alessandro Latini

Received: 3 October 2023
Revised: 20 October 2023
Accepted: 23 October 2023
Published: 24 October 2023

1. Introduction

With the growth of the human population, there is an increasing need for a more sustainable and more easily accessible source of energy [1], bringing prosperity, economic development, security, better health care, welfare, and the overall better social and environmental development of mankind [2]. In recent years, many challenges, such as the distribution of natural resources, growth of the population and its needs, economic instability, new war zones, etc. [3,4] have emerged in energy sources based on oil, gas, and coal. These challenges combined with geo-political challenges and environmental challenges such as greenhouse gases, environmental impact, sustainable development, etc. [2,5], are leading to increased efforts in research and the development of new solutions and options for new and more sustainable energy sources. The energy sources can be classified into natural fossil-based (oil, gas, and coal) and renewable types [6]. It is important to note that nuclear energy can be grouped on its own or as part of one of the previously mentioned groups. This is a highly controversial topic, mainly based on whether conventional or advanced nuclear power is discussed [6–9]. In this review, nuclear energy will be grouped on its own.

The current prediction of energy sources for the next 20 years (2030–2040) in the European Union (EU), predicted in the year 2020 [10,11], is shown in Figure 1. Currently, the production of energy is still dominated by fossil-fuel-based sources (70%). The nuclear-based sources have consistently maintained a similar ratio, while the renewable sources are constantly gaining an increasing share. For the next two decades, an increasing use

of renewable sources for energy production is predicted to increase by 300% in the EU alone by 2030 and by up to 450% by 2040 compared to the current state [10,11]. The nuclear energy source is predicted to remain a stable energy source throughout this period, especially if fusion is included [6–8]. Figure 1 and Table 1 also show the development of renewable energy sources in the EU over the next 20 years and the expected changes in the redistribution of energy sources within different sectors.

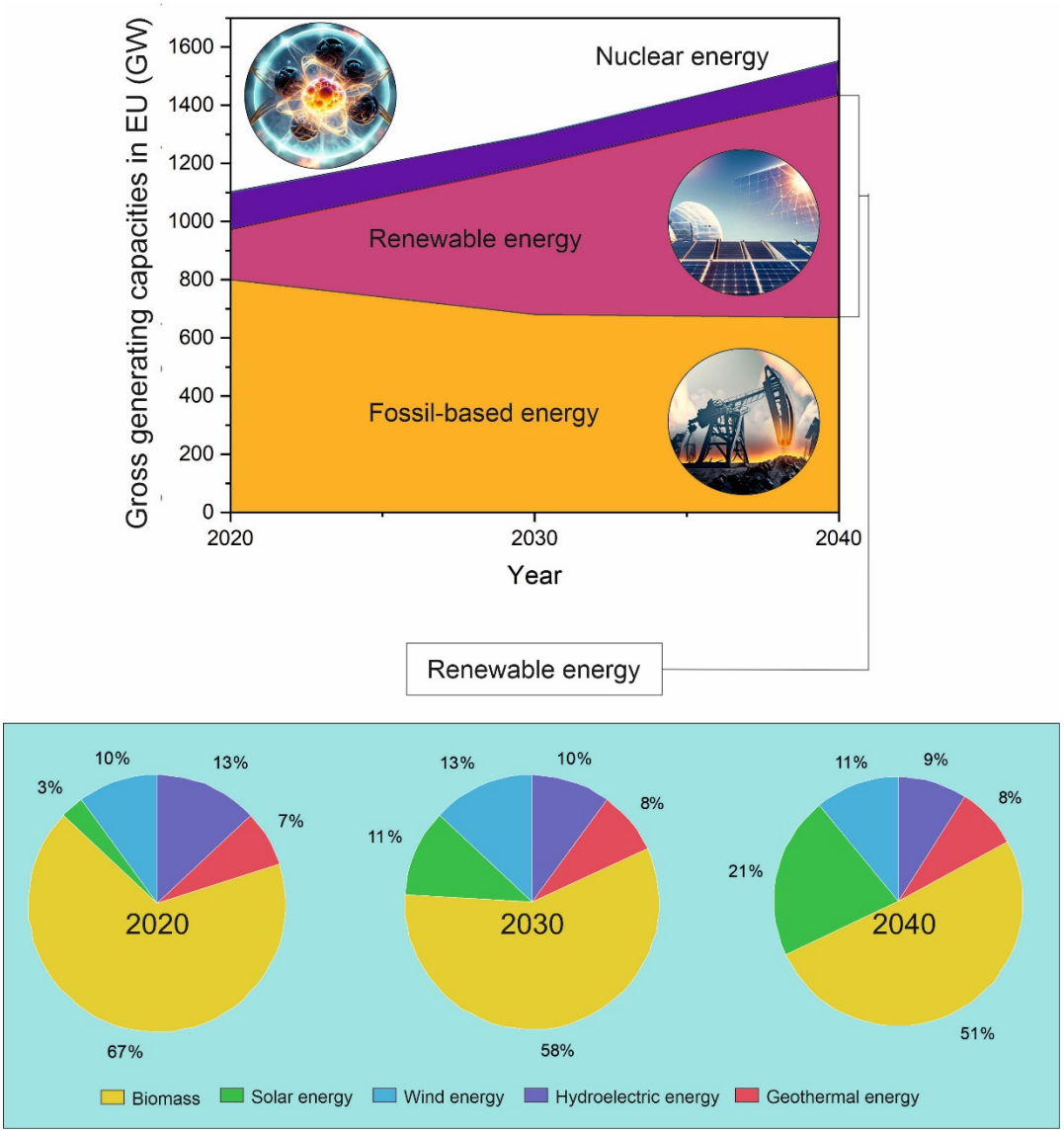

Figure 1. The square graph presents the prediction of gross energy-generating capacities within the EU from current state of 2020 up to the next 20 years (2030–2040) by each sector. The orange color stands for fossil fuels (oil, gas, and coal), red for renewables, and purple for nuclear. The lower pie charts represent the current (year 2020) and predicted (years 2030 and 2040) fractions of the different categories of renewable energy sources.

Production of Electricity per Year for Different Energy Sector

The production of electricity varies within the different categories of the energy sector, and also, the production costs can vary significantly depending on the energy source (Figure 2 and Table 2). Pricing is highly dependent on a variety of external factors, such as subsidies, various taxes, etc., which also vary depending on geopolitical locations and natural resources.

Table 1. Renewable source preconditions for next 20 years for the EU.

	Current State 2020	2030	2040
Hydroelectric energy			
• Land hydroelectric energy (rivers and lakes) • Marine hydroelectric energy (ocean currents, tidal stream, and waves)	13%	10%	9%
Geothermal energy	7%	8%	8%
Biomass	67%	58%	51%
Solar energy			
• Solar thermal • Photovoltaic	3%	11%	21%
Wind energy	10%	13%	11%
Combined contribution of the renewable energy and the total energy production	**~25%**	**~35%**	**~48%**

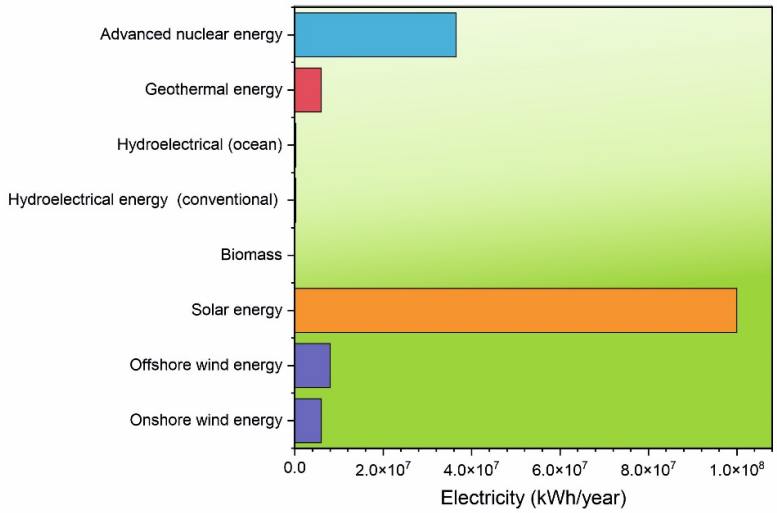

Figure 2. The highest electricity production in kWh/year is possible with solar energy [12,13] and nuclear energy [14]. This is followed by wind energy [15] and geothermal energy [16]. The lowest electricity production comes from the biomass sector [17,18].

In addition to the price of electricity, another important factor in energy production is also the so-called capacity factor (also known as CF). The CF is the unitless ratio of the actual electrical energy output over a given period to the theoretical maximum electrical energy output over the same period. The CF can also be thought of as production efficiency. CF is usually calculated over a year in order to average out temporal variations and to represent the realistic values of energy/electricity produced per maximum capacity of an energy source (Table 2). From Table 2, the cost of electricity for renewable energy sources varies due to different economic perspectives and also the source of production and maintenance and repair costs that need to be considered. The next capacity factors show that the most promising renewable energy sources are geothermal [16], hydroelectric [19–21], and wind [15,22], based on the lowest possible electricity cost and the highest capacity factor.

To cope with the increasing energy demand and consumption, new energy production pathways are expected to evolve and develop to provide greater energy security, reduce global carbon emissions, and lower the financial cost of energy production. The advancement of production processes in the energy sector will require the development and utilization of new materials. This is where metallic materials (metals and alloys) come into play, many of which have been scarcely used or even unused in energy production and will become the most important players in sustainable energy production (see Figure 1 and Table 1).

Table 2. Energy sectors presented in this manuscript and their cost of production and capacity factor [23].

Type of Energy Sector	Cost (EUR/MWh)	Capacity Factor (%)
Hydroelectric energy		
• Land hydroelectric energy	**53–326**	**31–66**
• Ocean hydroelectric energy	**130–280**	**39–45**
Geothermal energy	**49–353**	**80–90**
Biomass	**128**	**64**
Solar energy	**27–130**	**12–30**
Wind energy		
• Onshore wind energy	**24–67**	**29–52**
• Offshore wind energy	**60–130**	**12–48**
Advanced nuclear energy	**73**	**94**

The successful implementation of such materials will be particularly crucial in applications where high strength and dimensional flexibility combined with high temperature resistance are required. Today, more than 60 different metallic materials are used in one way or another in energy production (as base materials for reactors, storage and accumulation systems, and supporting infrastructure) [24]. Future energy security (Figure 3) requires a critical awareness of the availability, functionality, substitutability, recyclability, and production of metals and alloys [25–27]. Metallic materials are the type of materials that can be newly produced or reused and recycled. Additionally, their properties can be tailored through postprocessing, increasing their flexibility and versatility for various applications. Therefore, the adaptation and development of heat treatment and further processing steps of metallic materials for future applications must be under constant research [25–27]. The factors that influence the value of metallic materials are market availability, substitutability, recyclability, and socio-cultural and environmental impacts [26]. In addition, the development and consideration of new materials such as high-entropy alloys and materials for catalysis, energy generation, and storage applications will bring new challenges and benefits to the energy sector [28,29].

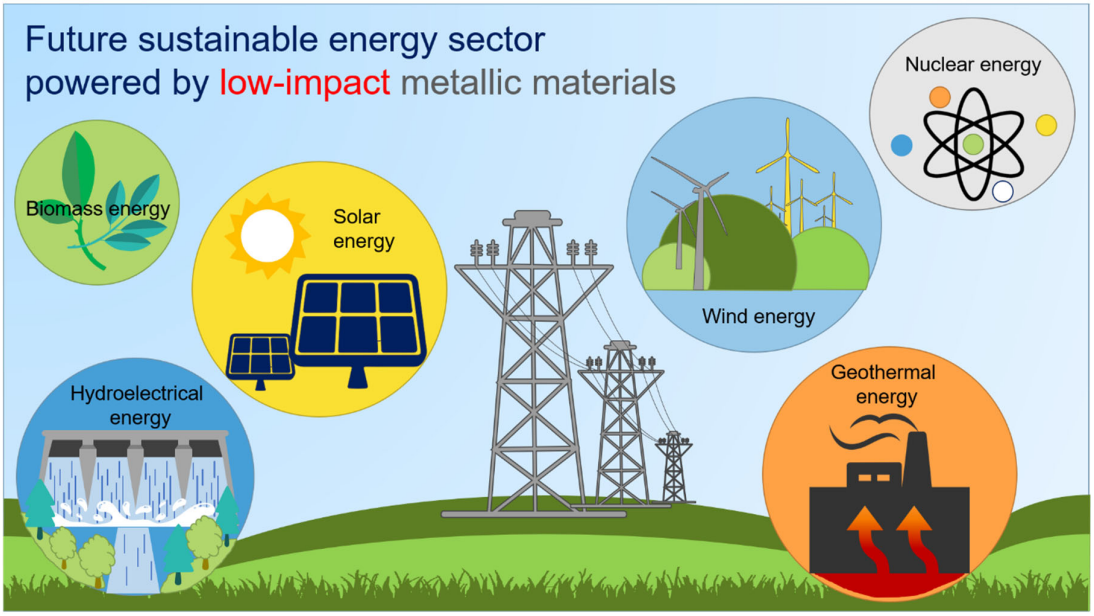

Figure 3. The future sustainable energy sector powered by low-impact metallic materials.

This review aims to provide a comprehensive overview of the metallic materials used in the advanced nuclear and renewable energy sectors of the future, including the challenges (environments) to which these materials are and planned to be exposed on a daily basis. Particularly, this review aims to present a possible novel way of processing metallic materials in a more environmentally friendly way, opening the possibility of improving material properties, extending the life cycle of components, and generating lower CO_2 emissions compared to conventional pathways.

The paper is structured in the following order: in Section 2, the future energy sector is presented, where the renewable energy and advanced nuclear energy sources are introduced and discussed. In the same chapter, the challenges and requirements of the metallic materials used in the given environments of the different energy sources are also presented. Section 3 introduces the emerging green technology of cryogenic heat treatment, which has a great potential to reduce the impact of the energy sector on the environment by improving material properties and extending the life cycle of components. Section 4 discusses the outlook for future technology and the energy sector and provides individual guidelines for future materials implementation in the energy sector.

2. Future Energy Sector

The future energy sector is divided into renewable energy sources and advanced nuclear energy based on fusion. The renewable energy sector is divided into hydroelectric energy, geothermal energy, and biomass, solar, and wind energy, with some subdivisions (see Figure 3 and Table 1).

2.1. Energy Sector and Selection of the Right Material

2.1.1. Advanced Nuclear Energy

For future advanced nuclear reactors, three major subtypes are considered: non-water-cooled reactors, advanced water-cooled reactors, and fusion reactors. The latter's design will be based on the current fission reactors; therefore, the use of similar metallic materials is expected. However, the research into the development of new, more resistant metallic materials and their protection is ongoing [30,31].

The non-water-cooled reactor subtype includes reactors and systems that are still based on fission reaction, but the coolants are either molten salts and are designated as Th-based reactors or high-temperature gases (or cooled with helium, using graphite as a moderator) [30,31]. This category also includes small modular reactors (SMRs), which are fast-cooled reactors based on Na, Pb, and gas cooling [32].

The next category is advanced water-cooled reactors, also based on the fission reaction and using water as a coolant and moderator, i.e., SMRs [30,31]. These reactors are cleaner, fundamentally safer, more fuel efficient, more reliable, and more sustainable than the current generation of reactors [33,34].

The last category is fusion reactors. Fusion reactors are based on fusion plasmas, which are still in the early stages of research and development. The working conditions of these reactors are much more intense compared to those of the fission reactors, reaching temperatures of several thousand degrees during the plasma generation. Therefore, complex testing and development of metallic materials is required for the construction and operation of such reactors. In fact, there are two types of fusion plasmas being considered for the development of future fusion reactors. The first type is based on strong magnetic fields and is known as magnetic confinement fusion (MFC). The second type is based on compressing the deuterium (DT) fuel and heating it rapidly that fusion occurs before the fuel expands; this method is also known as inertial confinement fusion (ICF). Due to the different primary principle compared to fission, the material for fusion application must have a specific non-equilibrium thermodynamic state, two or more main phases, complex grain boundaries; and dislocation systems. Compared to the traditional fission system/environment, the new challenges for metallic materials used in fusion will mainly

focus on adaptation to the higher resistance to neutron irradiation, cladding, and higher temperatures and stresses [30,31].

The benefits of a new, advanced generation of nuclear reactors can bring society lower energy costs, increased production, decarbonization of industry, increased efficiency, and significantly reduced environmental and waste hazards. The development and safety of future nuclear power systems depends not only on the type of fuel but also on the material design. In current and future advanced nuclear power, materials are exposed to high-energy particles, high temperatures, pressure changes, and highly corrosive environments. However, the degradation of metallic materials in this environment is complex due to the different materials used for the plant, the complex and highly variable environmental conditions, and the different loading conditions of the material in various applications [30].

The first factor to consider is the thermal ageing and fatigue of metallic materials that occurs in metals exposed to elevated temperatures. This is a critical aspect for metallic materials used in nuclear energy, as it can lead to a short life cycle of the metallic component. The reason for this is the altered microstructure, resulting from the diffusion activated process, which causes changes in mechanical properties and fatigue (including creep fatigue) [30,31].

The next factor (second) is irradiation, which causes changes in the dimensional stability of metallic materials and thus influences the final properties of the metallic component. This is caused by the following five radiation processes: (i) phase (microstructural) instability induced by neutron irradiation, forming increased precipitation and segregation of alloying elements; (ii) radiation-induced hardening and embrittlement; (iii) volume swelling due to void formation; (iv) high-temperature helium embrittlement caused by helium movement towards grain boundaries; and (v) irradiation creep caused by changes in the crystal lattice due to migration of interstitial atoms and dislocations [30,31].

The third factor is the water environment, where water is the primary reactor coolant. Exposure of metallic materials to water, especially with elevated temperatures, can lead to corrosion of metallic materials, which can cause degradation of properties and lead to component failures. The extent of the corrosion is a product of several factors, such as water pH, water purity, material composition, temperature, gas concentrations, etc.). The type of corrosion mechanisms can be divided into general and localized corrosion. General corrosion mechanisms include uniform corrosion, boric acid corrosion, erosion corrosion, and flow-accelerated corrosion. Localized corrosion mechanisms include crevice corrosion, galvanic corrosion, pitting, environmental assisted cracking, and biological corrosion. In addition, stress corrosion cracking (intergranular and transgranular stress corrosion cracking and low-temperature cracking) can also be present under high-loading conditions. In addition to water, molten salts and liquid metals can also cause corrosion and electrochemical reactions that affect the degradation of the metallic material (see Table 3) [30,31].

2.1.2. Hydroelectric Renewable Energy

Hydroelectric renewable energy currently represents 13% of all renewable energy sources in the EU [21]. Hydropower is based on the movement of water through a turbine, which in turn drives a generator to produce electricity. Hydroelectric power plants can be installed in oceans or on rivers and lakes, which are sources of continental hydroelectric power. Ocean electricity sources can be divided into wave energy, tidal current energy, tidal barrage, ocean thermal air conditioning, and ocean thermal energy conversion (also known as OTEC), where the last two options additionally produce heat.

OTEC relies on the steam from the warm surface water to interact with the turbines. However, OTEC is still at an early stage of development, and the application relies on the cold, deep ocean water, which condenses the steam back into water for reuse. For this application to be viable, there must be a temperature difference of at least 20 K between the two layers of the ocean water (surface/deep layer), which is mostly limited to the tropical regions. OTEC can also be combined with ocean thermal air conditioning [35].

Ocean thermal air conditioning can be used to control the air conditioning of buildings by using cold, deep water to cool the fresh water circulating through a building. The cold water must be between 277 K and 284 K. The same technique can also be used in lakes [36,37].

The next option for harvesting electricity from the ocean is tidal barrages. Tidal barrages are based on the normal hydroelectric concept, where instead of the typical river flow, the tide drives the turbines in the barrage and then generates electricity. However, the tidal difference between high and low tide must be at least 3 m for this technique to be viable [38,39].

The next option for generating electricity is tidal stream (current) energy, which uses similar technology as tidal barrages but relies on tidal currents [40]. In this type of installation, the turbines are anchored to the seabed or can be suspended from a buoy to generate electricity. The challenge of this technique is the preservation of the marine environment when deploying this type of energy solution [41–43].

The next type of the energy source is produced by wave power. This type of energy harvesting is based on the prediction of constant wave direction. It is estimated that wave power of solely 2100 TWh per year could be generated by harvesting the naturally occurring waves. To harvest wave energy, cells based on the pressure and then movement of hydraulic pumps are built, which then drive the generator into motion. However, the application of this technology is limited to the areas with constant waves [44–47]. In development are also hybrid wave and wind energy farms [44,48] that use a combination of the aforementioned techniques. The last type of the ocean-based hydroelectric renewable energy is related to the use of osmotic power, which is based on the salt concentration difference between seawater and fresh river water [49–51]. There are two known methods: one is reverse electrodialysis (known as RED) [50,52], and the other is pressure-retarded osmosis (PRO) [53,54].

The continental type of hydroelectric renewable energy can be divided into three parts. The best known and that with the longest tradition is hydroelectric power generation with dams on large rivers or lakes [55]. However, due to its environmental impact, the future of small hydro (also known as SHP) is a promising source of renewable and clean energy that provides significantly lower changes to the environment and disruption of the local ecosystem [49,55–57].

The next option for generating electricity from rivers is run-of-the-river (ROR) hydropower, where the natural flow of the river generates electricity, and the flow of the river determines the amount of electricity generated [58–60]. This type of source is ideal for streams and rivers that can sustain a minimum flow compared to other types. This type delivers cleaner power and generates less greenhouse gas for equivalent energy production compared to other types. Additionally, because these types do not require a reservoir, there is a reduced influence on the environment and flooding [61].

The last option is a special type of hydroelectric power generation using turbines that are completely submerged and, in some cases, anchored to the river bed [62,63]. The advantages of this type are its high efficiency, low maintenance, and high reliability compared to other hydroelectric types [64]. However, the environmental impact can be controversial, especially on the flora and fauna of the marine/lake/river environments [65].

The metallic materials used in the hydroelectric sector must be able to withstand the different environments (low temperature, high pressure, and highly corrosive environment (including chemical agents)) and also have low density, high strength, high toughness and high resistance to wear (especially abrasion), high resistance to corrosion, and high fatigue resistance [66]. The metallic materials used for the turbines are austenitic stainless steel (over 12% Cr content as an alloy), but the turbine blades can also be made of martensitic stainless steel due to the higher strength of the steel [66,67]. Low-head machine parts are made of weathering steel (Corten steel) and various types of stainless steel [68,69], high-strength steel [56,70], ACSR steel [71], cast steel [68], carbon steel [72–74], and ferritic steel [69] (see Section 2.2 for detailed description of metallic materials). Resistance to erosion and cavitation are also important factors to consider for metallic materials used in

the hydroelectric sector [66,75,76]. In addition, due to the biologically active environment of hydroelectric plants, biofouling occurs where invasive species grow and accumulate various bacteria [66]. As a result, the metallic materials need to either have self-cleaning capabilities or can be treated with surface specific process to provide resistance to biofouling. Alterative metallic materials that can also be used for turbines and components are also different Al alloys (including Al-Si alloys) [66,71,77], Ti alloys [66,78], Cu alloys [76,79,80], and Ni alloys [81] (see Table 3).

2.1.3. Biomass Renewable Energy

Biomass is a type of energy based on organic sources (animals and plants), the most common sources being plants, waste, and wood. Biomass energy can be used for electricity, heating or even biofuel [82–84].

One type of energy production is thermal conversion, where raw materials (paper or waste) are burned (pyrolysis, gasification, anaerobic decomposition, torrefaction, and co-firing) [83–87]. Most of the research and its emphasis has been on the pyrolysis technique, where the combustion of organic material is carried out in the absence of oxygen under temperatures up to 1173 K [85,88]. Different types of catalysts are used for the pyrolysis of different types of source based biomasses (waste, plants, etc.) [89,90].

Biomass also has great potential to be used in the production of steel for reducing the CO_2 impact of the steel industry, but this is still being researched [84].

The main challenges that are facing metallic materials in the biomass sector are corrosion (pitting corrosion, intergranular corrosion, etc.) [89], high-temperature corrosion, and microbial-assisted corrosion [89,91]. The factors that strongly influence all types of the corrosion are fluid dynamics (including different solutions), gas composition (N_2, CO_2, H_2O, Cl_2, H_2, etc. [90]), deposit composition, and temperature (573–1173 K) [89,90].

Other challenges that metallic materials face in biomass energy are abrasive wear [92], material degradation due to small dusty particles [93], and thermomechanical fatigue (high-temperature fatigue) [94–96].

The most common metals used in the biomass energy sector are carbon low-alloyed steels [97,98], austenitic and martensitic stainless steels [97], Al and Ni alloys [97], and some specialized non-ferrous alloys, such as nickel-cobalt-aluminum alloys (NCA). All these metallic materials are used for the main structure and various components in the biomass sector [82–84] (see Table 3).

2.1.4. Onshore and Off-Shore Renewable Energy

The highest demand and largest source of renewable energy in the global market is currently onshore and offshore wind [99]. Wind energy is based on the conversion of kinetic energy into rotational energy, which is then converted into electrical energy by means of a shaft [100]. It is important to note that some turbine designs can produce more energy compared to others (height, size, etc.). The other way to produce more energy is the so-called yawing technique, where the wind turbine is shifted to face directly into the wind, which can be freely manipulated on demand [101].

Wind energy can be produced both onshore and offshore. Onshore wind energy encompasses the energy produced by the wind on land that comes from the natural movement of air [102]. The advantages of onshore wind energy are cost-effective energy, faster installation and easier maintenance, and a reduced environmental impact compared to offshore energy [102]. However, there are disadvantages to onshore wind energy, such as lower power generation, inconsistent wind, varying wind speeds, and a greater impact on nature [102].

Offshore wind energy, i.e., offshore wind farms, are located out at sea where the wind (sea breeze) has higher speeds and greater consistency [102]. The advantages of this type or, more accurately, placement of wind farms include more space for placement, reduced environmental impact (although this is debatable due to the more complicated and invasive supporting infrastructure), and their greater efficiency compared to onshore

turbines. The disadvantages are their higher maintenance and repair costs and higher construction costs [101]. Offshore wind turbines can be anchored to the seabed, known as fixed-bottom turbines, or they can be placed on floating platforms, known as floating turbines [101,102].

Metallic materials are used in wind energy for the main foundation of the structure, tower, gearbox, turbines, bearings, bolts, controllers, casings, and many other components that require high corrosion and wear resistance, resistance to higher loads and dynamic forces (including fatigue), and higher contact pressures [103–105]. The material must also be highly resistant to solid particle erosion caused by dust particles [106].

For these reasons, the most common metallic materials used in the wind renewable energy sector (see Section 2.2) are structural steels, stainless steels (austenitic, duplex, and martensitic steels), electrical steels, cast iron, bearing steels, high Cr steels, low C nitrogen steels, and high Si nodular cast iron [103–105]. The most common non-ferrous alloys used in this sector are Cu-based alloys and Al-based alloys [103–105] (see Table 3).

2.1.5. Solar Renewable Energy

The next renewable energy sector is solar energy, which is based on the system of harvesting solar radiation (photovoltaic) for electricity or collecting solar thermal energy for heating [107]. The photovoltaic (PV) system for harvesting solar radiation is primarily based on solar panels, where solar radiation is absorbed by PV cells in the solar panel. This then creates electrical charges that move and respond to an internal electrical field in the PV cell, causing electricity to flow [108,109]. In addition, photocatalysis can provide additional support for solar energy production and storage by inhibiting the conversion of collected light after exposure when there is insufficient light incoming to the solar panel (night time, low radiance angle, or weather-related obstruction) [110,111].

Solar energy can also be harnessed using concentrating solar thermal power (also known as CSP), which uses a system of mirrors to reflect, concentrate, and convert solar energy into heat or even electricity [108,109].

The advantage of solar energy is that it is the most abundant natural energy source in the world, and solar energy can provide a solid and increasing output efficiency compared to other sources. It has minimal harmful effects on the environment, although this can also be highly controversial [108].

The future of solar energy is also being explored in the context of hydrogen production, which can later be used as a clean energy carrier [112]. H_2 production from sustainable solar energy is a possible environmentally friendly solution for the increasing demand for energy and fuel as well as energy storage and transportation. The production of H_2 from solar energy would be achieved by solar thermolysis and then by electrolysis from solar–thermally produced H_2 and photovoltaic-based hydrogen production [112]. Such systems will also require new adaptations of metallic materials to adapt to new challenges in terms of maintenance and repair in correlation to the high temperatures, hydrogen presence that can cause hydrogen embrittlement, and corrosive environments [112].

The challenges that metallic materials face in the solar energy sector include the corrosion effect between molten salts and thermal storage materials [113], high-temperature corrosion [114], mechanically assisted corrosion [114], localized corrosion (stress corrosion cracking and flow-accelerated corrosion) [114], creep fatigue [115,116], erosion [117,118], oxidation [117], and mechanical properties [119,120].

The most commonly used ferrous alloys in the solar energy sector are austenitic and martensitic stainless steels, carbon steels, Cr-Mo steels, duplex steels, FeCrAl steel, and ferritic-martensitic steels (see Section 2.2). The most-used non-ferrous alloys are Ni alloys, which represent more than 60% of all non-ferrous alloys used in this sector. The other non-ferrous alloys are Al-based alloys, high-entropy alloys (HEA), and Mg-based alloys [121] (see Section 2.2) (see Table 3).

2.1.6. Geothermal Renewable Energy

Geothermal renewable energy is the last renewable energy herein presented. Geothermal energy is a type of thermal energy that originates from the formation of the planet and from radioactive decay of elements [122–124]. The Earth's internal thermal energy flows to the surface by conduction at the rate of 44.2 TW [125] and by radioactive decay at the rate of 30 TW [123]. The output of geothermal energy can currently meet twice the current energy demand from all energy sources (including non-renewable sources), but the challenge lies in the non-renewable energy flow and its extraction [123]. Harvested geothermal energy can be used for electricity or for heating/cooling.

There are several ways to produce electricity directly from geothermal energy. The first and the oldest type is the dry-steam power plant, which is based on the underground steam source [124,126]. The next type is the flash-steam power plant, where the source is underground water (>180 °C) and steam. This is the most common type of electricity source based on geothermal energy [127,128]. The next type is an enhanced geothermal system, which uses fracturing, drilling, and injection to extract fluid from the subsurface, which is then used for heating and electricity generation [129,130]. The next type is the binary cycle power plant, where water is heated underground (100–180 °C), and then, the hot water circulates above ground and heats a liquid organic compound that has a lower boiling point than water. This compound then produces steam, which flows into the turbine and powers the generator to produce electricity [122,124,131].

In addition to electricity, geothermal energy can be used for heating and cooling. Thermal energy can be extracted from low-temperature geothermal plants, co-produced geothermal energy, or by geothermal heat pump [124]. The first type, low-temperature geothermal energy, is based on the extracting energy from the low-temperature pockets (around 150 °C) located a few meters below the surface [132]. The next type is the so-called co-produced geothermal energy, where heat is produced by water that has been heated [133,134]. The last type is the geothermal heat pump, which is installed at a depth of 3 to 90 m. In this system, the temperature difference between both ends of the system is used to transfer energy by either heating or cooling the upper part of the system [135,136].

One of the advantages of geothermal energy compared to other sources is that it can be harvested almost anywhere in the world. Additionally, the power plants can last for decades with proper maintenance, and because there is no seasonal variation in workload, the system can be adapted to different conditions depending on the application and environment [122,124].

The challenges facing metallic materials used for geothermal energy are corrosion (uniform corrosion, pitting corrosion, crack corrosion, stress corrosion cracking, sulfur-assisted corrosion cracking, and galvanic corrosion) [137,138], hydrogen bubbling [139,140], corrosion fatigue [141,142], fatigue [137,138], erosion [140,142–144], wear [145], high pressure [144], high temperature [144], and cavitation and decomposition of alloy structure [138]. The most common metallic materials used in the geothermal energy sector are duplex steels, austenitic and superaustenitic stainless steels, martensitic stainless steels, low-alloyed steels, carbon steels, superferritic steels, Cu-based alloys, Ni-based alloys, and Ti-based alloys (see references in Section 2.2) (see Table 3).

2.2. Cost of Maintenance and Repairs in Future Energy Sector and Search of the Solutions for Lowering the Costs

Cost of Maintenance and Repairs of Future Energy Sector

Maintenance costs vary for each of the described energy sectors due to the different technologies used to produce electricity or heat (see Figure 4a). For advanced nuclear power, projections are based on current nuclear power sources and can be up to 20% of the initial investment [146,147]. For biomass energy, maintenance costs are estimated to be up to 35% due to the unique environment. However, different technologies require different levels of maintenance and servicing of the components, so maintenance costs can also be as low as 15% of the investment over time [148,149].

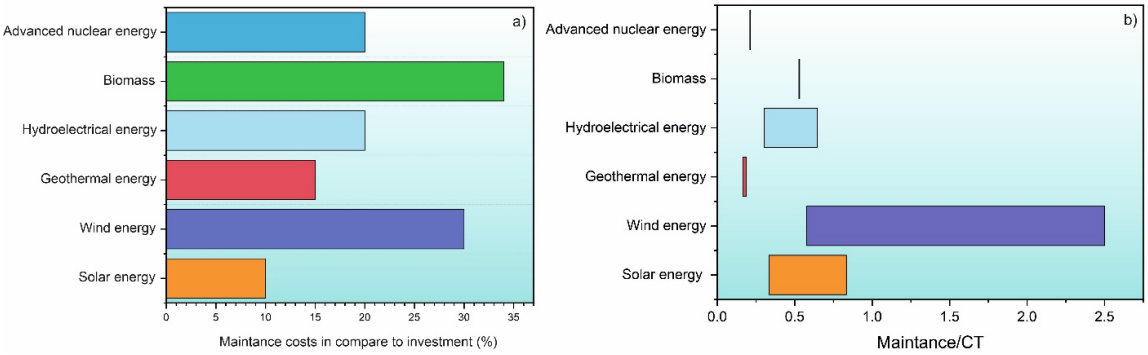

Figure 4. (**a**) Maintenance costs for each energy source type over time. Note that the figures are the maximum value that maintenance can cost in terms of investment over time, but this can vary due to different techniques. (**b**) Maintenance costs for each energy sector normalized by their corresponding maximum and minimum CF. The range of CF was taken from Table 2.

Maintenance costs for hydropower can vary from 1.5 to 20% depending on the type of technology used and the environment in which the plant is located [150,151]. The next sector is geothermal sector, where the maintenance costs can reach up to 15% of investment over the course of the life span of a typical power plant [152,153]. In the wind energy sector, the onshore or offshore location of the wind farms plays an important role in maintenance and repair costs, which can vary the costs somewhere between 20% and 30% of the total investment [103,154]. The last sector is solar energy, which has the one of the lowest maintenance costs (up to 10%) compared to all sectors. However, it is important to note that this does not reflect how much energy is actually produced by it (see Table 2) [155].

In order to put the maintenance cost in relation to the actual output of the individual energy source, the maintenance costs are normalized by the CF of the individual energy source, which is presented in Figure 4b. As can be seen, the wind energy has a very wide range due to the high maintenance costs that can be associated with specific maintenance issues of a wind farm. The solar, hydroelectric, and biomass sources show an intermediate influence of the maintenance costs, while geothermal and advanced nuclear energy have the lowest influence of maintenance costs in relation to their effective production capacity. This Figure 4 clearly shows that the improvement of materials will play an important role in the development and improved cost reduction of renewable energy power plants.

2.3. Metallic Mateirals Used in the Energy Sector

Table 3 summarizes the various metallic materials used in the advanced nuclear and renewable energy sectors.

Table 3. The list of metallic materials used in advanced nuclear energy and renewable energy sectors.

Energy Sector	Metallic Materials		Application
	Ferrous Alloys	**Non-Ferrous Alloys**	
Advanced Nuclear Energy		Zr-based alloys (Zircoaloy-4 (Zr-Sn-Fe-Cr), Zirlo, and M4 (Nb-based alloy)) [30,31]	Water reactors [30,31]
Advanced Nuclear Energy	Austenitic stainless steel (AISI 316 [31], AISI 316 SS [31], AISI 316L [156], AISI 316 LN [157], AISI 304 [31,157–160], AISI 304L [161–164], AISI 304 N [161], AISI 304 SS [31], AISI 347 [31], AISI 308L [157], AISI 308 SS [31], AISI 310 SS [156,165], AISI 309L [31], AISI 309 SS [31], AISI 321 SS [31], AISI 403 [31], AISI 410 [31]; AISI 347 SS [31], AISI 630 [31], AISI D9 [31], HT-UPS [31], AISI 4340)		Water reactors, piping, pressurizer, steam generator, pump, valve casing, plunger, control rod drive mechanism, and core internal structure [30,31]
Advanced Nuclear Energy	Cast-austenitic stainless steel (CF3, CF3A, CF3M, CF8, CF8A, CF8M, AISI 304 SS, AISI 304L SS, AISI 316 SS, AISI 316L SS, AISI 321 SS, AISI 347 SS) [31]		Primary cooling piping system, reactor coolant, auxiliary system, pump casing, valve bodies, and cooling circuit [30,31]
Advanced Nuclear Energy		Ni-based alloys (600 [161,166,167], 690 [161,168], 625 [31], 718 [31], X-750 [31], 800 [31], 800 H [165], 182 [31], 82 [31])	Piping, steam generators, tubes, and working component in high corrosive environments [30,31]
Advanced Nuclear Energy	Low-alloyed steel (Ferritic steels: A105 [169], A106 GrB [31], A182 [169], A216 GrWCB [31], A302 GrB [169,170], A333 Gr6 [31], SA212 B [169]; A508 Gr3 [169,171–174], A516 Gr70 [31], A533 A [31], A555 B [31], 15Kh2NMFA [175,176], 08Kh18N10T [177]; bainitic steels: 1Cr1Mo0.25v [31], 2Cr1MoGr 22 [31], NiCrMoV [31]; duplex steel: 2507 [159], DSS [178], Fe20Cr9Ni [179]; carbon steel: AISI 1018 [159])		Steamless piping, gorging, casting, bolting, plate, pressure vessels, piping, and feedwater lines; internal stainless steel cladding; steam generator channel heads [30,31]
Advanced Nuclear Energy	*Fusion RAFM steel (Eurofer97 [180–183], CLAM [31], Infrafm [31], FB2h [31]; Rusfer [31]; 9Cr-2WVTa [31]) Ferritic steel [31]		First wall at reactor, blanket, shield, vacuum vessel, and divertor [30,31]
Advanced Nuclear Energy		Fusion ODS alloy [31] ODS ferritic alloy [31]	
Advanced Nuclear Energy		Fusion other alloys SiC composites [31] W and W-based alloys [184–186] Cu-based alloys [186] Pb-Al alloy [187,188] HEA [189] Mo-based alloys [184] Nb-based alloy [184] V-based alloy [184] C-fiber components [190]	Structural and insulating application, joints, and filaments [30,31]

Table 3. *Cont.*

Energy Sector	Metallic Materials		Application
	Ferrous Alloys	**Non-Ferrous Alloys**	
Hydroelectrical Renewable Energy	Austenitic stainless steel (AISI 316/AISI 316L [71,191–193], AISI 304/AISI 304L [66,79,194,195], AISI 325 [71], ASTM A743 [79,196], ASTM CF20 [71])		Turbines and other components [66]
Hydroelectrical Renewable Energy		Non-ferrous alloys Al-based alloys [66,71,77] Ti-based alloys [66,78] Cu-based alloys [76,79,80] Ni-based alloys ([81,89])	
Hydroelectrical Renewable Energy	Martensitic stainless steel (AISI 410 [197–200] ASTM F6NM [201,202], 13Cr4Ni [202–204], AISI 410T [79], AISI 410 [71], AISI 430 [69], ASTM FV520B [205], ASTM CA6NM [196])		Turbines, shear pins, and other components [66]
Hydroelectrical Renewable Energy	Other steels High-strength steel [56,70,206] ACSR [71,77] Stainless steel [72,77,79,199,206] Cast steel [71] Nitronic steel [202] Carbon steel [72] High-speed steel [207] Electric steel [69] Constructional steel [69]		Supporting systems and other components [66]
Biomass Renewable Energy	Carbon steels and low-alloyed steels (2.25Cr-1Mo [97,98], 5Cr-1Mo [98], 9Cr-1Mo [98,208])		Construction of the plant, pumps, pipes, valves, fittings, and digester tanks [82–84,105,209]
Biomass Renewable Energy		Non-ferrous alloys Al-based alloys [97,210,211] Ni-based alloys [97,212] NCA [213]	Specialized components [82–84]
Biomass Renewable Energy	Stainless steels Austenitic (AISI 304 L [97,214], AISI 316 L [74]) Martensitic (AISI 409 [74], AISI 410 [74], AISI 416 [74])		Construction of the plant, pumps, pipes, valves, fittings, and digester tanks [82–84,105,209]
Biomass Renewable Energy	Cr-steels (12-13Cr [208], 13Cr [208], 14.5Cr [208], 16Cr [208], 12Cr-5Ni-2Mo [208], 11.5Cr-2Mo [208])		

Table 3. *Cont.*

Energy Sector	Metallic Materials		Application
	Ferrous Alloys	**Non-Ferrous Alloys**	
Wind and Offshore Wind Renewable Energy	Structural steel (S235J2 [215,216], S355J2 [215], S500G1 [215,216], S35G10 [217], S460 [216], S690 [216], S355 [216], S420M3Z [218], S500M3Z [219])		Foundation, tower, gear, and casing of the wind turbines [105]
Wind and Offshore Wind Renewable Energy	Stainless steel Duplex stainless steel (mostly AISI 2205 [220]) Austenitic stainless steel (22Cr25NiWCoCu [221], AISI 304L [222–224], AISI 904L [225,226]) Martensitic stainless steel (mainly from 4xx series, such as AISI 440 C [227,228])		
Wind and Off-shore Wind Renewable Energy		Non-ferrous alloys Cu-based alloys [229,230] Al-based alloys mostly from 2xxx and 6xxx series [218,231,232]	
Wind and Off-shore Wind Renewable Energy	Other types of steel Electric steels [233] Cast iron [234,235] High-Si nodular cast iron (EN GJS500-14 [235], EN GJS450-18 [235], EN GJS600-10 [235]) Bearing steels (mainly AISI 52100 [227,228]) High-Cr steel [227,228] Low-C nitrogen steel [227,228]		
Solar Renewable Energy	Austenitic stainless steel (AISI 304 [236,237], AISI 304L [238], AISI 316 [236,239], AISI 316L [237,240,241], AISI 321 [242,243], AISI 347 [242], AISI 347H [236])		Are used for base in solar-thermal panels, pumps, tanks, and heat exchangers [105]
Solar Renewable Energy	Martensitic stainless steel (AISI 420 [244], EN 1.4903 [236], EN 1.4923 [236], AISI T91 [245], VM12 [246])		
Solar Renewable Energy		Ni-based alloy (IN 230 [247], IN 600 [248,249], IN 617 [247,249], IN 625 [236,239,247], IN HT700 [250], IN 800H [251], C-276 [252], XH [249], H230 [249], HR120 [249])	
Solar Renewable Energy	Other steels Carbon steels [236,253] Cr-Mo steels [254] Duplex steels [255] FeCrAl steels [241] Ferritic-martensitic P91 [248]		
Solar Renewable Energy		Other non-ferrous alloys Al-based alloys, mostly from series 7xxx [256–259] HEA [260,261] Mg-based alloys, mostly Ti-Y combination [262,263]	

Table 3. *Cont.*

Energy Sector	Metallic Materials		Application
	Ferrous Alloys	**Non-Ferrous Alloys**	
Geothermal Renewable Energy	Duplex steels (2205 [264], 2507 [264], 2707 [264])		Heat exchangers, filters, pumps, valves, piping, and condensers [209]
Geothermal Renewable Energy	Austenitic and superaustenitic steels (AISI 304 [265], AISI 304L [264], AISI 310S [264], AISI 316L [264,266], AISI 321 [264], UNS N08031 [266], N08020 [267], N08026 [267], N08825 [267], N08330 [267], S31254 [267])		Construction of the plant [267]
Geothermal Renewable Energy	Martensitic stainless steels (mostly from 4xx series, AISI 400 [268,269], AISI 430 [269], AISI 431 [269])		
Geothermal Renewable Energy		Non-ferrous alloys Ti-based alloys [138] Ni-based alloys [138,264] Cu-based alloys [269]	
Geothermal Renewable Energy	Other steels Low-alloyed steels [266] Carbon steel [270] Superferritic steels (S44627 [267], S44700 [267], S44800 [267])		

2.4. Solutions for Lowering the Costs of Maintenance and Prolonging the Component Durability

As mentioned before, the major maintenance costs are the repair and replacement of materials used in the power plants. It is important to extend the service life of materials and to design materials and components that can be easily and cost-effectively replaced or repaired. A common solution to address these challenges for metallic materials used in different energy sectors is mostly by cathodic corrosion protection in combination with coatings [271,272]. Cathodic protection of the metallic materials is an electrochemical technique to protect and control corrosion of the material [273,274].

Coatings, especially organic coatings, can also be applied without the combination of cathodic protection, which is mainly used for materials that are immersed in water [275–277]; often, a combined use is chosen. Cathodic protection can be also achieved by some metallic coatings, such as zinc alloy coatings or by a combination of metallic and organic coatings (see, for example, [278,279]). However, coatings and linings can also be applied alone as a passive corrosion protection or in a so-called duplex system, where both coatings and linings are used simultaneously as a multilayer system [218,280].

Other options for surface treatment to improve resistance to environmental factors and prolong component life include surface treatments such as laser treatment, electron beam, induction heating, plasma nitriding, and selection of the appropriate heat treatment to achieve the desired microstructure [281–284]. While coatings and surface treatments can be a good technique to overcome many challenges, certain applications that require specialized metallic materials can make this technique very limited. This is particularly an issue when the application is under harsh conditions such as simultaneous high temperatures and high loads, which require either metallic materials that are difficult to coat or specialized coatings and surface treatments that can be very expensive and have limited-service life due to combined wear, erosion, and corrosion effects [285,286].

This requires a holistic approach to material treatment that is not limited to the surface of the material. A common approach for metallic materials is to use conventional heat treatments to tailor individual properties. However, conventional heat treatments typically involve a trade-off where certain properties are improved at the expense of others, typically resulting in metallic materials with high strength but low fatigue and corrosion properties and vice versa [287,288].

As a result, more sophisticated and complex processing and treatment of metallic materials are being explored to overcome such trade-offs. One of the new options, which has also been tested in the steel industry, is the use of cryogenic treatment, which can improve various properties of metallic materials, including corrosion performance, without adding a coating to the surface [289–292]. A more detailed presentation and explanation of cryogenic treatment and its application to surface and corrosion properties is described in Section 3.

3. Cryogenic Treatments in Energy Sector

The technology of cryogenic treatment (CT) has made tremendous progress in the last 10 years in its application on metallic materials in various sectors ranging from medicine, aerospace, robotics, materials science (including the steel industry), nanotechnology, and mining to even more specialized disciplines [289,293]. The technique has evolved from the first attempts to treat materials at cryogenic temperatures in the 19th century by James Dewar and Karol Olszewski using liquefied gases (nitrogen and hydrogen). Later, the first real scientific observation and documentation of CT was made by NASA (National Aeronautics and Space Administration) in the mid-20th century, when they observed changes in the properties of materials used in space shuttles returning from space [289,293]. The selected aluminum components were harder and more wear-resistant after returning to Earth than they were before the space mission [289,293]. Since then, CT has been slowly adapted with different techniques and applications to metallic materials in order to improve

macroscopic and microscopic properties. In the literature, CT can also be called sub-zero treatment, ultra-low temperature processing, or cryo-processing [289,293–296].

The application of CT in the energy sector can be of particular interest due to the variety of metallic materials that are used in extreme conditions (high-temperature and high-pressure environments, highly corrosive environments, highly abrasive environments, etc.), as discussed in Section 2. However, the application of CT in the energy sector is still in its infancy, mainly due to the slow introduction and development of this treatment scheme and the limited research focus on applications in the energy sector.

3.1. Mechanisms of Cryogenic Treatments

The mechanisms of CTs are based on the type, which is defined by the selected temperature regime for the CT (Figure 5). CT is usually applied after the material has been hardened and quenched and before being tempered, usually for 24 h at a predetermined temperature [289–293,297,298]. The most common and the one with the longest tradition is the conventional cryogenic treatment (CCT), where temperatures as low as 193 K are used [299].

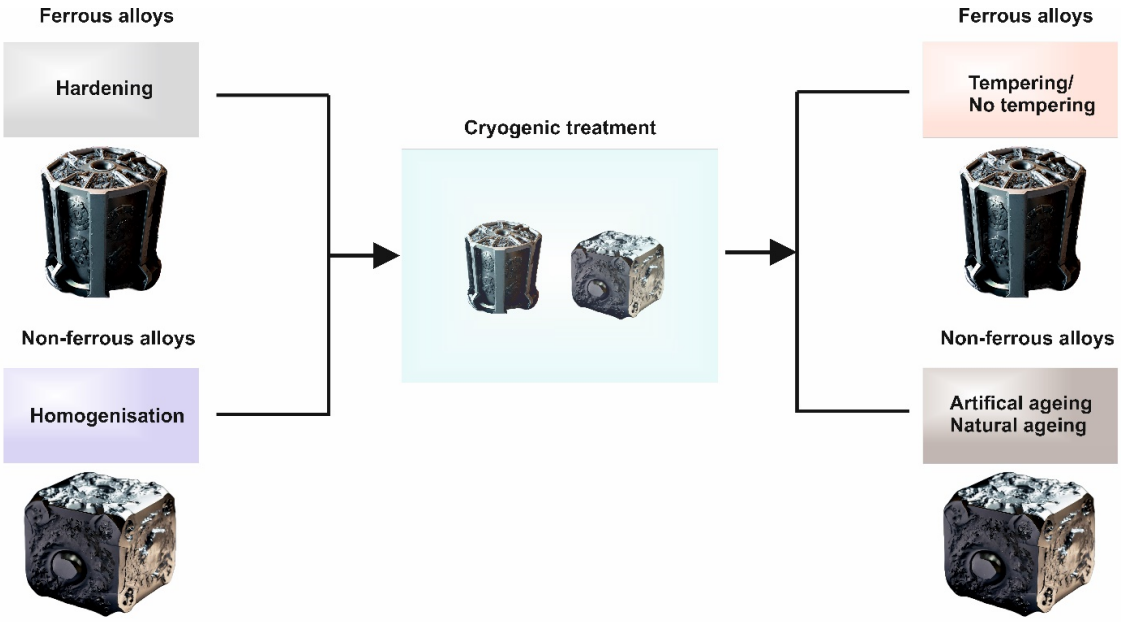

Figure 5. The heat treatment route(s) for both ferrous and non-ferrous alloys when CT is applied.

The reason for CCT being the most-used type in the past was the easy availability of media to which the material is exposed, namely dry ice (solid CO_2) [293,299]. In the past, it was also believed that temperatures as low as 193 K were sufficient to transform all the retained austenite (RA) in ferrous alloys to martensite, thereby increasing wear resistance and fatigue strength [293,299]. The transformation of RA to martensite, particularly in steels, was one of the key properties for which CTs were commonly applied, which also propagated the initial research on CT [293,299]. Unfortunately, the negative results of the first experiments with CCT led many companies to abandon the application and development of this treatment (1940s–1950s) [293,299]. This was mainly due to a misunderstanding of the martensitic transformation and its temperatures as well as simplistic and inconsistent treatment procedures [293,299]. It was not until years later, after NASA observations and detailed documentation of the changes at lower temperatures, that the next two types of CT were developed and tested for materials science applications: shallow (SCT) and deep cryogenic treatment (DCT) [293,299].

Shallow cryogenic treatment is defined between 193 K and 113 K. During SCT, more than 50% of the RA is converted to martensite for generally any ferrous alloy that has instable austenite formation during quenching, causing a change in mechanical prop-

erties (increased hardness), size reduction of carbides, and increased precipitation of carbides [300,301]. With the positive results of SCT, the research on CT blossomed and led to further research at even lower temperatures, resulting in the development of deep cryogenic treatment.

Temperatures for deep cryogenic treatment are below 113 K and typically go as low as 4 K, which is the temperature of liquid helium. However, the most-used temperature is 77 K, the temperature of liquid nitrogen, which is the most-used medium in DCT due to abundancy of the media and economic reasons. With DCT, for ferrous alloys, most of the RA is converted to martensite (>90%), the precipitation of carbides is increased, grain refinement and precipitation of nanocarbides occurs, and changes to residual stresses are formed [302]. Special mention should be made to a specific type of DCT, the multi-stage deep cryogenic treatment (MCT), where the DCT treatment of the material consists of rapid changes between SCT and DCT temperatures for a predefined time and number of cycles to manipulate predefined properties [303]. DCT performance is influenced by the selected cooling temperature, cooling–warming rate, time the material is exposed to DCT, type of metallic material (ferrous/non-ferrous alloy or type of steel), chemical composition of the metallic material, hardening process, tempering temperature, and also the microstructural phenomena present within the microstructure (such as transformation-induced plasticity (TRIP), austenite reversion transformation (ART), and twinning-induced plasticity (TWIP)) [304–310].

All types of CT alter the bulk and surface properties of metallic materials. The bulk properties affected by CT are mechanical properties ((micro)hardness [311–314], toughness [311,315–317], strength [318–320], and fatigue [307,321,322]) and magnetism [304,323]. The surface properties affected by CT are corrosion resistance [324–332], wear resistance [321,333–335], roughness [336], and oxide formation [324–326,336].

Bulk properties and, to some extent, selected surface properties have been studied in more detail than others. There are still many unknowns and great potential in surface properties and corrosion resistance, which is also the focus of the following section of this review.

3.2. Energy Sector and Position of Cryogenic Treatments

Cryogenic processing has a great potential in the energy sector due to the use of different materials, from metallic to non-metallic. The application of CT, especially for metallic materials, has a great potential because it improves the properties of metallic materials needed in different energy sectors, from corrosion and wear resistance to mechanical properties and surface modifications [337,338]. At the same time, it does not require the additional application of any other coating treatment to improve the properties (see Section 3.3.1).

However, the application of CT in this sector has not been widespread due to the lack of known test methods and quantification and qualification methods. Only a few attempts have been made to provide systematic guidelines for standards and application of CT for metallic materials [293,306,309,339–341]. An additional obstacle was that in the past, there were no large capacity tanks, and no providers of these services or systems were available on an industrial scale, but this is now changing and, in some cases, improving with the establishment of CT-specialized companies, communities, and even patents [294–296,332,342–347]. CT was also not well transferred to other disciplines, as CT was mainly reserved and developed for improving tools. The research was (and still is) mainly focused on tool steels, such as high-speed steels, hot work tool steels, and cold work tool steels, where the emphasis is on mechanical and wear properties [334,348–351].

As a result, the majority of other types of steels and alloys have been left out of the focus. There is some limited research on non-ferrous alloys, but even these are mostly related to aluminum alloys used or related to the tooling industry. The study of non-ferrous alloys (Al-, Ni-, and Ti-based alloys) showed the improvement of mechanical properties [352–358]

such as microhardness [352,354,359–361], fatigue [352], fracture toughness [362,363], impact toughness [352], and tensile strength [352,354].

The following sections present metallic materials that have been tested by cryogenic treatment, the results of which have the potential to be used in the energy sector.

3.3. Effect of Cryogenic Treatments on Surface, Interface, and Corrosion Properties of Metallic Mateirals Used in the Energy Sector

3.3.1. Metallic Materials Being Tested for the Use in the Energy Sector

There are many metallic materials (ferrous and non-ferrous alloys) that are suitable for use in the energy sector that have already been tested through various cryogenic treatments, and studies have resulted in changes in the microstructure of metallic materials, resulting in changes in the properties of the material. The following ferrous and non-ferrous alloys are used in the following sectors (Table 4).

Table 4. The list of ferrous alloys that were cryogenically treated and have the potential for use in the energy sector.

Ferrous Alloys	Grades of Steel	Tested Properties	Possibilities of Application in Selected Energy Sector
Austenitic stainless steel	AISI 304 [364–370], AISI 304L [308,319,371–374], AISI 304LN [374], AISI 316 [374–380], AISI 316L [192,341,348,381–384], AISI 316LN [374,385], AISI 321 [386,387], AISI 347 [388,389]	Hardness, microhardness, wear (abrasive wear), fracture toughness, impact toughness, compressive strength, tensile strength, yield strength, elongation, friction, erosion, strain-hardening exponent, surface roughness, machining of steel, fatigue, residual stress, surface chemistry, and oxidation	In all energy sectors
Martensitic stainless steel	AISI 410 [390], AISI 420 [349,390–392], AISI 420 MOD [392], AISI 430 [393,394], AISI 431 [304,309,395], AISI 440C [366], AISI P91 [396], 10Cr13Co13Mo5NiW1VE [397], 13Cr4NiMo [315], 10Cr [398].	Yield strength, elongation, tensile strength, wear, hardness, impact toughness, fracture toughness, magnetism tribocorrosion, electrochemistry, and corrosion resistance (also stress corrosion cracking)	In all energy sectors.
Duplex steels	AISI 2205 [399,400], AISI 2507 [401–404]	Hardness, wear, machinability, residual stress, and corrosion resistance	Mostly in wind and solar energy
Carbon steels	IS 2062 [405], AISI 1045 [406–412], AISI 1018 [413]	Hardness, wear, surface roughness, tensile strength, yield strength, ultimate tensile strength, elongation, and residual stress	Steels can be used in hydroelectrical, biomass, solar, and geothermal energy
Other steels	Nitronic steels 40 [414], 50 [415] High-strength steels ASTM A36 [416] Cast steels ASTM A743 [417], SAE J431 G10 [418] ACSR [419] Bearing steel AISI 52100 [326,328,420–422] Low-alloyed steels SAE 1008 [423], AISI 4340 [424], AISI 4140 [424] Structural steel S235 [425], S355 [426,427], S460 [428]	Residual tress, hardness, friction, wear, fatigue, impact toughness, corrosion resistance, and machinability	In all energy sectors

Table 5 presents the non-ferrous alloys that have been CT-treated and have potential in the current and future energy sectors.

3.4. Effect of Cryogenic Treatments on Metallic Materials Potenitally Used in the Energy Sector

The surface properties that are the focus of this review and that also need more attention in order to carry out more research on them are corrosion resistance and oxide formation, while wear resistance and roughness have been observed and researched by many studies in the cryogenic community (see Section 3).

Table 5. The list of non-ferrous alloys that were cryogenically treated and have potential for use in the energy sector.

Non-Ferrous Alloys	Grades of Alloys	Tested Properties	Possibilities of Application in Selected Energy Sector
Al-based alloy	2xxx series: 2024 [354,429] 3xxx series: A356 [430,431], A390 [432] 6xxx series: 6026 [352,433–435], 6061 [353,436,437], 6063 [362] 7xxx series: 7075 [330,331,361,438–442]	Hardness, wear (abrasion), corrosion resistance, tensile strength, machinability, fatigue, strain-hardening coefficient, residual stress, fracture toughness, and corrosion resistance	Mostly in hydroelectrical, biomass, wind, and solar energy
Ni-based alloy	Inconel: 200 [443], 600 [444,445], 617 [446], 625 [447–449], 690 [450], 800 [451], 800H [452–454] Hastelloy C276 [455], C22 [456,457], X [458] HEA [459]	Fatigue, surface roughness, machinability, durability, impact toughness, microhardness, and tensile strength	In all energy sectors
Other alloys	W-based alloys [460] Cu-based alloys [461] Ti-based alloys Ti6Al4V [451,462]	Microhardness, compressive strength, and plasticity	Mostly in advanced nuclear power (fusion), geothermal, and solar energy

3.4.1. Oxide Formation

Oxide formation is one of the properties that is seldomly researched and not fully understood in CT. The fact is that most of the studies focus on the corrosion resistance and its improvement by CT, and not many studies strive for deeper understanding of the origin of altered corrosion resistance by CT. A major contribution is provided by passive layers and oxide formation (corrosion products) that can be manipulated by CT and CT-induced changes to the bulk properties of the treated material. The influence of CT on oxide formation has been demonstrated for bearing, high-speed, and cold work tool steels [324–326,336]. The oxidation dynamics after the application of CT was mainly studied by Jovičević-Klug et al., where the observations showed a different development of oxides compared to conventional heat treatment (CHT).

Jovičević-Klug et al. 2021 [336] suggested that the chemical composition of the oxide formation directly corresponds to the higher number of precipitates and the higher surface-to-volume ratio of the carbides. Furthermore, the study indicates that the reduced amount of carbide clusters after CT could be directly correlated with the passivation layer and the oxidation state of the surface and the corresponding corrosion products.

In the next study, Jovičević-Klug et al. 2021 [325] suggested that the Cr oxide layer is thicker on the cryogenically treated samples compared to the CHT samples. These observations also suggest that due to the formation of the Cr-oxide-passivation layer on the CT sample, there is no microscopic-related stress corrosion cracking of the matrix, which in turn, combined with the thicker passivation layer, reduces corrosion propagation.

The next factor observed in relation to CT was the formation of Fe oxides. The study by Jovičević-Klug et al. [326] suggested that Fe-oxides form different layers compared to the CT sample, which is attributed to the local excessive corrosion damage in the CHT sample.

The same researchers, Jovičević-Klug et al. 2022 [324], also observed the different layering of the oxides in the samples. The results of ToF-SIMS provided the novel insight that nitrogen from CT is present in greater amounts in the CT samples, which then influences the complex oxide formations (corrosion products), which ultimately influence the corrosion resistance. Nitrogen acts as an exalter for the formation of green rust, which then acts as a precursor for the formation of the next layer (magnetite). As a result, corrosion propagation is greatly retarded due to the higher density and stability of magnetite. The same study also confirmed that the CT-induced passive film is more stable than its CHT counterpart. As a result, the CT-treated sample showed lower corrosion and wear loss, which was also confirmed in extreme environments (elevated temperatures and vibrations).

The above examples show that there is a need for research on oxide formation as the basis for successful tailoring of corrosion resistance and prolonged component life of treated materials. The studies only focused on tool and bearing steels, which means that other steels such as high-Cr steels, stainless steels, duplex steels, and non-ferrous

alloys are still potential research areas with great opportunities for the application of CT to manipulate oxide formation and modify corrosion resistance. To date, no similar studies or research have been conducted or found for non-ferrous alloys. Section 3.4.2 discusses corrosion resistance.

3.4.2. Corrosion Resistance

The influence of CT on corrosion resistance has not only been investigated in relation to tool steels, but many studies have also tested other ferrous (bearing steels and stainless steels) and non-ferrous (mostly Al-based alloys) alloys. The first part focuses on the corrosion testing of ferrous alloys, while the second part focuses on the non-ferrous alloys in relation to CT.

Corrosion Resistance of Ferrous Alloys

The studies on tool steels showed that corrosion resistance is influenced by CT [329,392,463–466]. The corrosion resistance of bearing and tool steels can be improved by up to 65% in an alkaline environment, with the improvement depending on the steel type and heat treatment strategy [326]. This was also observed by Senthilkumar 2014 [327], who found that in alkali conditions, CT improves corrosion resistance, which was postulated to be a result of formation of more stable passive film. Furthermore, in extreme alkaline environments, such as elevated temperatures and vibrations, the CT-treated samples (tool steels) suggested improvement of corrosion resistance by 90% in the study of Jovičević-Klug et al. 2022 [324]. Also, the study by Jovičević-Klug et al. 2021 [326] showed that in an alkaline environment, the formation of pits is modified by CT (for tool and bearing steels). The study showed that pits in CT specimens expand only in the exposed upper part and decrease continuously deeper into the material. It was suggested that this is due to the confinement of the corrosion attack to the grain boundaries and the exposure of the pit opening to the oxidative media, which is limited by the change in orientation of the crack with respect to the sample surface. In addition, the 2021 study by Jovičević-Klug et al. [325] also showed that in the alkaline environment, the CT samples did not show any stress corrosion cracking of the passivation layer, and the presence of Mo in the steel allowed the continuous growth of the protective Cr oxide layer, which reduced the formation and growth of pits. The results show that CT samples have a 3× slower corrosion rate of pitting corrosion, which can be directly correlated to the slower material degradation and prolonged functionality of the metallic material.

Only a few studies have been conducted on stainless steels and a few other types of steels that are more commonly used in energy sector applications. The studies showed different results of CT on the corrosion resistance of steels used in the energy sector. A study by Wang et al. 2020 [467] showed that there is an increase in corrosion resistance for high-strength stainless steel. On contrary, a study by Baldissera and Delprete 2010 [468] postulated that CT has no effect on austenitic stainless steel. Another study by Cai et al. 2016 [469] indicated that for austenitic stainless steel, CT could improve corrosion resistance, which is suggested through Cr-carbide precipitation at the austenite grain boundary, which then reduces the intergranular corrosion. For martensitic stainless steels, CT has been shown to improve corrosion resistance in correlation with both the general and pitting corrosion, as was shown by Ramos et al. 2017 [366]. Another explanation for the higher pitting corrosion potential was proposed by He et al. 2021 [470], in which pitting corrosion was reduced by increased carbide precipitation and Si segregation at the interface boundaries between $M_{23}C_6$ and martensite in the matrix. For structural steels, a 95% improvement in corrosion resistance was determined by Ramesh et al. 2019 [392], which is suggested to be a consequence of uniform and homogenous carbide precipitation and microstructure modification.

The above literature review shows that there has been some research on corrosion enhancement with CT but only on a limited selection of ferrous alloys. Furthermore, the review shows that there is a great need for research on the corrosion resistance of ferrous

alloys used in the energy sector in combination with CT. Such research could open up new avenues and applications for CT to improve corrosion resistance alone or in combination with coatings, which could further expand the energy sector from both an economic and sustainable point of view.

Corrosion Resistance of Non-Ferrous Alloys

The corrosion resistance of CT-treated non-ferrous alloys has been mainly focused on the Al-based alloys of the 2xxx [471], 5xxx [355], and 7xxx [330,331,440] series. The study by Cabeza et al. 2015 [471] on Al-based alloys from the 2xxx series suggested that CT improves the resistance to stress corrosion cracking due to changes in compressive residual stresses. Another study by Aamir et al. 2016 [355] showed that for the 5xxx Al-alloy, the corrosion resistance is increased due to the minimization of dislocation densities and noncontinuous distribution of the β-phase. From the 7xxx series, the tested representative was the 7075 Al-alloy. A study by Ma et al. 2021 [440] showed an improvement in corrosion resistance after the application of CT, which was attributed to the increased precipitation of the η′ phase. They postulated that the grain boundary from the η′ resulted in short chains of carbides, which then blocked corrosion channeling, thus enhancing the corrosion resistance of the alloy. Similar observations were also made by Su et al. 2021 [331]. Ma et al., from their study in 2022 [330], additionally showed that the optimized combination of aging and CT can influence the rate of the corrosion improvement when CT is applied.

Compared to ferrous alloys, research on non-ferrous alloys is also considered to be lacking and is mostly focused on specific alloys, mainly aluminum alloys. The review clearly confirms the lack of research on non-ferrous alloys, which have a great potential for use in the future energy sector. The lack of research can be particularly evident in the case of Ni alloys and corrosion resistance in combination with CT, which are one of the main non-ferrous alloys used in different energy sectors due to their versatility. Other non-ferrous alloys such as Cu-based, Mg-based, V-based, W-based, etc., are also completely excluded from the studies, and therefore, this could be another potentially interesting niche to study in more depth the influence of CT on these alloys, which could be applied to the future energy sector. Furthermore, in most cases, the reasons for improved or sometimes reduced corrosion performance are based on speculation. Fundamental research is needed to elucidate the reasons for the effects of CT on corrosion performance.

4. Economic and Ecological Aspects and Future Role of Cryogenic Treatment in Future Energy Sector

While it is clear that the application of CT to ferrous and non-ferrous alloys has great potential due to its versatile effect on bulk and surface properties, the next question that comes to mind is the economic and environmental aspects of its application. CT uses mostly liquid N_2 as a coolant media, which is highly considered as a viable option for the conventional heat treatment of metallic materials. After CT treatment, LN_2 evaporates to become nitrogen gas (N_2) and becomes part of the air (78% of air consists of N_2). It leaves no harmful residue to the industry and the environment and no health hazards compared to other processing/machining techniques [369]. Therefore, it is considered as a recycling and environmentally friendly approach to improve the materials. Furthermore, it is suggested in some works, see, e.g., Hong and Broomer [369] and Dosset [472], showing a cost reduction of about 50%; however, more insight into the economic advantages is expected in the near future, which is expected to cause an increasing interest in the energy sector. In conclusion, CT shows great potential to improve the corrosion performance of materials, and the process is environmentally unharmful.

Based on all these facts, CT has a bright future in the future energy sector, where advanced knowledge of more economical and ecological impacts on the environment is being considered. Not only that, but with the trend of diminishing natural resources and more recycling options, CT also has an answer, as no additional treatment is required. CT

is also expected to play an important role in emerging materials for energy applications and storage (HEA and catalytic materials), which have not yet been explored and applied.

5. Conclusions

This review first provides an overview of the metallic materials used in the energy sector and then of the application of CT on metallic materials used in different energy sectors. In addition, this review also presents a synopsis of the current work and results on surface properties and corrosion, with critical comments to provide a future possibility for metallic materials in relation to CT and oxide formation and corrosion resistance. The review also highlights which materials should be prioritized for CT testing due to lack of research but are of high importance for applications (or are already in use) in different energy sectors.

The main conclusions of the study can be summarized as follows:

- The energy sector has a great demand for the improvement of metallic materials;
- Available green and cost-effective CT technology has been proven to effectively improve the bulk and surface properties of metallic materials;
- CT improves corrosion resistance by up to 90% depending on metallic materials and environmental conditions;
- CT also produces a unique sequence of oxide formation that effectively influences the improved corrosion resistance of cryogenically treated metallic materials;
- The result of CT is a reduction in material degradation and a possible 3-fold increase in the service life of the treated metallic material;
- Further detailed and systematic investigation of the effectiveness of CT is required, using both experiments and modeling of both ferrous and non-ferrous alloys. Combined with detailed microstructural investigations, the mechanisms responsible for changes in metallic material properties can be clearly identified, and standards for the application of CT in the energy sector can be established.

Author Contributions: Conceptualization, P.J.-K.; investigation, P.J.-K.; resources, P.J.-K. and M.R.; data curation, P.J.-K.; writing—original draft preparation, P.J.-K.; writing—review and editing, P.J.-K. and M.R.; visualization, P.J.-K.; supervision, M.R.; project administration, P.J.-K.; funding acquisition, P.J.-K. All authors have read and agreed to the published version of the manuscript.

Funding: The financial support was provided by Alexander von Humboldt Foundation throughout the Humboldt Research Fellowship Programme for PostDocs.

Institutional Review Board Statement: Not applicable.

Informed Consent Statement: Not applicable.

Data Availability Statement: Data will be available upon request.

Conflicts of Interest: The authors declare no conflict of interest.

References

1. Candra, O.; Chammam, A.; Alvarez, J.R.N.; Muda, I.; Aybar, H. The Impact of Renewable Energy Sources on the Sustainable Development of the Economy and Greenhouse Gas Emissions. *Sustainability* **2023**, *15*, 2104. [CrossRef]
2. Owusu, P.A.; Asumadu-Sarkodie, S. A Review of Renewable Energy Sources, Sustainability Issues and Climate Change Mitigation. *Cogent Eng.* **2016**, *3*, 1167990. [CrossRef]
3. Sinha, A.; Sengupta, T. Impact of Natural Resource Rents on Human Development: What Is the Role of Globalization in Asia Pacific Countries? *Resour. Policy* **2019**, *63*, 101413. [CrossRef]
4. Zallé, O. Natural Resources and Economic Growth in Africa: The Role of Institutional Quality and Human Capital. *Resour. Policy* **2019**, *62*, 616–624. [CrossRef]
5. Kumar, M. Social, Economic, and Environemtal of Renewable Energy Resources. In *Wind Solar Hybrid Renewable Energy System*; DoB-Books on Demand: Norderstedt, Germany, 2020; pp. 237–247.
6. Zohuri, B.; McDaniel, P. Energy Insight: An Energy Essential Guide. In *Introduction to Energy Essentials*; Academic Press: Cambridge, MA, USA, 2021; pp. 321–370. [CrossRef]
7. Smith, C.L.; Cowley, S. The Path to Fusion Power. *Philos. Trans. A Math. Phys. Eng. Sci.* **2010**, *368*, 1091. [CrossRef] [PubMed]

8. Dream of Unlimited, Clean Nuclear Fusion Energy within Reach | Research and Innovation. Available online: https://ec.europa.eu/research-and-innovation/en/horizon-magazine/dream-unlimited-clean-nuclear-fusion-energy-within-reach (accessed on 23 July 2023).
9. Carter, T.; Baalrud, S.; Betti, R.; Ellis, T.; Foster, J.; Geddes, C.; Gleason, A.; Holland, C.; Humrickhouse, P.; Kessel, C.; et al. *Powering the Future: Fusion and Plasmas*; US Department of Energy (USDOE): Loa Alamos, NM, USA, 2018.
10. EU Energy Outlook 2050—How Will Europe Evolve over the Next 30 Years?—Energy BrainBlog. Available online: https://blog.energybrainpool.com/en/eu-energy-outlook-2050-how-will-europe-evolve-over-the-next-30-years-3/ (accessed on 28 June 2023).
11. Renewable Energy on the Rise: 37% of EU's Electricity—Products Eurostat News—Eurostat. Available online: https://ec.europa.eu/eurostat/web/products-eurostat-news/-/ddn-20220126-1 (accessed on 28 June 2023).
12. Forbes Home. Solar. Available online: https://www.forbes.com/home-improvement/solar/ (accessed on 23 July 2023).
13. How Much Energy Does a Solar Farm Produce? [Solar Farms Explained]. Available online: https://solarenergyhackers.com/how-much-energy-does-a-solar-farm-produce/ (accessed on 23 July 2023).
14. U.S. Energy Information Administration (EIA). Frequently Asked Questions (FAQs). Available online: https://www.eia.gov/tools/faqs/faq.php?id=104&t=3 (accessed on 23 July 2023).
15. Pearce-Higgins, J.W.; Stephen, L.; Douse, A.; Langston, R.H.W. Greater Impacts of Wind Farms on Bird Populations during Construction than Subsequent Operation: Results of a Multi-Site and Multi-Species Analysis. *J. Appl. Ecol.* **2012**, *49*, 386–394. [CrossRef]
16. Kjeld, A.; Bjarnadottir, H.J.; Olafsdottir, R. Life Cycle Assessment of the Theistareykir Geothermal Power Plant in Iceland. *Geothermics* **2022**, *105*, 102530. [CrossRef]
17. Whole Building Design Guide. Biomass for Electricity Generation | WBDG. Available online: https://www.wbdg.org/resources/biomass-electricity-generation (accessed on 23 July 2023).
18. Fachagentur Nachwachsende Rohstoffe eV Agency for Renewable Resources. *Bioenergy in Germany Facts and Figures 2020*; Fachagentur Nachwachsende Rohstoffe eV Agency for Renewable Resources: Gülzow-Prüzen, Germany, 2020.
19. Tidal Energy: Can It Be Used to Generate Electricity. Available online: https://justenergy.com/blog/tidal-energy-electricity/ (accessed on 23 July 2023).
20. Hallidays. How Much Energy Does Hydropower Produce Each Year. Available online: https://www.hallidayshydropower.com/how-much-energy-hydropower/ (accessed on 23 July 2023).
21. IEA. Hydropower. Available online: https://www.iea.org/energy-system/renewables/hydropower (accessed on 23 July 2023).
22. Global Offshore Wind Capacity Factor 2021 | Statista. Available online: https://www.statista.com/statistics/1368679/global-offshore-wind-capacity-factor/ (accessed on 23 July 2023).
23. Agency, I.R.E. *Renewable Power Generation Costs in 2019*; International Renewable Energy Agency (IRENA): Abu Dhabi, United Arab Emirates, 2020; ISBN 978-92-9260-244-4.
24. IEA. Executive Summary—The Role of Critical Minerals in Clean Energy Transitions—Analysis. Available online: https://www.iea.org/reports/the-role-of-critical-minerals-in-clean-energy-transitions/executive-summary (accessed on 23 July 2023).
25. Watari, T.; Nansai, K.; Nakajima, K. Review of Critical Metal Dynamics to 2050 for 48 Elements. *Resour. Conserv. Recycl.* **2020**, *155*, 104669. [CrossRef]
26. Zepf, V.; Simmons, J.; Reller, A.; Ashfield, M.; Rennie, C. *Materials Critical to the Energy Industry An Introduction*, 2nd ed.; BP p.l.c.: London, UK, 2014.
27. McKinsey. The Raw-Materials Challenge: How the Metals and Mining Sector Will Be at the Core of Enabling the Energy Transition. Available online: https://www.mckinsey.com/industries/metals-and-mining/our-insights/the-raw-materials-challenge-how-the-metals-and-mining-sector-will-be-at-the-core-of-enabling-the-energy-transition (accessed on 23 July 2023).
28. Fu, M.; Ma, X.; Zhao, K.; Li, X.; Su, D. High-Entropy Materials for Energy-Related Applications. *iScience* **2021**, *24*, 102177. [CrossRef]
29. Xin, Y.; Li, S.; Qian, Y.; Zhu, W.; Yuan, H.; Jiang, P.; Guo, R.; Wang, L. High-Entropy Alloys as a Platform for Catalysis: Progress, Challenges, and Opportunities. *ACS Catal.* **2020**, *10*, 11280–11306. [CrossRef]
30. Allen, T.; Busby, J.; Meyer, M.; Petti, D. Materials Challenges for Nuclear Systems. *Mater. Today* **2010**, *13*, 14–23. [CrossRef]
31. Odette, R.G.; Zinkle, S.J. (Eds.) *Structural Alloys for Nuclear Energy Applications*; Elsevier: Amsterdam, The Netherlands, 2019. Available online: https://books.google.de/books?hl=en&lr=&id=KAF0AwAAQBAJ&oi=fnd&pg=PP1&dq=alloys+in+nuclear+energy&ots=kPDtxJjGm_&sig=0_gOE-NqXXv-PV27O1LfuvFqJBM&redir_esc=y#v=onepage&q=alloys%20in%20nuclear%20energy&f=false (accessed on 3 July 2023).
32. Advanced Nuclear Reactors 101. Available online: https://www.rff.org/publications/explainers/advanced-nuclear-reactors-101/ (accessed on 23 July 2023).
33. IAEA. *Advanced Large Water Cooled Reactors. A Supplement to: IAEA Advanced Reactors Information System (ARIS) 2020 Edition*; IAEA: Vienna, Austria, 2020.
34. Tian, W. Grand Challenges in Advanced Nuclear Reactor Design. *Front. Nucl. Eng.* **2022**, *1*, 1000754. [CrossRef]
35. Xiao, C.; Gulfam, R. Opinion on Ocean Thermal Energy Conversion (OTEC). *Front. Energy Res.* **2023**, *11*, 1115695. [CrossRef]
36. Elahee, K.; Jugoo, S. Ocean Thermal Energy for Air-Conditioning: Case Study of a Green Data Center. *Energy Sources Part A Recovery Util. Environ. Eff.* **2013**, *35*, 679–684. [CrossRef]

37. Hunt, J.D.; Zakeri, B.; Nascimento, A.; Garnier, B.; Pereira, M.G.; Bellezoni, R.A.; de Assis Brasil Weber, N.; Schneider, P.S.; Machado, P.P.B.; Ramos, D.S. High Velocity Seawater Air-Conditioning with Thermal Energy Storage and Its Operation with Intermittent Renewable Energies. *Energy Effic.* **2020**, *13*, 1825–1840. [CrossRef]
38. Etemadi, A.; Emami, Y.; AsefAfshar, O.; Emdadi, A. Electricity Generation by the Tidal Barrages. *Energy Procedia* **2011**, *12*, 928–935. [CrossRef]
39. Ringwood, J.V.; Faedo, N. Tidal Barrage Operational Optimisation Using Wave Energy Control Techniques. *IFAC-PapersOnLine* **2022**, *55*, 148–153. [CrossRef]
40. Walker, S.R.J.; Thies, P.R. A Life Cycle Assessment Comparison of Materials for a Tidal Stream Turbine Blade. *Appl. Energy* **2022**, *309*, 118353. [CrossRef]
41. Zheng, J.; Dai, P.; Zhang, J. Tidal Stream Energy in China. *Procedia Eng.* **2015**, *116*, 880–887. [CrossRef]
42. Radfar, S.; Panahi, R.; Javaherchi, T.; Filom, S.; Mazyaki, A.R. A Comprehensive Insight into Tidal Stream Energy Farms in Iran. *Renew. Sustain. Energy Rev.* **2017**, *79*, 323–338. [CrossRef]
43. Blunden, L.S.; Bahaj, A.S. Tidal Energy Resource Assessment for Tidal Stream Generators. *Proc. Inst. Mech. Eng. Part A J. Power Energy* **2007**, *221*, 137–146. [CrossRef]
44. Watson, S.; Moro, A.; Reis, V.; Baniotopoulos, C.; Barth, S.; Bartoli, G.; Bauer, F.; Boelman, E.; Bosse, D.; Cherubini, A.; et al. Future Emerging Technologies in the Wind Power Sector: A European Perspective. *Renew. Sustain. Energy Rev.* **2019**, *113*, 109270. [CrossRef]
45. Majidi, A.G.; Bingölbali, B.; Akpınar, A.; Rusu, E. Wave Power Performance of Wave Energy Converters at High-Energy Areas of a Semi-Enclosed Sea. *Energy* **2021**, *220*, 119705. [CrossRef]
46. Langhamer, O.; Haikonen, K.; Sundberg, J. Wave Power—Sustainable Energy or Environmentally Costly? A Review with Special Emphasis on Linear Wave Energy Converters. *Renew. Sustain. Energy Rev.* **2010**, *14*, 1329–1335. [CrossRef]
47. Clément, A.; McCullen, P.; Falcão, A.; Fiorentino, A.; Gardner, F.; Hammarlund, K.; Lemonis, G.; Lewis, T.; Nielsen, K.; Petroncini, S.; et al. Wave Energy in Europe: Current Status and Perspectives. *Renew. Sustain. Energy Rev.* **2002**, *6*, 405–431. [CrossRef]
48. Rusu, L. The Wave and Wind Power Potential in the Western Black Sea. *Renew. Energy* **2019**, *139*, 1146–1158. [CrossRef]
49. Rahman, A.; Farrok, O.; Haque, M.M. Environmental Impact of Renewable Energy Source Based Electrical Power Plants: Solar, Wind, Hydroelectric, Biomass, Geothermal, Tidal, Ocean, and Osmotic. *Renew. Sustain. Energy Rev.* **2022**, *161*, 112279. [CrossRef]
50. Zhang, Z.; Wen, L.; Jiang, L. Nanofluidics for Osmotic Energy Conversion. *Nat. Rev. Mater.* **2021**, *6*, 622–639. [CrossRef]
51. Xin, W.; Zhang, Z.; Huang, X.; Hu, Y.; Zhou, T.; Zhu, C.; Kong, X.Y.; Jiang, L.; Wen, L. High-Performance Silk-Based Hybrid Membranes Employed for Osmotic Energy Conversion. *Nat. Commun.* **2019**, *10*, 3876. [CrossRef]
52. Wang, Q.; Gao, X.; Zhang, Y.; He, Z.; Ji, Z.; Wang, X.; Gao, C. Hybrid RED/ED System: Simultaneous Osmotic Energy Recovery and Desalination of High-Salinity Wastewater. *Desalination* **2017**, *405*, 59–67. [CrossRef]
53. Han, G.; Zhang, S.; Li, X.; Chung, T.S. Progress in Pressure Retarded Osmosis (PRO) Membranes for Osmotic Power Generation. *Prog. Polym. Sci.* **2015**, *51*, 1–27. [CrossRef]
54. Kim, J.; Jeong, K.; Park, M.J.; Shon, H.K.; Kim, J.H. Recent Advances in Osmotic Energy Generation via Pressure-Retarded Osmosis (PRO): A Review. *Energies* **2015**, *8*, 11821–11845. [CrossRef]
55. Llamosas, C.; Sovacool, B.K. The Future of Hydropower? A Systematic Review of the Drivers, Benefits and Governance Dynamics of Transboundary Dams. *Renew. Sustain. Energy Rev.* **2021**, *137*, 110495. [CrossRef]
56. Kumar, R.; Singal, S.K. Penstock Material Selection in Small Hydropower Plants Using MADM Methods. *Renew. Sustain. Energy Rev.* **2015**, *52*, 240–255. [CrossRef]
57. Gemechu, E.; Kumar, A. A Review of How Life Cycle Assessment Has Been Used to Assess the Environmental Impacts of Hydropower Energy. *Renew. Sustain. Energy Rev.* **2022**, *167*, 112684. [CrossRef]
58. Borkowski, D.; Cholewa, D.; Korzeń, A. Run-of-the-River Hydro-PV Battery Hybrid System as an Energy Supplier for Local Loads. *Energies* **2021**, *14*, 5160. [CrossRef]
59. Venus, T.E.; Hinzmann, M.; Bakken, T.H.; Gerdes, H.; Godinho, F.N.; Hansen, B.; Pinheiro, A.; Sauer, J. The Public's Perception of Run-of-the-River Hydropower across Europe. *Energy Policy* **2020**, *140*, 111422. [CrossRef]
60. François, B.; Hingray, B.; Raynaud, D.; Borga, M.; Creutin, J.D. Increasing Climate-Related-Energy Penetration by Integrating Run-of-the River Hydropower to Wind/Solar Mix. *Renew. Energy* **2016**, *87*, 686–696. [CrossRef]
61. Douglas, T.; Broomhall, P.; Orr, C. *Run-of-River Hydropower in BC A Citizen's Guide to Understanding Approvals, Impacts and Sustainability of Independent Power Projects*; British Columbia Ministry of Environment: Coquitlam, BC, Canada, 2007.
62. Ramadan, A.; Nawar, M.A.A.; Mohamed, M.H. Performance Evaluation of a Drag Hydro Kinetic Turbine for Rivers Current Energy Extraction—A Case Study. *Ocean Eng.* **2020**, *195*, 106699. [CrossRef]
63. Badrul Salleh, M.; Kamaruddin, N.M.; Mohamed-Kassim, Z. Savonius Hydrokinetic Turbines for a Sustainable River-Based Energy Extraction: A Review of the Technology and Potential Applications in Malaysia. *Sustain. Energy Technol. Assess.* **2019**, *36*, 100554. [CrossRef]
64. EduRev. Which One of the Following Turbines Is Used in under Water Powerstations? (a) Pelton Turbine (b) Deriaz Turbine (c) Tubular Turbined (d) Turgo-Impulse Turbine. Correct Answer Is Option "C". Can You Explain This Answer? | EduRev Mechanical Engineering Question. Available online: https://edurev.in/question/1587343/Which-one-of-the-following-turbines-is-used-in-under-water-powerstations-a-Pelton-turbineb-Deriaz-tu (accessed on 24 July 2023).

65. Farr, H.; Ruttenberg, B.; Walter, R.K.; Wang, Y.H.; White, C. Potential Environmental Effects of Deepwater Floating Offshore Wind Energy Facilities. *Ocean Coast. Manag.* **2021**, *207*, 105611. [CrossRef]
66. Quaranta, E.; Davies, P. Emerging and Innovative Materials for Hydropower Engineering Applications: Turbines, Bearings, Sealing, Dams and Waterways, and Ocean Power. *Engineering* **2022**, *8*, 148–158. [CrossRef]
67. Tong, C. Introduction to Materials for Advanced Energy Systems. *MRS Bull.* **2020**, *45*, 317. [CrossRef]
68. Quaranta, E. Estimation of the Permanent Weight Load of Water Wheels for Civil Engineering and Hydropower Applications and Dataset Collection. *Sustain. Energy Technol. Assess.* **2020**, *40*, 100776. [CrossRef]
69. Hoffer, A.E.; Tapia, J.A.; Petrov, I.; Pyrhönen, J. Design of a Stainless Core Submersible Permanent Magnet Generator for Tidal Energy. In Proceedings of the IECON 2019-45th Annual Conference of the IEEE Industrial Electronics Society, Lisbon, Portugal, 14–17 October 2019; pp. 1010–1015. [CrossRef]
70. Rodiouchkina, M.; Lindsjö, H.; Berglund, K.; Hardell, J. Effect of Stroke Length on Friction and Wear of Self-Lubricating Polymer Composites during Dry Sliding against Stainless Steel at High Contact Pressures. *Wear* **2022**, *502–503*, 204393. [CrossRef]
71. Arun, K.; Kumar, K.M.; Karthikeyan, K.M.B.; Mohanasutan, S. Analysis on Influence of Bucket Angle of Pelton Wheel Turbine for Its Structural Integrity Using Aluminium Alloy (A390), Austenitic Stainless Steel (CF20), Grey Cast Iron (325) and Martensitic Stainless Steel (410). *Mater. Today Proc.* **2022**, *62*, 1045–1053. [CrossRef]
72. Musabikha, S.; Pratikno, H.; Utama, I.K.A.P.; Mukhtasor. Material Selection for Vertical Axis Tidal Current Turbine Using Multiple Attribute Decision Making (MADM). *IOP Conf. Ser. Mater. Sci. Eng.* **2021**, *1158*, 012001. [CrossRef]
73. Salter, S.H.; Taylor, J.R.M.; Caldwell, N.J. Power Conversion Mechanisms for Wave Energy. *Proc. Inst. Mech. Eng. Part M J. Eng. Marit. Environ.* **2002**, *216*, 1–27. [CrossRef]
74. Kofoed, J.P.; Frigaard, P.; Friis-Madsen, E.; Sørensen, H.C. Prototype Testing of the Wave Energy Converter Wave Dragon. *Renew. Energy* **2006**, *31*, 181–189. [CrossRef]
75. Jiang, X.; Overman, N.; Canfield, N.; Ross, K. Friction Stir Processing of Dual Certified 304/304L Austenitic Stainless Steel for Improved Cavitation Erosion Resistance. *Appl. Surf. Sci.* **2019**, *471*, 387–393. [CrossRef]
76. Suwanit, W.; Gheewala, S.H. Life Cycle Assessment of Mini-Hydropower Plants in Thailand. *Int. J. Life Cycle Assess.* **2011**, *16*, 849–858. [CrossRef]
77. Azevedo, C.R.F.; Cescon, T. Failure Analysis of Aluminum Cable Steel Reinforced (ACSR) Conductor of the Transmission Line Crossing the Paraná River. *Eng. Fail. Anal.* **2002**, *9*, 645–664. [CrossRef]
78. Ujwala, M.M.; Chaithanya, M.P.; Chowdary, K.; Naik, M.L.S. Design and Analysis of Low Head, Light Weight Kaplan Turbine Blade. *Int. Ref. J. Eng. Sci. IRJES* **2017**, *6*, 17–25.
79. Marangoni, P.R.D.; Robl, D.; Berton, M.A.C.; Garcia, C.M.; Bozza, A.; Porsani, M.V.; Dalzoto, P.D.R.; Vicente, V.A.; Pimentel, I.C. Occurrence of Sulphate Reducing Bacteria (SRB) Associated with Biocorrosion on Metallic Surfaces in a Hydroelectric Power Station in Ibirama (SC)—Brazil. *Braz. Arch. Biol. Technol.* **2013**, *56*, 801–809. [CrossRef]
80. Linhardt, P. Unusual Corrosion of Nickel-Aluminium Bronze in a Hydroelectric Power Plant. *Mater. Corros.* **2015**, *66*, 1536–1541. [CrossRef]
81. Ebrahimi, A. *Advances in Modelling and Control of Wind and Hydrogenerators Edited*, 1st ed.; Ebrahimi, A., Ed.; IntechOpen: London, UK, 2020.
82. Suopajärvi, H.; Umeki, K.; Mousa, E.; Hedayati, A.; Romar, H.; Kemppainen, A.; Wang, C.; Phounglamcheik, A.; Tuomikoski, S.; Norberg, N.; et al. Use of Biomass in Integrated Steelmaking—Status Quo, Future Needs and Comparison to Other Low-CO2 Steel Production Technologies. *Appl. Energy* **2018**, *213*, 384–407. [CrossRef]
83. Ropital, F. Current and Future Corrosion Challenges for a Reliable and Sustainable Development of the Chemical, Refinery, and Petrochemical Industries. *Mater. Corros.* **2009**, *60*, 495–500. [CrossRef]
84. Mousa, E.; Wang, C.; Riesbeck, J.; Larsson, M. Biomass Applications in Iron and Steel Industry: An Overview of Challenges and Opportunities. *Renew. Sustain. Energy Rev.* **2016**, *65*, 1247–1266. [CrossRef]
85. ORNL. Degradation of Structural Alloys In Biomass-Derived Pyrolysis Oil. Available online: https://www.ornl.gov/publication/degradation-structural-alloys-biomass-derived-pyrolysis-oil (accessed on 12 July 2023).
86. Giudicianni, P.; Gargiulo, V.; Grottola, C.M.; Alfè, M.; Ferreiro, A.I.; Mendes, M.A.A.; Fagnano, M.; Ragucci, R. Inherent Metal Elements in Biomass Pyrolysis: A Review. *Energy Fuels* **2021**, *35*, 5407–5478. [CrossRef]
87. Biomass Energy. Available online: https://education.nationalgeographic.org/resource/biomass-energy/ (accessed on 12 July 2023).
88. Miandad, R.; Rehan, M.; Barakat, M.A.; Aburiazaiza, A.S.; Khan, H.; Ismail, I.M.I.; Dhavamani, J.; Gardy, J.; Hassanpour, A.; Nizami, A.S. Catalytic Pyrolysis of Plastic Waste: Moving toward Pyrolysis Based Biorefineries. *Front. Energy Res.* **2019**, *7*, 27. [CrossRef]
89. Wei, L.; Wang, S.; Liu, G.; Hao, W.; Liang, K.; Yang, X.; Diao, W. Corrosion Behavior of High-Cr-Ni Materials in Biomass Incineration Atmospheres. *ACS Omega* **2022**, *7*, 21546–21553. [CrossRef] [PubMed]
90. Berlanga, C.; Ruiz, J.A. Study of Corrosion in a Biomass Boiler. *J. Chem.* **2013**, *2013*, 272090. [CrossRef]
91. Perego, P.; Fabiano, B.; Pastorino, R.; Randi, G. Microbiological Corrosion in Aerobic and Anaerobic Waste Purification Plants: Safety and Efficiency Problems. *Bioprocess Eng.* **1997**, *17*, 103–109. [CrossRef]

92. Miryalkar, P.; Chavitlo, S.; Tandekar, N.; Valleti, K. Improving the Abrasive Wear Resistance of Biomass Briquetting Machine Components Using Cathodic Arc Physical Vapor Deposition Coatings: A Comparative Study. *J. Vac. Sci. Technol. A Vac. Surf. Film.* **2021**, *39*, 63404. [CrossRef]
93. Bojanowska, M.; Chmiel, J.; Sozańska, M.; Chmiela, B.; Grudzień, J.; Halska, J. Issues of Corrosion and Degradation under Dusty Deposits of Energy Biomass. *Energies* **2021**, *14*, 534. [CrossRef]
94. Calmunger, M.; Wärner, H.; Chai, G.; Segersäll, M. Thermomechanical Fatigue of Heat Resistant Austenitic Alloys. *Procedia Struct. Integr.* **2023**, *43*, 130–135. [CrossRef]
95. Wärner, H.; Chai, G.; Moverare, J.; Calmunger, M. High Temperature Fatigue of Aged Heavy Section Austenitic Stainless Steels. *Materials* **2021**, *15*, 84. [CrossRef] [PubMed]
96. Wärner, H.; Calmunger, M.; Chai, G.; Johansson, S.; Moverare, J. Thermomechanical Fatigue Behaviour of Aged Heat Resistant Austenitic Alloys. *Int. J. Fatigue* **2019**, *127*, 509–521. [CrossRef]
97. Jun, J.; Warrington, G.L.; Keiser, J.R.; Connatser, R.M.; Sulejmanovic, D.; Brady, M.P.; Kass, M.D. Corrosion of Ferrous Structural Alloys in Biomass Derived Fuels and Organic Acids. *Energy Fuels* **2021**, *35*, 12175–12186. [CrossRef]
98. Jun, J.; Frith, M.G.; Connatser, R.M.; Keiser, J.R.; Brady, M.P.; Lewis, S. Corrosion Susceptibility of Cr-Mo Steels and Ferritic Stainless Steels in Biomass-Derived Pyrolysis Oil Constituents. *Energy Fuels* **2020**, *34*, 6220–6228. [CrossRef]
99. Vinnes, M.K.; Worth, N.A.; Segalini, A.; Hearst, R.J. The Flow in the Induction and Entrance Regions of Lab-Scale Wind Farms. *Wind Energy* **2023**, *26*, 1049–1065. [CrossRef]
100. Wind Energy. Available online: https://www.irena.org/Energy-Transition/Technology/Wind-energy (accessed on 19 July 2023).
101. NREL. Wind Energy Basics. Available online: https://www.nrel.gov/research/re-wind.html (accessed on 19 July 2023).
102. National Grid Group. Onshore vs Offshore Wind Energy: What's the Difference? Available online: https://www.nationalgrid.com/stories/energy-explained/onshore-vs-offshore-wind-energy (accessed on 19 July 2023).
103. Greco, A.; Sheng, S.; Keller, J.; Erdemir, A. Material Wear and Fatigue in Wind Turbine Systems. *Wear* **2013**, *302*, 1583–1591. [CrossRef]
104. Reddy, S.S.P.; Suresh, R.; Hanamantraygouda, M.B.; Shivakumar, B.P. Use of Composite Materials and Hybrid Composites in Wind Turbine Blades. *Mater. Today Proc.* **2021**, *46*, 2827–2830. [CrossRef]
105. Worldsteel.Org. Energy. Available online: https://worldsteel.org/steel-topics/steel-markets/energy/ (accessed on 16 July 2023).
106. Khalfallah, M.G.; Koliub, A.M. Effect of Dust on the Performance of Wind Turbines. *Desalination* **2007**, *209*, 209–220. [CrossRef]
107. German Energy Solutions. Solar Thermal Energy. Available online: https://www.german-energy-solutions.de/GES/Redaktion/EN/Text-Collections/EnergySolutions/EnergyGeneration/solar-thermal-energy.html (accessed on 23 July 2023).
108. Kannan, N.; Vakeesan, D. Solar Energy for Future World:—A Review. *Renew. Sustain. Energy Rev.* **2016**, *62*, 1092–1105. [CrossRef]
109. Department of Energy. How Does Solar Work? Available online: https://www.energy.gov/eere/solar/how-does-solar-work (accessed on 19 July 2023).
110. Negi, C.; Kandwal, P.; Rawat, J.; Sharma, M.; Sharma, H.; Dalapati, G.; Dwivedi, C. Carbon-Doped Titanium Dioxide Nanoparticles for Visible Light Driven Photocatalytic Activity. *Appl. Surf. Sci.* **2021**, *554*, 149553. [CrossRef]
111. Yang, X.; Wang, D. Photocatalysis: From Fundamental Principles to Materials and Applications. *ACS Appl. Energy Mater.* **2018**, *1*, 6657–6693. [CrossRef]
112. Hosseini, S.E.; Wahid, M.A. Hydrogen from Solar Energy, a Clean Energy Carrier from a Sustainable Source of Energy. *Int. J. Energy Res.* **2020**, *44*, 4110–4131. [CrossRef]
113. Guillot, S.; Faik, A.; Rakhmatullin, A.; Lambert, J.; Veron, E.; Echegut, P.; Bessada, C.; Calvet, N.; Py, X. Corrosion Effects between Molten Salts and Thermal Storage Material for Concentrated Solar Power Plants. *Appl. Energy* **2012**, *94*, 174–181. [CrossRef]
114. Walczak, M.; Pineda, F.; Fernández, Á.G.; Mata-Torres, C.; Escobar, R.A. Materials Corrosion for Thermal Energy Storage Systems in Concentrated Solar Power Plants. *Renew. Sustain. Energy Rev.* **2018**, *86*, 22–44. [CrossRef]
115. González-Gómez, P.A.; Rodríguez-Sánchez, M.R.; Laporte-Azcué, M.; Santana, D. Calculating Molten-Salt Central-Receiver Lifetime under Creep-Fatigue Damage. *Sol. Energy* **2021**, *213*, 180–197. [CrossRef]
116. Rabelo, M.; Zahid, M.A.; Khokhar, M.Q.; Sim, K.; Oh, H.; Cho, E.C.; Yi, J. Mechanical Fatigue Life Analysis of Solar Panels under Cyclic Load Conditions for Design Improvement. *J. Braz. Soc. Mech. Sci. Eng.* **2022**, *44*, 87. [CrossRef]
117. Galiullin, T.; Gobereit, B.; Naumenko, D.; Buck, R.; Amsbeck, L.; Neises-von Puttkamer, M.; Quadakkers, W.J. High Temperature Oxidation and Erosion of Candidate Materials for Particle Receivers of Concentrated Solar Power Tower Systems. *Sol. Energy* **2019**, *188*, 883–889. [CrossRef]
118. Ali, H.M. Phase Change Materials Based Thermal Energy Storage for Solar Energy Systems. *J. Build. Eng.* **2022**, *56*, 104731. [CrossRef]
119. Ma, T.; Yang, C.; Guo, W.; Lin, H.; Zhang, F.; Liu, H.; Zhao, L.; Zhang, Y.; Wang, Y.; Cui, Y.; et al. Flexible Pt3Ni-S-Deposited Teflon Membrane with High Surface Mechanical Properties for Efficient Solar-Driven Strong Acidic/Alkaline Water Evaporation. *ACS Appl. Mater. Interfaces* **2020**, *12*, 27140–27149. [CrossRef] [PubMed]
120. Li, F.; Li, N.; Wang, S.; Qiao, L.; Yu, L.; Murto, P.; Xu, X.; Li, F.; Li, N.; Wang, S.; et al. Self-Repairing and Damage-Tolerant Hydrogels for Efficient Solar-Powered Water Purification and Desalination. *Adv. Funct. Mater.* **2021**, *31*, 2104464. [CrossRef]
121. Rojas-Morín, A.; Flores-Salgado, Y.; Alvarez-Brito, O.; Jaramillo-Mora, J.; Barba-Pingarrón, A. Thermal Analysis Using Induction and Concentrated Solar Radiation for the Heating of Metals. *Results Eng.* **2022**, *14*, 1000431. [CrossRef]

122. Department of Energy. Geothermal Basics. Available online: https://www.energy.gov/eere/geothermal/geothermal-basics (accessed on 19 July 2023).
123. Wayback Machine. Available online: https://web.archive.org/web/20120217184740/http://geoheat.oit.edu/bulletin/bull28-3/art2.pdf (accessed on 19 July 2023).
124. Geothermal Energy. Available online: https://education.nationalgeographic.org/resource/geothermal-energy/ (accessed on 19 July 2023).
125. Vacquier, V. A Theory of the Origin of the Earth's Internal Heat. *Tectonophysics* **1998**, *291*, 1–7. [CrossRef]
126. Zarrouk, S.J.; Moon, H. Efficiency of Geothermal Power Plants: A Worldwide Review. *Geothermics* **2014**, *51*, 142–153. [CrossRef]
127. Tomarov, G.V.; Borzenko, V.I.; Shipkov, A.A. Application of Hydrogen–Oxygen Steam Generators for Secondary Flash Steam Superheating at Geothermal Power Plants. *Therm. Eng.* **2021**, *68*, 45–53. [CrossRef]
128. Farsi, A.; Rosen, M.A. Comparison of Thermodynamic Performances in Three Geothermal Power Plants Using Flash Steam. *ASME Open J. Eng.* **2022**, *1*, 011016. [CrossRef]
129. Wu, Y.; Li, P. The Potential of Coupled Carbon Storage and Geothermal Extraction in a CO_2-Enhanced Geothermal System: A Review. *Geotherm. Energy* **2020**, *8*, 19. [CrossRef]
130. Kumari, W.G.P.; Ranjith, P.G. Sustainable Development of Enhanced Geothermal Systems Based on Geotechnical Research—A Review. *Earth Sci. Rev.* **2019**, *199*, 102955. [CrossRef]
131. Nasruddin, N.; Dwi Saputra, I.; Mentari, T.; Bardow, A.; Marcelina, O.; Berlin, S. Exergy, Exergoeconomic, and Exergoenvironmental Optimization of the Geothermal Binary Cycle Power Plant at Ampallas, West Sulawesi, Indonesia. *Therm. Sci. Eng. Prog.* **2020**, *19*, 100625. [CrossRef]
132. Duggal, R.; Rayudu, R.; Hinkley, J.; Burnell, J.; Wieland, C.; Keim, M. A Comprehensive Review of Energy Extraction from Low-Temperature Geothermal Resources in Hydrocarbon Fields. *Renew. Sustain. Energy Rev.* **2022**, *154*, 111865. [CrossRef]
133. Van Nimwegen, D.; Van 't Westende, J.; Shoeibi-Omrani, P.; Dinkelman, D.; Peters, E. Sustainability of Geothermal Energy: Handling Co-Produced Gas. In Proceedings of the 3rd EAGE Global Energy Transition, GET 2022, The Hague, The Netherlands, 7–9 November 2022; Volume 2022, pp. 51–55. [CrossRef]
134. Nash, S.S. Offshore Co-Produced Critical Minerals and Geothermal Energy Generation. In Proceedings of the Offshore Technology Conference, Houston, TX, USA, 2–5 May 2022. [CrossRef]
135. Maddah, S.; Goodarzi, M.; Safaei, M.R. Comparative Study of the Performance of Air and Geothermal Sources of Heat Pumps Cycle Operating with Various Refrigerants and Vapor Injection. *Alex. Eng. J.* **2020**, *59*, 4037–4047. [CrossRef]
136. Farzanehkhameneh, P.; Soltani, M.; Moradi Kashkooli, F.; Ziabasharhagh, M. Optimization and Energy-Economic Assessment of a Geothermal Heat Pump System. *Renew. Sustain. Energy Rev.* **2020**, *133*, 110282. [CrossRef]
137. Mahmoud, M.; Ramadan, M.; Pullen, K.; Abdelkareem, M.A.; Wilberforce, T.; Olabi, A.G.; Naher, S. A Review of Grout Materials in Geothermal Energy Applications. *Int. J. Thermofluids* **2021**, *10*, 100070. [CrossRef]
138. Kaya, T.; Hoşhan, P.; Jeotermal Mühendislik, O.; ve Ticaret AŞAnkara, S.; Araştırma Merkezi, T. Corrosion and Material Selection for Geothermal Systems. In Proceedings of the World Geothermal Congress, Antalya, Turkey, 24–29 April 2005; pp. 24–29.
139. Kittel, J.; Ropital, F.; Grosjean, F.; Joshi, G. Evaluation of the Interactions Between Hydrogen and Steel in Geothermal Conditions with H2S. In Proceedings of the World Geothermal Congress, Antalya, Turkey, 24–29 April 2005.
140. Brownlie, F.; Hodgkiess, T.; Pearson, A.; Galloway, A.M. A Study on the Erosion-Corrosion Behaviour of Engineering Materials Used in the Geothermal Industry. *Wear* **2021**, *477*, 203821. [CrossRef]
141. Steel, Q.; Wang, P.; Qiu, B.; Chen, A.; Fink, C.G.; Turner, W.D.; Paul, G.T.; Wolf, M.; Pfennig, A. Failure of Standard Duplex Stainless Steel X2CrNiMoN22-5-3 under Corrosion Fatigue in Geothermal Environment. *IOP Conf. Ser. Mater. Sci. Eng.* **2020**, *894*, 012015. [CrossRef]
142. Tayactac, R.G.; Basilia, B. Corrosion in the Geothermal Systems: A Review of Corrosion Resistance Alloy (CRA) Weld Overlay Cladding Applications. *IOP Conf. Ser. Earth Environ. Sci.* **2022**, *1008*, 012018. [CrossRef]
143. Jasper, S.; Gradzki, D.P.; Bracke, R.; Hussong, J.; Petermann, M.; Lindken, R. Nozzle Cavitation and Rock Erosion Experiments Reveal Insight into the Jet Drilling Process. *Chem. Ing. Tech.* **2021**, *93*, 1610–1618. [CrossRef]
144. Phi, T.; Elgaddafi, R.; Al Ramadan, M.; Fahd, K.; Ahmed, R.; Teodoriu, C. Well Integrity Issues: Extreme High-Pressure High-Temperature Wells and Geothermal Wells a Review. In Proceedings of the Society of Petroleum Engineers—SPE Thermal Well Integrity and Design Symposium 2019, TWID 2019, Banff, AB, Canada, 19–21 November 2019. [CrossRef]
145. Boakye, G.O.; Kovalov, D.; Thorhallsson, A.I.; Karlsdottir, S.N.; Oppong Boakye, G.; Thórhallsson, A.Í.; Karlsdóttir, S.N.; Motoiu, V. Friction and Wear Behaviour of Surface Coatings for Geothermal Applications. In Proceedings of the World Geothermal Congress, Reykjavik, Iceland, 24–27 October 2021.
146. Bates, M.; Valderrama, B.; Bickford, E.; Chan, V.; Tian, L.; Programs, L.; Shah, J.; Wagner, J. *Pathways to Commercial Liftoff: Advanced Nuclear*; US Department of Energy: Washington, DC, USA, 2023.
147. Energy Options Network. *An Energy Innovation Reform Project Report Prepared by the Energy Options Network What Will Advanced Nuclear Power Plants Cost? A Standardized Cost Analysis of Advanced Nuclear Technologies in Commercial Development*; Energy Options Network: New York, NY, USA, 2018.
148. Claverton Group. Owning and Operating Costs of Waste and Biomass Power Plants. Available online: https://claverton-energy.com/owning-and-operating-costs-of-waste-and-biomass-power-plants.html (accessed on 19 July 2023).

149. International Renewable Energy Agency. *Renewable Energy Technologies: Cost Analysis Series Biomass for Power Generation Acknowledgement*; International Renewable Energy Agency: Abu Dhabi, United Arab Emirates, 2012.
150. Blakers, A.; Stocks, M.; Lu, B.; Cheng, C. A Review of Pumped Hydro Energy Storage. *Prog. Energy* **2021**, *3*, 022003. [CrossRef]
151. ETSAP. *Giorgio Hydropower*; Energy Technology Systems Analysis Programme: Paris, France, 2010.
152. Whole Building Design Guide (WBDG). Geothermal Electric Technology. Available online: https://www.wbdg.org/resources/geothermal-electric-technology (accessed on 19 July 2023).
153. LinkedIn. Cost of Geothermal Energy. Available online: https://www.linkedin.com/pulse/cost-geothermal-energy-abdelilah-soni/ (accessed on 19 July 2023).
154. Carroll, J.; McDonald, A.; McMillan, D. Failure Rate, Repair Time and Unscheduled O&M Cost Analysis of Offshore Wind Turbines. *Wind Energy* **2016**, *19*, 1107–1119. [CrossRef]
155. Deb, D.; Brahmbhatt, N.L. Review of Yield Increase of Solar Panels through Soiling Prevention, and a Proposed Water-Free Automated Cleaning Solution. *Renew. Sustain. Energy Rev.* **2018**, *82*, 3306–3313. [CrossRef]
156. Sabzi, M.; Mousavi Anijdan, S.H.; Eivani, A.R.; Park, N.; Jafarian, H.R. The Effect of Pulse Current Changes in PCGTAW on Microstructural Evolution, Drastic Improvement in Mechanical Properties, and Fracture Mode of Dissimilar Welded Joint of AISI 316L-AISI 310S Stainless Steels. *Mater. Sci. Eng. A* **2021**, *823*, 141700. [CrossRef]
157. Tan, J.; Zhang, Z.; Zheng, H.; Wang, X.; Gao, J.; Wu, X.; Han, E.H.; Yang, S.; Huang, P. Corrosion Fatigue Model of Austenitic Stainless Steels Used in Pressurized Water Reactor Nuclear Power Plants. *J. Nucl. Mater.* **2020**, *541*, 152407. [CrossRef]
158. Jo, B.; Okamoto, K.; Kasahara, N. Creep Buckling of 304 Stainless-Steel Tubes Subjected to External Pressure for Nuclear Power Plant Applications. *Metals* **2019**, *9*, 536. [CrossRef]
159. Sadawy, M.M.; El Shazly, R.M. Nuclear Radiation Shielding Effectiveness and Corrosion Behavior of Some Steel Alloys for Nuclear Reactor Systems. *Def. Technol.* **2019**, *15*, 621–628. [CrossRef]
160. Deng, P.; Peng, Q.; Han, E.H.; Ke, W.; Sun, C. Proton Irradiation Assisted Localized Corrosion and Stress Corrosion Cracking in 304 Nuclear Grade Stainless Steel in Simulated Primary PWR Water. *J. Mater. Sci. Technol.* **2021**, *65*, 61–71. [CrossRef]
161. Macdonald, D.D.; Engelhardt, G.R.; Petrov, A. A Critical Review of Radiolysis Issues in Water-Cooled Fission and Fusion Reactors: Part I, Assessment of Radiolysis Models. *Corros. Mater. Degrad.* **2022**, *3*, 470–535. [CrossRef]
162. Chen, X.; Cheng, G.; Hou, Y.; Li, J. Oxide-Inclusion Evolution in the Steelmaking Process of 304L Stainless Steel for Nuclear Power. *Metals* **2019**, *9*, 257. [CrossRef]
163. Yeh, C.P.; Tsai, K.C.; Huang, J.Y. Effects of Relative Humidity on Crevice Corrosion Behavior of 304L Stainless-Steel Nuclear Material in a Chloride Environment. *Metals* **2019**, *9*, 1185. [CrossRef]
164. Yeom, H.; Dabney, T.; Pocquette, N.; Ross, K.; Pfefferkorn, F.E.; Sridharan, K. Cold Spray Deposition of 304L Stainless Steel to Mitigate Chloride-Induced Stress Corrosion Cracking in Canisters for Used Nuclear Fuel Storage. *J. Nucl. Mater.* **2020**, *538*, 152254. [CrossRef]
165. Guo, X.; Liu, Z.; Li, L.; Cheng, J.; Su, H.; Zhang, L. Revealing the Long-Term Oxidation and Carburization Mechanism of 310S SS and Alloy 800H Exposed to Supercritical Carbon Dioxide. *Mater. Charact.* **2022**, *183*, 111603. [CrossRef]
166. Scott, P.M.; Combrade, P. General Corrosion and Stress Corrosion Cracking of Alloy 600 in Light Water Reactor Primary Coolants. *J. Nucl. Mater.* **2019**, *524*, 340–375. [CrossRef]
167. Ahn, T.M. Long-Term Initiation Time for Stress-Corrosion Cracking of Alloy 600 with Implications in Stainless Steel: Review and Analysis for Nuclear Application. *Prog. Nucl. Energy* **2021**, *137*, 103760. [CrossRef]
168. Chakrabarti, C.K.; Kumar, N.; Mishra, R.K.; Bhattacharya, S.; Sengupta, P.; Kaushik, C.P. Palladium Telluride within Nuclear Waste Containing Borosilicate Glass. *Prog. Nucl. Energy* **2022**, *148*, 104236. [CrossRef]
169. Zhou, L.; Dai, J.; Li, Y.; Dai, X.; Xie, C.; Li, L.; Chen, L. Research Progress of Steels for Nuclear Reactor Pressure Vessels. *Materials* **2022**, *15*, 8761. [CrossRef]
170. Bandaru, S.V.R.; Villanueva, W.; Thakre, S.; Bechta, S. Multi-Nozzle Spray Cooling of a Reactor Pressure Vessel Steel Plate for the Application of Ex-Vessel Cooling. *Nucl. Eng. Des.* **2021**, *375*, 111101. [CrossRef]
171. Gao, Z.; Lu, C.; He, Y.; Liu, R.; He, H.; Wang, W.; Zheng, W.; Yang, J. Influence of Phase Transformation on the Creep Deformation Mechanism of SA508 Gr.3 Steel for Nuclear Reactor Pressure Vessels. *J. Nucl. Mater.* **2019**, *519*, 292–301. [CrossRef]
172. Hong, S.; Hyun, S.M.; Kim, J.M.; Lee, Y.S.; Kim, M.C. Effect of Mo and V Addition on Microstructure and Mechanical Properties of SA508 Gr.1A Steel for Pipeline in Nuclear Power Plants. *Met. Mater. Trans. A Phys. Met. Mater. Sci.* **2022**, *53*, 1499–1511. [CrossRef]
173. Carter, M.; Gasparrini, C.; Douglas, J.O.; Riddle, N.; Edwards, L.; Bagot, P.A.J.; Hardie, C.D.; Wenman, M.R.; Moody, M.P. On the Influence of Microstructure on the Neutron Irradiation Response of HIPed SA508 Steel for Nuclear Applications. *J. Nucl. Mater.* **2022**, *559*, 153435. [CrossRef]
174. Ma, X.; She, M.; Zhang, W.; Song, L.; Qiu, S.; Liu, X.; Zhang, R. Microstructure Characterization of Reactor Pressure Vessel Steel A508-3 Irradiated by Heavy Ion. *J. Phys. Conf. Ser.* **2021**, *2133*, 012015. [CrossRef]
175. Vértesy, G.; Gasparics, A.; Szenthe, I.; Gillemot, F.; Uytdenhouwen, I. Inspection of Reactor Steel Degradation by Magnetic Adaptive Testing. *Materials* **2019**, *12*, 963. [CrossRef] [PubMed]
176. Loktionov, V.; Lyubashevskaya, I.; Terentyev, E. The Regularities of Creep Deformation and Failure of the VVER's Pressure Vessel Steel 15Kh2NMFA-A in Air and Argon at Temperature Range 500–900 °C. *Nucl. Mater. Energy* **2021**, *28*, 101019. [CrossRef]

177. Voevodyn, V.; Mytrofanov, S.; Hozhenko, S.V.; Vasylenko, R.L.; Krainyuk, E.; Bazhukov, V.; Palii; Mel'nyk, P.E. Nonmetallic Inclusions in 08Kh18N10T Steel as the Cause of Initiation of Defects in Heat-Exchange Tubes of Steam Generators of Nuclear Power Plants. *Mater. Sci.* **2019**, *55*, 152–159. [CrossRef]
178. Fan, Y.; Liu, T.G.; Xin, L.; Han, Y.M.; Lu, Y.H.; Shoji, T. Thermal Aging Behaviors of Duplex Stainless Steels Used in Nuclear Power Plant: A Review. *J. Nucl. Mater.* **2021**, *544*, 152693. [CrossRef]
179. Chen, Y.; Yang, B.; Zhou, Y.; Wu, Y.; Zhu, H. Evaluation of Pitting Corrosion in Duplex Stainless Steel Fe20Cr9Ni for Nuclear Power Application. *Acta Mater.* **2020**, *197*, 172–183. [CrossRef]
180. Rieth, M.; Dürrschnabel, M.; Bonk, S.; Jäntsch, U.; Bergfeldt, T.; Hoffmann, J.; Antusch, S.; Simondon, E.; Klimenkov, M.; Bonnekoh, C.; et al. Technological Processes for Steel Applications in Nuclear Fusion. *Appl. Sci.* **2021**, *11*, 11653. [CrossRef]
181. Duerrschnabel, M.; Jäntsch, U.; Gaisin, R.; Rieth, M. Microstructural Insights into EUROFER97 Batch 3 Steels. *Nucl. Mater. Energy* **2023**, *35*, 101445. [CrossRef]
182. Klimenkov, M.; Jäntsch, U.; Rieth, M.; Möslang, A. Correlation of Microstructural and Mechanical Properties of Neutron Irradiated EUROFER97 Steel. *J. Nucl. Mater.* **2020**, *538*, 152231. [CrossRef]
183. Cabet, C.; Dalle, F.; Gaganidze, E.; Henry, J.; Tanigawa, H. Ferritic-Martensitic Steels for Fission and Fusion Applications. *J. Nucl. Mater.* **2019**, *523*, 510–537. [CrossRef]
184. Snead, L.L.; Hoelzer, D.T.; Rieth, M.; Nemith, A.A.N. Refractory Alloys: Vanadium, Niobium, Molybdenum, Tungsten. In *Structural Alloys for Nuclear Energy Applications*; Elsevier: Amsterdam, The Netherlands, 2019; pp. 585–640. [CrossRef]
185. Fu, T.; Cui, K.; Zhang, Y.; Wang, J.; Shen, F.; Yu, L.; Qie, J.; Zhang, X. Oxidation Protection of Tungsten Alloys for Nuclear Fusion Applications: A Comprehensive Review. *J. Alloys Compd.* **2021**, *884*, 161057. [CrossRef]
186. Terentyev, D.; Rieth, M.; Pintsuk, G.; Riesch, J.; Von Müller, A.; Antusch, S.; Mergia, K.; Gaganidze, E.; Schneider, H.C.; Wirtz, M.; et al. Recent Progress in the Assessment of Irradiation Effects for In-Vessel Fusion Materials: Tungsten and Copper Alloys. *Nucl. Fusion* **2022**, *62*, 026045. [CrossRef]
187. Alzahrani, J.S.; Alrowaili, Z.A.; Eke, C.; Mahmoud, Z.M.M.; Mutuwong, C.; Al-Buriahi, M.S. Nuclear Shielding Properties of Ni-, Fe-, Pb-, and W-Based Alloys. *Radiat. Phys. Chem.* **2022**, *195*, 110090. [CrossRef]
188. Alzahrani, J.S.; Alrowaili, Z.A.; Saleh, H.H.; Hammoud, A.; Alomairy, S.; Sriwunkum, C.; Al-Buriahi, M.S. Synthesis, Physical and Nuclear Shielding Properties of Novel Pb–Al Alloys. *Prog. Nucl. Energy* **2021**, *142*, 103992. [CrossRef]
189. Pickering, E.J.; Carruthers, A.W.; Barron, P.J.; Middleburgh, S.C.; Armstrong, D.E.J.; Gandy, A.S. High-Entropy Alloys for Advanced Nuclear Applications. *Entropy* **2021**, *23*, 98. [CrossRef]
190. Xin, Z.; Ma, Y.; Chen, Y.; Wang, B.; Xiao, H.; Duan, Y. Fusion-Bonding Performance of Short and Continuous Carbon Fiber Synergistic Reinforced Composites Using Fused Filament Fabrication. *Compos. B Eng.* **2023**, *248*, 110370. [CrossRef]
191. Jiang, X.; Overman, N.; Smith, C.; Ross, K. Microstructure, Hardness and Cavitation Erosion Resistance of Different Cold Spray Coatings on Stainless Steel 316 for Hydropower Applications. *Mater. Today Commun.* **2020**, *25*, 101305. [CrossRef]
192. Kumar, M.; Singh Sidhu, H.; Singh Sidhu, B. Influence of Ultra-Low Temperature Treatments on the Slurry Erosion Performance of Stainless Steel-316L. In *Advances in Mechanical and Materials Technology*; Lecture Notes in Mechanical Engineering; Springer: Singapore, 2022; pp. 1273–1286. [CrossRef]
193. Pitsikoulis, S.A.; Tekumalla, S.; Sharma, A.; Wong, W.L.E.; Turkmen, S.; Liu, P. Cavitation Hydrodynamic Performance of 3-D Printed Highly Skewed Stainless Steel Tidal Turbine Rotors. *Energies* **2023**, *16*, 3675. [CrossRef]
194. Jung, H.J.; Jabbar, H.; Song, Y.; Sung, T.H. Hybrid-Type (D33 and D31) Impact-Based Piezoelectric Hydroelectric Energy Harvester for Watt-Level Electrical Devices. *Sens. Actuators A Phys.* **2016**, *245*, 40–48. [CrossRef]
195. Gavriilidis, I.; Huang, Y. Finite Element Analysis of Tidal Turbine Blade Subjected to Impact Loads from Sea Animals. *Energies* **2021**, *14*, 7208. [CrossRef]
196. Saenz-Betancourt, C.C.; Rodríguez, S.A.; Coronado, J.J. Effect of Boronising on the Cavitation Erosion Resistance of Stainless Steel Used for Hydromachinery Applications. *Wear* **2022**, *498–499*, 204330. [CrossRef]
197. Azevedo, C.R.F.; Magarotto, D.; Araújo, J.A.; Ferreira, J.L.A. Bending Fatigue of Stainless Steel Shear Pins Belonging to a Hydroelectric Plant. *Eng. Fail. Anal.* **2009**, *16*, 1126–1140. [CrossRef]
198. Sankar, S.; Nataraj, M.; Raja, V.P. Failure Analysis of Shear Pins in Wind Turbine Generator. *Eng. Fail. Anal.* **2011**, *18*, 325–339. [CrossRef]
199. Zhang, Q.L.; Hu, L.; Hu, C.; Wu, H.G. Low-Cycle Fatigue Issue of Steel Spiral Cases in Pumped-Storage Power Plants under China's and US's Design Philosophies: A Comparative Numerical Case Study. *Int. J. Press. Vessel. Pip.* **2019**, *172*, 134–144. [CrossRef]
200. Moreira, D.C.; Furtado, H.C.; Buarque, J.S.; Cardoso, B.R.; Merlin, B.; Moreira, D.D.C. Failure Analysis of AISI 410 Stainless-Steel Piston Rod in Spillway Floodgate. *Eng. Fail. Anal.* **2019**, *97*, 506–517. [CrossRef]
201. Maekai, I.A.; Harmain, G.A.; Zehab-ud-Din; Masoodi, J.H. Resistance to Slurry Erosion by WC-10Co-4Cr and Cr3C2 − 25(Ni20Cr) Coatings Deposited by HVOF Stainless Steel F6NM. *Int. J. Refract. Met. Hard Mater.* **2022**, *105*, 105830. [CrossRef]
202. Chauhan, A.K.; Goel, D.B.; Prakash, S. Erosion Behaviour of Hydro Turbine Steels. *Bull. Mater. Sci.* **2008**, *31*, 115–120. [CrossRef]
203. Kumar, S.; Chaudhari, G.P.; Nath, S.K.; Basu, B. Effect of Preheat Temperature on Weldability of Martensitic Stainless Steel. *Mater. Manuf. Process.* **2012**, *27*, 1382–1386. [CrossRef]

204. Rückle, D.; Schellenberg, G.; Ottens, W.; Leibing, B.; Locquenghien, F. Corrosion Fatigue of CrNi13-4 Martensitic Stainless Steel for Francis Runners in Dependency of Water Quality. In Proceedings of the Eurocorr 2022, Berlin, Germany, 28 August–1 September 2022.
205. Kevin, P.S.; Tiwari, A.; Seman, S.; Mohamed, S.A.B.; Jayaganthan, R. Erosion-Corrosion Protection Due to Cr_3C_2-NiCr Cermet Coating on Stainless Steel. *Coatings* **2020**, *10*, 1042. [CrossRef]
206. Titus, J.; Ayalur, B. Design and Fabrication of In-Line Turbine for Pico Hydro Energy Recovery in Treated Sewage Water Distribution Line. *Energy Procedia* **2019**, *156*, 133–138. [CrossRef]
207. Turnock, S.R.; Muller, G.; Nicholls-Lee, R.F.; Denchfield, S.; Hindley, S.; Shelmerdine, R.; Stevens, S. Development of a Floating Tidal Energy System Suitable for Use in Shallow Water. In Proceedings of the 7th European Wave and Tidal Energy Conference, Porto, Portugal, 11–13 September 2007.
208. Keiser, J. *Materials Degradation of Biomass-Derived Oils*; U.S. Department of Energy: Washington, DC, USA, 2021.
209. Special Piping Materials. Stainless Steel and Renewable Energy. Available online: https://specialpipingmaterials.com/stainless-steel-and-renewable-energy/ (accessed on 16 July 2023).
210. Guerrero, G.R.; Sevilla, L.; Soriano, C. Laser and Pyrolysis Removal of Fluorinated Ethylene Propylene Thin Layers Applied on EN AW-5251 Aluminium Substrates. *Appl. Surf. Sci.* **2015**, *353*, 686–692. [CrossRef]
211. Divandari, M.; Jamali, V.; Shabestari, S.G. Effect of Strips Size and Coating Thickness on Fluidity of A356 Aluminium Alloy in Lost Foam Casting Process. *Int. J. Cast Met. Res.* **2013**, *23*, 23–29. [CrossRef]
212. Jun, J.; Su, Y.F.; Keiser, J.R.; Wade, J.E.; Kass, M.D.; Ferrell, J.R.; Christensen, E.; Olarte, M.V.; Sulejmanovic, D. Corrosion Compatibility of Stainless Steels and Nickel in Pyrolysis Biomass-Derived Oil at Elevated Storage Temperatures. *Sustainability* **2022**, *15*, 22. [CrossRef]
213. Diaz, F.; Wang, Y.; Moorthy, T.; Friedrich, B. Degradation Mechanism of Nickel-Cobalt-Aluminum (NCA) Cathode Material from Spent Lithium-Ion Batteries in Microwave-Assisted Pyrolysis. *Metals* **2018**, *8*, 565. [CrossRef]
214. Brady, M.P.; Leonard, D.N.; Keiser, J.R.; Cakmak, E.; Whitmer, L.E. Degradation of Components After Exposure in a Biomass Pyrolysis System. *Corrosion* **2019**, *75*, 1136–1145. [CrossRef]
215. Braun, M. Statistical Analysis of Sub-Zero Temperature Effects on Fatigue Strength of Welded Joints. *Weld. World* **2022**, *66*, 159–172. [CrossRef]
216. Braun, M.; Scheffer, R.; Fricke, W.; Ehlers, S. Fatigue Strength of Fillet-Welded Joints at Subzero Temperatures. *Fatigue Fract. Eng. Mater. Struct.* **2020**, *43*, 403–416. [CrossRef]
217. Igwemezie, V.; Mehmanparast, A.; Kolios, A. Materials Selection for XL Wind Turbine Support Structures: A Corrosion-Fatigue Perspective. *Mar. Struct.* **2018**, *61*, 381–397. [CrossRef]
218. Momber, A. Corrosion and Corrosion Protection of Support Structures for Offshore Wind Energy Devices (OWEA). *Mater. Corros.* **2011**, *62*, 391–404. [CrossRef]
219. Martin, F.; Schröter, F. Stahllösungen Für Offshore-Windkraftanlagen. *Stahlbau* **2005**, *74*, 435–442. [CrossRef]
220. Ferro, P.; Berto, F.; Tang, K. UNS S32205 Duplex Stainless Steel SED-Critical Radius Characterization. *Metall. Ital.* **2020**, 29–38.
221. Sroka, M.; Zielinski, A.; Puszczalo, T.; Sówka, K.; Hadzima, B. Structure of 22Cr25NiWCoCu Austenitic Stainless Steel After Ageing. *Arch. Metall. Mater.* **2022**, *67*, 175–180. [CrossRef]
222. Ermakova, A.; Mehmanparast, A.; Ganguly, S. A Review of Present Status and Challenges of Using Additive Manufacturing Technology for Offshore Wind Applications. *Procedia Struct. Integr.* **2019**, *17*, 29–36. [CrossRef]
223. Nakagawa, T.; Matsushima, H.; Ueda, M.; Ito, H. Corrosion Behavior of SUS 304L Steel in Concentrated K_2CO_3 Solution. *ECS Meet. Abstr.* **2020**, *MA2020-02*, 1228. [CrossRef]
224. Röhsler, A.; Sobol, O.; Hänninen, H.; Böllinghaus, T. In-Situ ToF-SIMS Analyses of Deuterium Re-Distribution in Austenitic Steel AISI 304L under Mechanical Load. *Sci. Rep.* **2020**, *10*, 10545. [CrossRef]
225. Yang, D.; Huang, Y.; Peng, P.; Liu, X.; Zhang, B. Passivation Behavior and Corrosion Resistance of 904L Austenitic Stainless Steels in Static Seawater. *Int. J. Electrochem. Sci.* **2019**, *14*, 6133–6146. [CrossRef]
226. Sanni, O.; Popoola, A.P.I.; Fayomi, O.S.I. Electrochemical Analysis of Austenitic Stainless Steel (Type 904) Corrosion Using Egg Shell Powder in Sulphuric Acid Solution. *Energy Procedia* **2019**, *157*, 619–625. [CrossRef]
227. Evans, M.H. White Structure Flaking (WSF) in Wind Turbine Gearbox Bearings: Effects of 'Butterflies' and White Etching Cracks (WECs). *Mater. Sci. Technol.* **2013**, *28*, 3–22. [CrossRef]
228. Gooch, D.J. Materials Issues in Renewable Energy Power Generation. *Int. Mater. Rev.* **2013**, *45*, 1–14. [CrossRef]
229. Chen, Y.; Cai, G.; Bai, R.; Ke, S.; Wang, W.; Chen, X.; Li, P.; Zhang, Y.; Gao, L.; Nie, S.; et al. Spatiotemporally Explicit Pathway and Material-Energy-Emission Nexus of Offshore Wind Energy Development in China up to the Year 2060. *Resour. Conserv. Recycl.* **2022**, *183*, 106349. [CrossRef]
230. Lloberas-Valls, J.; Benveniste Perez, G.; Gomis-Bellmunt, O. Life-Cycle Assessment Comparison between 15-MW Second-Generation High Temperature Superconductor and Permanent-Magnet Direct-Drive Synchronous Generators for Offshore Wind Energy Applications. *IEEE Trans. Appl. Supercond.* **2015**, *25*, 5204209. [CrossRef]
231. Kumar, A.; Dwivedi, A.; Paliwal, V.; Patil, P.P. Free Vibration Analysis of Al 2024 Wind Turbine Blade Designed for Uttarakhand Region Based on FEA. *Procedia Technol.* **2014**, *14*, 336–347. [CrossRef]
232. Siddiqui, R.A.; Abdullah, H.A.; Al-Belushi, K.R. Influence of Aging Parameters on the Mechanical Properties of 6063 Aluminium Alloy. *J. Mater. Process. Technol.* **2000**, *102*, 234–240. [CrossRef]

233. Wang, H.; Lamichhane, T.N.; Paranthaman, M.P. Review of Additive Manufacturing of Permanent Magnets for Electrical Machines: A Prospective on Wind Turbine. *Mater. Today Phys.* **2022**, *24*, 100675. [CrossRef]
234. Lüddecke, F.; Rücker, W.; Seidel, M.; Assheuer, J. Tragverhalten von Stahlgussbauteilen in Offshore-Windenergie-Anlagen Unter Vorwiegend Ruhender Und Nicht Ruhender Beanspruchung. *Stahlbau* **2008**, *77*, 639–646. [CrossRef]
235. Bleicher, C.; Niewiadomski, J.; Kansy, A.; Kaufmann, H. High-Silicon Nodular Cast Iron for Lightweight Optimized Wind Energy Components. *Int. J. Offshore Polar Eng.* **2022**, *32*, 201–209. [CrossRef]
236. Soleimani Dorcheh, A.; Durham, R.N.; Galetz, M.C. Corrosion Behavior of Stainless and Low-Chromium Steels and IN625 in Molten Nitrate Salts at 600 °C. *Sol. Energy Mater. Sol. Cells* **2016**, *144*, 109–116. [CrossRef]
237. Li, H.; Feng, X.; Wang, X.; Yang, X.; Tang, J.; Gong, J. Impact of Temperature on Corrosion Behavior of Austenitic Stainless Steels in Solar Salt for CSP Application: An Electrochemical Study. *Sol. Energy Mater. Sol. Cells* **2022**, *239*, 111661. [CrossRef]
238. Pantelis, D.I.; Griniari, A.; Sarafoglou, C. Surface Alloying of Pre-Deposited Molybdenum-Based Powder on 304L Stainless Steel Using Concentrated Solar Energy. *Sol. Energy Mater. Sol. Cells* **2005**, *89*, 1–11. [CrossRef]
239. Wang, M.; Zeng, S.; Zhang, H.; Zhu, M.; Lei, C.; Li, B. Corrosion Behaviors of 316 Stainless Steel and Inconel 625 Alloy in Chloride Molten Salts for Solar Energy Storage. *High. Temp. Mater. Process.* **2020**, *39*, 340–350. [CrossRef]
240. Yin, Y.; Rumman, R.; Sarvghad, M.; Bell, S.; Ong, T.C.; Jacob, R.; Liu, M.; Flewell-Smith, R.; Sheoran, S.; Severino, J.; et al. Role of Headspace Environment for Phase Change Carbonates on the Corrosion of Stainless Steel 316L: High Temperature Thermal Storage Cycling in Concentrated Solar Power Plants. *Sol. Energy Mater. Sol. Cells* **2023**, *251*, 112170. [CrossRef]
241. Cionea, C.; Abad, M.D.; Aussat, Y.; Frazer, D.; Gubser, A.J.; Hosemann, P. Oxide Scale Formation on 316L and FeCrAl Steels Exposed to Oxygen Controlled Static LBE at Temperatures up to 800 °C. *Sol. Energy Mater. Sol. Cells* **2016**, *144*, 235–246. [CrossRef]
242. Liu, Q.; Qian, J.; Neville, A.; Pessu, F. Solar Thermal Irradiation Cycles and Their Influence on the Corrosion Behaviour of Stainless Steels with Molten Salt Used in Concentrated Solar Power Plants. *Sol. Energy Mater. Sol. Cells* **2023**, *251*, 112141. [CrossRef]
243. Brown-Shaklee, H.J.; Carty, W.; Edwards, D.D. Spectral Selectivity of Composite Enamel Coatings on 321 Stainless Steel. *Sol. Energy Mater. Sol. Cells* **2009**, *93*, 1404–1410. [CrossRef]
244. Sierra, C.; Vázquez, A.J. High Solar Energy Concentration with a Fresnel Lens. *J. Mater. Sci.* **2005**, *40*, 1339–1343. [CrossRef]
245. Mallco, A.; Pineda, F.; Mendoza, M.; Henriquez, M.; Carrasco, C.; Vergara, V.; Fuentealba, E.; Fernandez, A.G. Evaluation of Flow Accelerated Corrosion and Mechanical Performance of Martensitic Steel T91 for a Ternary Mixture of Molten Salts for CSP Plants. *Sol. Energy Mater. Sol. Cells* **2022**, *238*, 111623. [CrossRef]
246. Pineda, F.; Mallco, A.; De Barbieri, F.; Carrasco, C.; Henriquez, M.; Fuentealba, E.; Fernández, Á.G. Corrosion Evaluation by Electrochemical Real-Time Tracking of VM12 Martensitic Steel in a Ternary Molten Salt Mixture with Lithium Nitrates for CSP Plants. *Sol. Energy Mater. Sol. Cells* **2021**, *231*, 111302. [CrossRef]
247. The Amazing Role of High-Temperature Nickel Alloys and Stainless Steels for Concentrated Solar Power. Available online: https://nickelinstitute.org/en/blog/2021/september/the-amazing-role-of-high-temperature-nickel-alloys-and-stainless-steels-for-concentrated-solar-power/ (accessed on 18 July 2023).
248. Grégoire, B.; Oskay, C.; Meißner, T.M.; Galetz, M.C. Corrosion Mechanisms of Ferritic-Martensitic P91 Steel and Inconel 600 Nickel-Based Alloy in Molten Chlorides. Part II: NaCl-KCl-$MgCl_2$ Ternary System. *Sol. Energy Mater. Sol. Cells* **2020**, *216*, 110675. [CrossRef]
249. Balat-Pichelin, M.; Sans, J.L.; Bêche, E.; Charpentier, L.; Ferrière, A.; Chomette, S. Emissivity at High Temperature of Ni-Based Superalloys for the Design of Solar Receivers for Future Tower Power Plants. *Sol. Energy Mater. Sol. Cells* **2021**, *227*, 111066. [CrossRef]
250. Zhu, M.; Yi, H.; Lu, J.; Huang, C.; Zhang, H.; Bo, P.; Huang, J. Corrosion of Ni–Fe Based Alloy in Chloride Molten Salts for Concentrating Solar Power Containing Aluminum as Corrosion Inhibitor. *Sol. Energy Mater. Sol. Cells* **2022**, *241*, 111737. [CrossRef]
251. Peng, Y.; Shinde, P.S.; Reddy, R.G. High-Temperature Corrosion Rate and Diffusion Modelling of Ni-Coated Incoloy 800H Alloy in MgCl2–KCl Heat Transfer Fluid. *Sol. Energy Mater. Sol. Cells* **2022**, *243*, 111767. [CrossRef]
252. Bell, S.; de Bruyn, M.; Steinberg, T.; Will, G. C-276 Nickel Alloy Corrosion in Eutectic Na_2CO_3/NaCl Molten Salt under Isothermal and Thermal Cycling Conditions. *Sol. Energy Mater. Sol. Cells* **2022**, *240*, 111695. [CrossRef]
253. García-Martín, G.; Lasanta, M.I.; Encinas-Sánchez, V.; de Miguel, M.T.; Pérez, F.J. Evaluation of Corrosion Resistance of A516 Steel in a Molten Nitrate Salt Mixture Using a Pilot Plant Facility for Application in CSP Plants. *Sol. Energy Mater. Sol. Cells* **2017**, *161*, 226–231. [CrossRef]
254. Cheng, W.J.; Chen, D.J.; Wang, C.J. High-Temperature Corrosion of Cr–Mo Steel in Molten LiNO3–NaNO3–KNO3 Eutectic Salt for Thermal Energy Storage. *Sol. Energy Mater. Sol. Cells* **2015**, *132*, 563–569. [CrossRef]
255. Sarvghad, M.; Will, G.; Steinberg, T.A. Corrosion of Steel Alloys in Molten NaCl + Na_2SO_4 at 700 °C for Thermal Energy Storage. *Sol. Energy Mater. Sol. Cells* **2018**, *179*, 207–216. [CrossRef]
256. Karalis, D.G.; Pantelis, D.I.; Papazoglou, V.J. On the Investigation of 7075 Aluminum Alloy Welding Using Concentrated Solar Energy. *Sol. Energy Mater. Sol. Cells* **2005**, *86*, 145–163. [CrossRef]
257. Shimizu, Y.; Kawaguchi, T.; Sakai, H.; Dong, K.; Kurniawan, A.; Nomura, T. Al–Ni Alloy-Based Core-Shell Type Microencapsulated Phase Change Material for High Temperature Thermal Energy Utilization. *Sol. Energy Mater. Sol. Cells* **2022**, *246*, 111874. [CrossRef]

258. Sugianto, A.; Tjahjono, B.S.; Mai, L.; Wenham, S.R. Investigation of Unusual Shunting Behavior Due to Phototransistor Effect in N-Type Aluminum-Alloyed Rear Junction Solar Cells. *Sol. Energy Mater. Sol. Cells* **2009**, *93*, 1986–1993. [CrossRef]
259. Krause, J.; Woehl, R.; Rauer, M.; Schmiga, C.; Wilde, J.; Biro, D. Microstructural and Electrical Properties of Different-Sized Aluminum-Alloyed Contacts and Their Layer System on Silicon Surfaces. *Sol. Energy Mater. Sol. Cells* **2011**, *95*, 2151–2160. [CrossRef]
260. Patel, K.; Sadeghilaridjani, M.; Pole, M.; Mukherjee, S. Hot Corrosion Behavior of Refractory High Entropy Alloys in Molten Chloride Salt for Concentrating Solar Power Systems. *Sol. Energy Mater. Sol. Cells* **2021**, *230*, 111222. [CrossRef]
261. He, C.Y.; Gao, X.H.; Dong, M.; Qiu, X.L.; An, J.H.; Guo, H.X.; Liu, G. Further Investigation of a Novel High Entropy Alloy MoNbHfZrTi Based Solar Absorber Coating with Double Antireflective Layers. *Sol. Energy Mater. Sol. Cells* **2020**, *217*, 110709. [CrossRef]
262. Yamada, Y.; Miura, M.; Tajima, K.; Okada, M.; Yoshimura, K. Optical Switching Durability of Switchable Mirrors Based on Magnesium–Yttrium Alloy Thin Films. *Sol. Energy Mater. Sol. Cells* **2013**, *117*, 396–399. [CrossRef]
263. Bao, S.; Tajima, K.; Yamada, Y.; Okada, M.; Yoshimura, K. Magnesium–Titanium Alloy Thin-Film Switchable Mirrors. *Sol. Energy Mater. Sol. Cells* **2008**, *92*, 224–227. [CrossRef]
264. Hot Rocks—Geothermal and the Role of Nickel. Available online: https://nickelinstitute.org/en/blog/2021/august/hot-rocks-geothermal-and-the-role-of-nickel/ (accessed on 18 July 2023).
265. Wang, G.G.; Zhu, L.Q.; Liu, H.C.; Li, W.P. Galvanic Corrosion of Ni–Cu–Al Composite Coating and Its Anti-Fouling Property for Metal Pipeline in Simulated Geothermal Water. *Surf. Coat. Technol.* **2012**, *206*, 3728–3732. [CrossRef]
266. Keserović, A.; Bäßler, R.; Kamah, Y. *Suitability of Alloyed Steels in Highly Acidic Geothermal Environments*; NACE: San Antonio, TX, USA, 2014.
267. Nogara, J.; Zarrouk, S.J. Corrosion in Geothermal Environment Part 2: Metals and Alloys. *Renew. Sustain. Energy Rev.* **2018**, *82*, 1347–1363. [CrossRef]
268. Jalaluddin; Miyara, A.; Tsubaki, K.; Inoue, S.; Yoshida, K. Experimental Study of Several Types of Ground Heat Exchanger Using a Steel Pile Foundation. *Renew. Energy* **2011**, *36*, 764–771. [CrossRef]
269. Faizal, M.; Bouazza, A.; Singh, R.M. Heat Transfer Enhancement of Geothermal Energy Piles. *Renew. Sustain. Energy Rev.* **2016**, *57*, 16–33. [CrossRef]
270. Vitaller, A.V.; Angst, U.M.; Elsener, B. Corrosion Behaviour of L80 Steel Grade in Geothermal Power Plants in Switzerland. *Metals* **2019**, *9*, 331. [CrossRef]
271. AI Technology Inc. Solar Energy Enhancement Protection Coating, Sealant and Adhesive. Available online: https://www.aitechnology.com/products/solar/solar-energy-coating/ (accessed on 23 July 2023).
272. Strom-Forschung De. Protecting Wind Turbines from Corrosion. Available online: https://www.strom-forschung.de/projects/wind-energy/protecting-wind-turbines-from-corrosion/ (accessed on 23 July 2023).
273. Wang, C.; Gao, W.; Liu, N.; Xin, Y.; Liu, X.; Wang, X.; Tian, Y.; Chen, X.; Hou, B. Covalent Organic Framework Decorated TiO_2 Nanotube Arrays for Photoelectrochemical Cathodic Protection of Steel. *Corros. Sci.* **2020**, *176*, 108920. [CrossRef]
274. Angst, U.M. A Critical Review of the Science and Engineering of Cathodic Protection of Steel in Soil and Concrete. *Corrosion* **2019**, *75*, 1420–1433. [CrossRef] [PubMed]
275. Brenna, A.; Beretta, S.; Ormellese, M. AC Corrosion of Carbon Steel under Cathodic Protection Condition: Assessment, Criteria and Mechanism. A Review. *Materials* **2020**, *13*, 2158. [CrossRef] [PubMed]
276. Zhang, R.; Yu, X.; Yang, Q.; Cui, G.; Li, Z. The Role of Graphene in Anti-Corrosion Coatings: A Review. *Constr. Build. Mater.* **2021**, *294*, 123613. [CrossRef]
277. Hussain, A.K.; Seetharamaiah, N.; Pichumani, M.; Chakra, C.S. Research Progress in Organic Zinc Rich Primer Coatings for Cathodic Protection of Metals—A Comprehensive Review. *Prog. Org. Coat.* **2021**, *153*, 106040. [CrossRef]
278. Krieg, R.; Vimalanandan, A.; Rohwerder, M. Corrosion of Zinc and Zn-Mg Alloys with Varying Microstructures and Magnesium Contents. *J. Electrochem. Soc.* **2014**, *161*, C156–C161. [CrossRef]
279. Hausbrand, R.; Stratmann, M.; Rohwerder, M. Corrosion of Zinc–Magnesium Coatings: Mechanism of Paint Delamination. *Corros. Sci.* **2009**, *51*, 2107–2114. [CrossRef]
280. Sun, W.; Wang, N.; Li, J.; Xu, S.; Song, L.; Liu, Y.; Wang, D. Humidity-Resistant Triboelectric Nanogenerator and Its Applications in Wind Energy Harvesting and Self-Powered Cathodic Protection. *Electrochim. Acta* **2021**, *391*, 138994. [CrossRef]
281. Hautfenne, C.; Nardone, S.; De Bruycker, E.; Hautfenne, C. Influence of Heat Treatments and Build Orientation on the Creep Strength of Additive Manufactured IN718 Contact Data. In Proceedings of the 4th International ECCC Conference, Düsseldorf, Germany, 10–14 September 2017.
282. Reisgen, U.; Olschok, S.; Jakobs, S. Laser Beam Welding in Vacuum of Thick Plate Structural Steel. In Proceedings of the ICALEO 2013—32nd International Congress on Applications of Lasers and Electro-Optics, Orlando, FL, USA, 23–27 October 2013; pp. 341–350.
283. Vázquez, A.J.; Rodriguez, G.P.; de Damborenea, J. Surface Treatment of Steels by Solar Energy. *Sol. Energy Mater.* **1991**, *24*, 751–759. [CrossRef]
284. Pisarek, J.; Frączek, T.; Popławski, T.; Szota, M. Practical and Economical Effects of the Use of Screen Meshes for Steel Nitriding Processes with Glow Plasma. *Energies* **2021**, *14*, 3808. [CrossRef]

285. Micallef, C.; Zhuk, Y.; Aria, A.I. Recent Progress in Precision Machining and Surface Finishing of Tungsten Carbide Hard Composite Coatings. *Coatings* **2020**, *10*, 731. [CrossRef]
286. Pan, X.; Shi, Z.; Shi, C.; Ling, T.C.; Li, N. A Review on Concrete Surface Treatment Part I: Types and Mechanisms. *Constr. Build. Mater.* **2017**, *132*, 578–590. [CrossRef]
287. Poulain, R.; Amann, F.; Deya, J.; Bourgon, J.; Delannoy, S.; Prima, F. Short-Time Heat Treatments in Oxygen Strengthened Ti-Zr α Titanium Alloys: A Simple Approach for Optimized Strength-Ductility Trade-Off. *Mater. Lett.* **2022**, *317*, 132114. [CrossRef]
288. Osunbunmi, I.S.; Ajide, O.O.; Oluwole, O.O. Effect of Heat Treatment on the Mechanical and Microstructural Properties of a Low Carbon Steel. In Proceedings of the International Conference of Mechanical Engineering, Energy Technology and Management, IMEETMCON 2018, Ibadan, Nigeria, 4–7 September 2018.
289. Jovičević-Klug, P.; Podgornik, B. Review on the Effect of Deep Cryogenic Treatment of Metallic Materials in Automotive Applications. *Metals* **2020**, *10*, 434. [CrossRef]
290. Baldissera, P.; Delprete, C. Deep Cryogenic Treatment: A Bibliographic Review. *Open Mech. Eng. J.* **2008**, *2*, 32–39. [CrossRef]
291. Vengatesh, M.; Srivignesh, R.; Pradeep, T.; Karthik, N.R. Review on Cryogenic Trearment of Steels. *Int. Res. J. Eng. Technol.* **2016**, *3*, 417–422.
292. Sonar, T.; Lomte, S.; Gogte, C. Cryogenic Treatment of Metal—A Review. *Mater. Today Proc.* **2018**, *5*, 25219–25228. [CrossRef]
293. Jovičević-Klug, P. *Mechanisms and Effect of Deep Cryogenic Treatment on Steel Properties*; Institute of Metals and Technology: Ljubljana, Slovenia, 2022.
294. Workman, K.J.; Pitts, D.W. Method of Treating Brake Pads. U.S. Patent US5447035A, 29 September 1994.
295. Leach, J.M.; Harvey, W.L. Method of Cryogenically Hardening an Insert in an Article. U.S. Patent No. 4,336,077, 3 March 1980.
296. Voorhees, J.E. Process for Treating Materials to Improve Their Structural Characteristics. U.S. Patent No. 4,482,005, 13 November 1984.
297. Yildiz, Y.; Nalbant, M. A Review of Cryogenic Cooling in Machining Processes. *Int. J. Mach. Tools Manuf.* **2008**, *48*, 947–964. [CrossRef]
298. Akincioğlu, S.; Gökkaya, H.; Uygur, İ. A Review of Cryogenic Treatment on Cutting Tools. *Int. J. Adv. Manuf. Technol.* **2015**, *78*, 1609–1627. [CrossRef]
299. Barron, R.F. Cryogenic Treatment of Metals to Improve Wear Resistance. *Cryogenics* **1982**, *22*, 409–413. [CrossRef]
300. Senthilkumar, D.; Rajendran, I. Influence of Shallow and Deep Cryogenic Treatment on Tribological Behavior of En 19 Steel. *J. Iron Steel Res. Int.* **2011**, *18*, 53–59. [CrossRef]
301. Senthilkumar, D.; Rajendran, I.; Pellizzari, M.; Siiriainen, J. Influence of Shallow and Deep Cryogenic Treatment on the Residual State of Stress of 4140 Steel. *J. Mater. Process. Technol.* **2011**, *211*, 396–401. [CrossRef]
302. Senthilkumar, D. Cryogenic Treatment: Shallow and Deep. In *Encyclopedia of Iron, Steel, and Their Alloys*; Totten, G.E., Colas, R., Eds.; Taylor and Francis: New York, NY, USA, 2016; pp. 995–1007. ISBN 9781351254496.
303. Ciski, A.; Nawrocki, P.; Babul, T.; Hradil, D. Multistage Cryogenic Treatment of X153CrMoV12 Cold Work Steel. In Proceedings of the 5th International Conference Recent Trends in Structural Materials, Pilsen, Czech Republic, 14–16 November 2018; Volume 461, pp. 0120121–0120126.
304. Jovičević-Klug, P.; Jovičević-Klug, M.; Thormählen, L.; McCord, J.; Rohwerder, M.; Godec, M.; Podgornik, B. Austenite Reversion Suppression with Deep Cryogenic Treatment: A Novel Pathway towards 3rd Generation Advanced High-Strength Steels. *Mater. Sci. Eng. A* **2023**, *873*, 145033. [CrossRef]
305. Jovičević-Klug, P.; Tegg, L.; Jovičević-Klug, M.; Parmar, R.; Amati, M.; Gregoratti, L.; Almasy, L.; Cairney, J.M.; Podgornik, B. Understanding Carbide Evolution and Surface Chemistry during Deep Cryogenic Treatment in High-Alloyed Ferrous Alloy. *Appl. Surf. Sci.* **2023**, *610*, 155497. [CrossRef]
306. Jovičević-Klug, P.; Puš, G.; Jovičević-Klug, M.; Žužek, B.; Podgornik, B. Influence of Heat Treatment Parameters on Effectiveness of Deep Cryogenic Treatment on Properties of High-Speed Steels. *Mater. Sci. Eng. A* **2022**, *829*, 142157. [CrossRef]
307. Jovičević-Klug, P.; Guštin, A.Z.; Jovičević-Klug, M.; Šetina Batič, B.; Lebar, A.; Podgornik, B. Coupled Role of Alloying and Manufacturing on Deep Cryogenic Treatment Performance on High-Alloyed Ferrous Alloys. *J. Mater. Res. Technol.* **2022**, *18*, 3184–3197. [CrossRef]
308. Jovičević-Klug, P.; Lipovšek, N.; Jovičević-Klug, M.; Mrak, M.; Ekar, J.; Ambrožič, B.; Dražić, G.; Kovač, J.; Podgornik, B. Assessment of Deep Cryogenic Heat-Treatment Impact on the Microstructure and Surface Chemistry of Austenitic Stainless Steel. *Surf. Interfaces* **2022**, *35*, 102456. [CrossRef]
309. Jovičević-Klug, P.; Jovičević-Klug, M.; Sever, T.; Feizpour, D.; Podgornik, B. Impact of Steel Type, Composition and Heat Treatment Parameters on Effectiveness of Deep Cryogenic Treatment. *J. Mater. Res. Technol.* **2021**, *14*, 1007–1020. [CrossRef]
310. Pellizzari, M. Influence of Deep Cryogenic Treatment on the Properties of Conventional and PM High Speed Steels. *Metall. Ital.* **2008**, *100*, 17–22.
311. Senthilkumar, D. Influence of Deep Cryogenic Treatment on Hardness and Toughness of En31 Steel. *Adv. Mater. Process. Technol.* **2019**, *5*, 114–122. [CrossRef]
312. Baldissera, P. Deep Cryogenic Treatment of AISI 302 Stainless Steel: Part I—Hardness and Tensile Properties. *Mater. Des.* **2010**, *31*, 4725–4730. [CrossRef]
313. Amini, K.; Negahbani, M.; Ghayour, H. The Effect of Deep Cryogenic Treatment on Hardness and Wear Behavior of the H13 Tool Steel. *Metall. Ital.* **2015**, *107*, 53–58.

314. Elango, G.; Raghunath, B.K.; Thamizhmaran, K. Effect of Cryogenic Treatment on Microstructure and Micro Hardness of Aluminium (LM25)—SiC Metal Matrix Composite. *J. Eng. Res.* **2014**, *10*, 64–68. [CrossRef]
315. Peng, J.; Zhou, B.; Li, Z.; Huo, D.; Xiong, J.; Zhang, S. Effect of Tempering Process on the Cryogenic Impact Toughness of 13Cr4NiMo Martensitic Stainless Steel. *J. Mater. Res. Technol.* **2023**, *23*, 5618–5630. [CrossRef]
316. Çakir, F.H.; Çelik, O.N. The Effects of Cryogenic Treatment on the Toughness and Tribological Behaviors of Eutectoid Steel. *J. Mech. Sci. Technol.* **2017**, *31*, 3233–3239. [CrossRef]
317. Sola, R.; Giovanardi, R.; Parigi, G.; Veronesi, P. A Novel Method for Fracture Toughness Evaluation of Tool Steels with Post-Tempering Cryogenic Treatment. *Metals* **2017**, *7*, 75. [CrossRef]
318. Nanesa, C.H.; Jahazi, M. Simultaneous Enhancement of Strength and Ductility in Cryogenically Treated AISI D2 Tool Steel. *Mater. Sci. Eng. A* **2014**, *598*, 413–419. [CrossRef]
319. Jovičević-Klug, P.; Jovičević-Klug, M.; Rohwerder, M.; Godec, M.; Podgornik, B. Complex Interdependency of Microstructure, Mechanical Properties, Fatigue Resistance and Residual Stress of Austenitic Stainless Steels AISI 304L. *Materials* **2023**, *16*, 2638. [CrossRef]
320. Weng, Z.; Gu, K.; Wang, K.; Liu, X.; Wang, J. The Reinforcement Role of Deep Cryogenic Treatment on the Strength and Toughness of Alloy Structural Steel. *Mater. Sci. Eng. A* **2020**, *772*, 138698. [CrossRef]
321. Korade, D.; Ramana, K.V.; Jagtap, K. Wear and Fatigue Behaviour of Deep Cryogenically Treated H21 Tool Steel. *Trans. Indian Inst. Met.* **2020**, *73*, 843–851. [CrossRef]
322. Bensely, A.; Shyamala, L.; Harish, S.; Mohan Lal, D.; Nagarajan, G.; Junik, K.; Rajadurai, A. Fatigue Behaviour and Fracture Mechanism of Cryogenically Treated En 353 Steel. *Mater. Des.* **2009**, *30*, 2955–2962. [CrossRef]
323. Jovicevic-Klug, M.; Jovicevic-Klug, P.; McCord, J.; Podgornik, B. Investigation of Microstructural Attributes of Steel Surfaces through Magneto-Optical Kerr Effect. *J. Mater. Res. Technol.* **2021**, *11*, 1245–1259. [CrossRef]
324. Jovičević-Klug, P.; Jovičević-Klug, M.; Podgornik, B. Unravelling the Role of Nitrogen in Surface Chemistry and Oxidation Evolution of Deep Cryogenic Treated High-Alloyed Ferrous Alloy. *Coatings* **2022**, *12*, 213. [CrossRef]
325. Jovičević-Klug, M.; Jovičević-Klug, P.; Kranjec, T.; Podgornik, B. Cross-Effect of Surface Finishing and Deep Cryogenic Treatment on Corrosion Resistance of AISI M35 Steel. *J. Mater. Res. Technol.* **2021**, *14*, 2365–2381. [CrossRef]
326. Jovičević-Klug, P.; Kranjec, T.; Jovičević-Klug, M.; Kosec, T.; Podgornik, B. Influence of the Deep Cryogenic Treatment on AISI 52100 and AISI D3 Steel's Corrosion Resistance. *Materials* **2021**, *14*, 6357. [CrossRef]
327. Senthilkumar, D.; Bracke, J.; Slootsman, N. Corrosion and Elastic Behaviour of Cryogenically Treated En 19 Steel. *Corros. Manag.* **2014**, *117*, 16–21.
328. Wang, W.; Srinivasan, V.; Siva, S.; Albert, B.; Lal, M.; Alfantazi, A. Corrosion Behavior of Deep Cryogenically Treated AISI 420 and AISI 52100 Steel. *Corrosion* **2014**, *70*, 708–720. [CrossRef]
329. Ramesh, S.; Bhuvaneswari, B.; Palani, G.S.; Lal, D.M.; Iyer, N.R. Effects on Corrosion Resistance of Rebar Subjected to Deep Cryogenic Treatment. *J. Mech. Sci. Technol.* **2017**, *31*, 123–132. [CrossRef]
330. Ma, S.; Su, R.; Li, G.; Qu, Y.; Li, R. Effect of Deep Cryogenic Treatment on Corrosion Resistance of AA7075-RRA. *J. Phys. Chem. Solids* **2022**, *167*, 110747. [CrossRef]
331. Su, R.; Ma, S.; Wang, K.; Li, G.; Qu, Y.; Li, R. Effect of Cyclic Deep Cryogenic Treatment on Corrosion Resistance of 7075 Alloy. *Met. Mater. Int.* **2022**, *28*, 862–870. [CrossRef]
332. Garrison, T.C. Process for Improving the Corrosion Resistance of Metals. CN1795278A, 24 May 2004.
333. Gunes, I.; Uzun, M.; Cetin, A.; Aslantas, K.; Cicek, A. Evaluation of Wear Performance of Cryogenically Treated Vanadis 4 Extra Tool Steel. *Kov. Mater.* **2016**, *54*, 195–204. [CrossRef]
334. Koneshlou, M.; Meshinchi, A.K.; Khomamizadeh, F. Effect of Cryogenic Tratment on Microstucture, Mechanical and Wear Behaviors of AISI H13 Hot Work Tool Steel. *Cryogenics* **2011**, *51*, 55–61. [CrossRef]
335. Senthilkumar, D.; Rajendran, I. Optimization of Deep Cryogenic Treatment to Reduce Wear Loss of 4140 Steel. *Mater. Manuf. Process.* **2011**, *27*, 567–572. [CrossRef]
336. Jovičević-Klug, P.; Jenko, M.; Jovičević-Klug, M.; Šetina Batič, B.; Kovač, J.; Podgornik, B. Effect of Deep Cryogenic Treatment on Surface Chemistry and Microstructure of Selected High-Speed Steels. *Appl. Surf. Sci.* **2021**, *548*, 149257. [CrossRef]
337. Cryogenic Treatment Applications Find Potential in the Energy Sector. Available online: https://www.cryogenicsociety.org/index.php?option=com_dailyplanetblog&view=entry&year=2023&month=05&day=02&id=188:cryogenic-treatment-applications-find-potential-in-the-energy-sector (accessed on 20 July 2023).
338. Industrial Heating. Deep Cryogenic Treatment for Marine and Oil-and-Gas Applications. 3 December 2018. Available online: https://www.industrialheating.com/articles/94598-deep-cryogenic-treatment-for-marine-and-oil-and-gas-applications (accessed on 20 July 2023).
339. Darwin, J.D.; Mohan Lal, D.; Nagarajan, G. Optimization of Cryogenic Treatment to Maximize the Wear Resistance of 18% Cr Martensitic Stainless Steel by Taguchi Method. *J. Mater. Process Technol.* **2008**, *195*, 241–247. [CrossRef]
340. Kumar, M.C.; Vijayakumar, P.; Narayan, B. Optimization of Cryogenic Treatment Parameters to Maximise the Tool Wear of HSS Tools by Taguchi Method. *Int. J. Mod. Eng. Res.* **2012**, *2*, 3051–3055.
341. Baloji, D.; Anil, K.; Satyanarayana, K.; Ul Haq, A.; Singh, S.K.; Naik, M.T. Evaluation and Optimization of Material Properties of ASS316L at Sub-Zero Temperature Using Taguchi Robust Design. *Mater. Today Proc.* **2019**, *18*, 4475–4481. [CrossRef]
342. Lance, J.W.; Jones, H.M. Material Treatment by Cryogenic Cooling. U.S. Patent No. 3,891,477, 9 September 1971.

343. Jin, F.; Wu, L.; Xiong, C.; Wei, J.; Wen, X. A Kind of Cryogenic Treating Process of Cast Aluminium Alloy Piston Piece. CN103498117B, 29 September 2013.
344. De Carvalho Eduardo, A.; Atem De Carvalho, R. Special Steels; Cryogenic Process for the Production Thereof; Use of Special Steels in a Saline and/or High-Pressure Environment. WO2014008564A1, 9 July 2013.
345. Jin, F.; Zhou, Z.; Wei, J.; Xiong, C.; Wu, L. High-Speed Steel Cryogenic Treatment Process. CN103525997A, 29 September 2013.
346. Pang, B.; Wang, B.; Zhao, X. High-Efficiency Energy-Saving Apparatus Used for Cryogenic Treatment. CN103589840A, 26 November 2013.
347. Kamody, D.J. Process for the Cryogenic Treatment of Metal Containing Materials. US5875636A, 1 October 1997.
348. Li, Z.; Wang, Y.; Wang, J.; Zhang, Y. Effect of Cryogenic Heat Treatment and Heat Treatment on the Influence of Mechanical, Energy, and Wear Properties of 316L Stainless Steel by Selective Laser Melting. *JOM* **2022**, *74*, 3855–3868. [CrossRef]
349. Prieto, G.; Ipiña, J.E.P.; Tuckart, W.R. Cryogenic Treatments on AISI 420 Stainless Steel: Microstructure and Mechanical Properties. *Mater. Sci. Eng. A* **2014**, *605*, 236–243. [CrossRef]
350. Zhirafar, S.; Rezaeian, A.; Pugh, M. Effect of Cryogenic Treatment on the Mechanical Properties of 4340 Steel. *J. Mater. Process. Technol.* **2007**, *186*, 298–303. [CrossRef]
351. Baldissera, P.; Delprete, C. Effects of Deep Cryogenic Treatment on Static Mechanical Properties of 18NiCrMo5 Carburized Steel. *Mater. Des.* **2009**, *30*, 1435–1440. [CrossRef]
352. Jovičević-Klug, M.; Rezar, R.; Jovičević-Klug, P.; Podgornik, B. Influence of Deep Cryogenic Treatment on Natural and Artificial Aging of Al-Mg-Si Alloy EN AW 6026. *J. Alloys Compd.* **2022**, *899*, 163323. [CrossRef]
353. Nageswara Rao, P.; Jayaganthan, R. Effects of Warm Rolling and Ageing after Cryogenic Rolling on Mechanical Properties and Microstructure of Al 6061 Alloy. *Mater. Des.* **2012**, *39*, 226–233. [CrossRef]
354. Shahsavari, A.; Karimzadeh, F.; Rezaeian, A.; Heydari, H. Significant Increase in Tensile Strength and Hardness in 2024 Aluminum Alloy by Cryogenic Rolling. *Procedia Mater. Sci.* **2015**, *11*, 84–88. [CrossRef]
355. Aamir, A.; Lei, P.; Lixiang, D.; Zengmin, Z. Effects of Deep Cryogenic Treatment, Cryogenic and Annealing Temperatures on Mechanical Properties and Corrosion Resistance of AA5083 Aluminium Alloy. *Int. J. Microstruct. Mater. Prop.* **2016**, *11*, 339–358. [CrossRef]
356. Gu, K.; Zhang, H.; Zhao, B.; Wang, J.; Zhou, Y.; Li, Z. Effect of Cryogenic Treatment and Aging Treatment on the Tensile Properties and Microstructure of Ti-6Al-4V Alloy. *Mater. Sci. Eng. A* **2013**, *584*, 170–176. [CrossRef]
357. Vinothkumar, T.S.; Kandaswamy, D.; Prabhakaran, G.; Rajadurai, A. Effect of Dry Cryogenic Treatment on Vickers Hardness and Wear Resistance of New Martensitic Shape Memory Nickel-Titanium Alloy. *Eur. J. Dent.* **2015**, *9*, 513–517. [CrossRef]
358. Anil Kumar, B.K.; Ananthaprasad, M.G.; Gopalakrishna, K. Action of Cryogenic Chill on Mechanical Properties of Nickel Alloy Metal Matrix Composites. In Proceedings of the International Conference on Advances in Materials and Manufacturing Applications, Bangalore, India, 14–16 July 2016; pp. 1–11.
359. Khedekar, D.; Gogte, C.L. Development of the Cryogenic Processing Cycle for Age Hardenable AA7075 Aluminium Alloy and Optimization of the Process for Surface Quality Using Gray Relational Analysis. *Mater. Today Proc.* **2018**, *5*, 4995–5003. [CrossRef]
360. Yuanchun, H.; Li, Y.; Ren, X.; Xiao, Z. Effect of Deep Cryogenic Treatment on Aging Processes of Al–Mg–Si Alloy. *Phys. Met. Metallogr.* **2019**, *120*, 914–918. [CrossRef]
361. Adin, M.Ş. Performances of Cryo-Treated and Untreated Cutting Tools in Machining of AA7075 Aerospace Aluminium Alloy. *Eur. Mech. Sci.* **2023**, *7*, 70–81. [CrossRef]
362. Vendra, S.S.L.; Goel, S.; Kumar, N.; Jayaganthan, R. A Study on Fracture Toughness and Strain Rate Sensitivity of Severely Deformed Al 6063 Alloys Processed by Multiaxial Forging and Rolling at Cryogenic Temperature. *Mater. Sci. Eng. A* **2017**, *686*, 82–92. [CrossRef]
363. Sonia, P.; Verma, V.; Saxena, K.K.; Kishore, N.; Rana, R.S. Effect of Cryogenic Treatment on Mechanical Properties and Microstructure of Aluminium 6082 Alloy. *Mater. Today Proc.* **2020**, *26*, 2248–2253. [CrossRef]
364. Özbek, N.A.; ÇİÇek, A.; GülesİN, M.; Özbek, O. Application of Deep Cryogenic Treatment to Uncoated Tungsten Carbide Inserts in the Turning of AISI 304 Stainless Steel. *Met. Mater. Trans. A Phys. Met. Mater. Sci.* **2016**, *47*, 6270–6280. [CrossRef]
365. Çiçek, A.; Kıvak, T.; Ekici, E. Optimization of Drilling Parameters Using Taguchi Technique and Response Surface Methodology (RSM) in Drilling of AISI 304 Steel with Cryogenically Treated HSS Drills. *J. Intell. Manuf.* **2015**, *26*, 295–305. [CrossRef]
366. Ramos, L.B.; Simoni, L.; Mielczarski, R.G.; Vega, M.R.O.; Schroeder, R.M.; De Fraga Malfatti, C. Tribocorrosion and Electrochemical Behavior of DIN 1.4110 Martensitic Stainless Steels After Cryogenic Heat Treatment. *Mater. Res.* **2017**, *20*, 460–468. [CrossRef]
367. Ben Fredj, N.; Sidhom, H. Effects of the Cryogenic Cooling on the Fatigue Strength of the AISI 304 Stainless Steel Ground Components. *Cryogenics* **2006**, *46*, 439–448. [CrossRef]
368. Nalbant, M.; Yildiz, Y. Effect of Cryogenic Cooling in Milling Process of AISI 304 Stainless Steel. *Trans. Nonferrous Met. Soc. China* **2011**, *21*, 72–79. [CrossRef]
369. Hong, S.Y.; Broomer, M.; Hong, S.Y.; Broomer, M. Economical and Ecological Cryogenic Machining of AISI 304 Austenitic Stainless Steel. *Clean Technol. Environ. Policy* **2000**, *2*, 157–166. [CrossRef]
370. Dhananchezian, M.; Pradeep Kumar, M.; Sornakumar, T. Cryogenic Turning of AISI 304 Stainless Steel with Modified Tungsten Carbide Tool Inserts. *Mater. Manuf. Process.* **2011**, *26*, 781–785. [CrossRef]
371. Johan Singh, P.; Guha, B.; Achar, D.R.G. Fatigue Life Improvement of AISI 304L Cruciform Welded Joints by Cryogenic Treatment. *Eng. Fail. Anal.* **2003**, *10*, 1–12. [CrossRef]

372. Singh, P.J.; Mannan, S.L.; Jayakumar, T.; Achar, D.R.G. Fatigue Life Extension of Notches in AISI 304L Weldments Using Deep Cryogenic Treatment. *Eng. Fail. Anal.* **2005**, *12*, 263–271. [CrossRef]
373. Oh, D.; Song, S.; Kim, N.; Kim, M. Effect of Cryogenic Temperature on Low-Cycle Fatigue Behavior of AISI 304L Welded Joint. *Metals* **2018**, *8*, 657. [CrossRef]
374. Read, D.T.; Reed, R.P. Fracture and Strength Properties of Selected Austenitic Stainless Steels at Cryogenic Temperatures. *Cryogenics* **1981**, *21*, 415–417. [CrossRef]
375. Manimaran, G.; Pradeep Kumar, M.; Venkatasamy, R. Influence of Cryogenic Cooling on Surface Grinding of Stainless Steel 316. *Cryogenics* **2014**, *59*, 76–83. [CrossRef]
376. Kennedy, F.E.; Ye, Y.; Baker, I.; White, R.R.; Barry, R.L.; Tang, A.Y.; Song, M. Development of a New Cryogenic Tribotester and Its Application to the Study of Cryogenic Wear of AISI 316 Stainless Steel. *Wear* **2022**, *496–497*, 204309. [CrossRef]
377. Bhaskar, L.; Raj, D.S. Evaluation of the Effect of Cryogenic Treatment of HSS Drills at Different Holding Time in Drilling AISI 316-SS. *Eng. Res. Express* **2020**, *2*, 025005. [CrossRef]
378. Norberto López de Lacalle, L.; Gandarias, A.; López de Lacalle, L.N.; Aizpitarte, X.; Lamikiz, A. High Performance Drilling of Austenitic Stainless Steels. *Int. J. Mach. Mach. Mater.* **2008**, *3*, 1–17. [CrossRef]
379. Uhlář, R.; Hlaváč, L.; Gembalová, L.; Jonšta, P.; Zuchnický, O. Abrasive Water Jet Cutting of the Steels Samples Cooled by Liquid Nitrogen. *Appl. Mech. Mater.* **2013**, *308*, 7–12. [CrossRef]
380. Çiçek, A.; Uygur, I.; Kvak, T.; Altan Zbek, N. Machinability of AISI 316 Austenitic Stainless Steel with Cryogenically Treated M35 High-Speed Steel Twist Drills. *J. Manuf. Sci. Eng.* **2012**, *134*, 061003. [CrossRef]
381. Gao, Q.; Jiang, X.; Sun, H.; Zhang, Y.; Fang, Y.; Mo, D.; Li, X. Performance and Microstructure of TC4/Nb/Cu/316L Welded Joints Subjected to Cryogenic Treatment. *Mater. Lett.* **2022**, *321*, 132453. [CrossRef]
382. Sugavaneswaran, M.; Kulkarni, A. Effect of Cryogenic Treatment on the Wear Behavior of Additive Manufactured 316L Stainless Steel. *Tribol. Ind.* **2019**, *41*, 33–42. [CrossRef]
383. Wang, C.; Lin, X.; Wang, L.; Zhang, S.; Huang, W. Cryogenic Mechanical Properties of 316L Stainless Steel Fabricated by Selective Laser Melting. *Mater. Sci. Eng. A* **2021**, *815*, 141317. [CrossRef]
384. Kosaraju, S.; Singh, S.K.; Buddi, T.; Kalluri, A.; Ul Haq, A. Evaluation and Characterisation of ASS316L at Sub-Zero Temperature. *Adv. Mater. Process. Technol.* **2020**, *6*, 445–455. [CrossRef]
385. Kvackaj, T.; Rozsypalova, A.; Kocisko, R.; Bidulska, J.; Petrousek, P.; Vlado, M.; Pokorny, I.; Sas, J.; Weiss, K.P.; Duchek, M.; et al. Influence of Processing Conditions on Properties of AISI 316LN Steel Grade. *J. Mater. Eng. Perform.* **2020**, *29*, 1509–1514. [CrossRef]
386. Salehi, M.; Eskandari, M.; Yeganeh, M. Characterizations of the Microstructure and Texture of 321 Austenitic Stainless Steel After Cryo-Rolling and Annealing Treatments. *J. Mater. Eng. Perform.* **2023**, *32*, 816–834. [CrossRef]
387. Aletdinov, A.; Mironov, S.; Korznikova, G.; Konkova, T.; Zaripova, R.; Myshlyaev, M.; Semiatin, S.L. EBSD Investigation of Microstructure Evolution during Cryogenic Rolling of Type 321 Metastable Austenitic Steel. *Mater. Sci. Eng. A* **2019**, *745*, 460–473. [CrossRef]
388. Aurich, J.C.; Mayer, P.; Kirsch, B.; Eifler, D.; Smaga, M.; Skorupski, R. Characterization of Deformation Induced Surface Hardening during Cryogenic Turning of AISI 347. *CIRP Ann.* **2014**, *63*, 65–68. [CrossRef]
389. Mayer, P.; Skorupski, R.; Smaga, M.; Eifler, D.; Aurich, J.C. Deformation Induced Surface Hardening When Turning Metastable Austenitic Steel AISI 347 with Different Cryogenic Cooling Strategies. *Procedia CIRP* **2014**, *14*, 101–106. [CrossRef]
390. Laksanasittiphan, S.; Tuchinda, K.; Manonukul, A.; Suranuntchai, S. Use of Deep Cryogenic Treatment to Reduce Particle Contamination Induced Problem in Hard Disk Drive. *Key Eng. Mater.* **2017**, *730*, 265–271. [CrossRef]
391. Prieto, G.; Tuckart, W.R. Influence of Cryogenic Treatments on the Wear Behavior of AISI 420 Martensitic Stainless Steel. *J. Mater. Eng. Perform.* **2017**, *26*, 5262–5271. [CrossRef]
392. Ramesh, S.; Bhuvaneshwari, B.; Palani, G.S.; Mohan Lal, D.; Mondal, K.; Gupta, R.K. Enhancing the Corrosion Resistance Performance of Structural Steel via a Novel Deep Cryogenic Treatment Process. *Vacuum* **2019**, *159*, 468–475. [CrossRef]
393. Makalesi, A.; Şenel, S.; Koçar, O.; Kocaman, E.; Özdamar, O.; Bülent, Z.; Üniversitesi, E.; Fakültesi, M.; Bölümü, M.M. AISI 430 Çeliklerin Derin Kroyonejik İşlem Sonrası Mekanik ve Mikroyapısal Özelliklerinin İncelenmesi. *Eur. J. Sci. Technol.* **2021**, *32*, 1000–1005. [CrossRef]
394. ŞİRİN, Ş.; AKINCIOĞLU, S. Investigation of Friction Performance and Surface Integrity of Cryogenically Treated AISI 430 Ferritic Stainless Steel. *Int. Adv. Res. Eng. J.* **2021**, *5*, 194–201. [CrossRef]
395. Yıldız, E.; Altan Özbek, N.; Ankara Hidrolik Mak San Tic Ltd.; Şti, H. Effect of cryogenic treatment and tempering temperature on mechanical and microstructural properties of aisi 431 steel. *Int. J. 3D Print. Technol. Digit. Ind.* **2022**, *6*, 74–82. [CrossRef]
396. Tembwa, E.N. Softening Response of As-Normalized and Cryogenic-Soaked P91 Martensitic Steels p y g P91 Martensitic Steels. Master's Thesis, University of Johannesburg, Johannesburg, South Africa, 2018.
397. Zhao, Z.; Yu, M.; Han, C.; Yang, Z.; Teng, P.; Zhong, J.; Li, S.; Liu, J. Effects of Carbide Evolution on SCC Behaviors of 10Cr13Co13Mo5NiW1VE Martensitic Stainless Steel. Available online: https://papers.ssrn.com/sol3/papers.cfm?abstract_id=4400821 (accessed on 2 October 2023).
398. Zhang, H.; Ji, X.; Ma, D.; Tong, M.; Wang, T.; Xu, B.; Sun, M.; Li, D. Effect of Aging Temperature on the Austenite Reversion and Mechanical Properties of a Fe–10Cr–10Ni Cryogenic Maraging Steel. *J. Mater. Res. Technol.* **2021**, *11*, 98–111. [CrossRef]
399. Dhananchezian, M.; Priyan, M.R.; Rajashekar, G.; Narayanan, S.S. Study the Effect of Cryogenic Cooling On Machinability Characteristics During Turning Duplex Stainless Steel 2205. *Mater. Today Proc.* **2018**, *5*, 12062–12070. [CrossRef]

400. Koppula, S.; Rajkumar, A.; Krishna, S.H.; Prudhvi, R.S.; Aparna, S.; Subbiah, R. Improving the Mechanical Properties of AISI 2205 Duplex Stainless Steel by Cryogenic Treatment Process. *E3S Web Conf.* **2020**, *184*, 01019. [CrossRef]
401. Narayanan, D.; Jagadeesha, T. Process Capability Improvement Using Internally Cooled Cutting Tool Insert in Cryogenic Machining of Super Duplex Stainless Steel 2507. In *Innovative Product Design and Intelligent Manufacturing Systems*; Lecture Notes in Mechanical Engineering; Springer: Singapore, 2020; pp. 323–330. [CrossRef]
402. Narayanan, D.; Salunkhe, V.G.; Dhinakaran, V.; Jagadeesha, T. Experimental Evaluation of Cutting Process Parameters in Cryogenic Machining of Duplex Stainless Steel. In *Advances in Industrial Automation and Smart Manufacturing*; Lecture Notes in Mechanical Engineering; Springer: Singapore, 2021; Volume 23, pp. 505–516. [CrossRef]
403. Kanagaraju, T.; Boopathy, S.R.; Gowthaman, B. Effect of Cryogenic and Wet Coolant Performance on Drilling of Super Duplex Stainless Steel (2507). *Mater. Express* **2020**, *10*, 81–93. [CrossRef]
404. Sastry, C.C.; Abeens, M.; Pradeep, N.; Manickam, M.A.M. Microstructural Analysis, Radiography, Tool Wear Characterization, Induced Residual Stress and Corrosion Behavior of Conventional and Cryogenic Trepanning of DSS 2507. *J. Mech. Sci. Technol.* **2020**, *34*, 2535–2547. [CrossRef]
405. Pradeep Samuel, A.; Arul, S. Effect of Cryogenic Treatment on the Mechanical Properties of Low Carbon Steel IS 2062. *Mater. Today Proc.* **2018**, *5*, 25065–25074. [CrossRef]
406. Thornton, R.; Slatter, T.; Lewis, R. Effects of Deep Cryogenic Treatment on the Wear Development of H13A Tungsten Carbide Inserts When Machining AISI 1045 Steel. *Prod. Eng.* **2014**, *8*, 355–364. [CrossRef]
407. Govindaraju, N.; Shakeel Ahmed, L.; Pradeep Kumar, M. Experimental Investigations on Cryogenic Cooling in the Drilling of AISI 1045 Steel. *Mater. Manuf. Process.* **2014**, *29*, 1417–1421. [CrossRef]
408. Dilip Jerold, B.; Pradeep Kumar, M. Experimental Investigation of Turning AISI 1045 Steel Using Cryogenic Carbon Dioxide as the Cutting Fluid. *J. Manuf. Process.* **2011**, *13*, 113–119. [CrossRef]
409. Mahendran, R.; Rajkumar, P.; Nirmal Raj, L.; Karthikeyan, S.; Rajeshkumar, L. Effect of Deep Cryogenic Treatment on Tool Life of Multilayer Coated Carbide Inserts by Shoulder Milling of EN8 Steel. *J. Braz. Soc. Mech. Sci. Eng.* **2021**, *43*, 378. [CrossRef]
410. Karnan, B.; Kuppusamy, A.; Latchoumi, T.P.; Banerjee, A.; Sinha, A.; Biswas, A.; Subramanian, A.K. Multi-Response Optimization of Turning Parameters for Cryogenically Treated and Tempered WC–Co Inserts. *J. Inst. Eng. India Ser. D* **2022**, *103*, 263–274. [CrossRef]
411. Senthilkumar, D. Deep Cryogenic Treatment of En 31 and En 8 Steel for the Development of Wear Resistance. *Adv. Mater. Process. Technol.* **2021**, *8*, 1769–1776. [CrossRef]
412. Senthilkumar, D. Effect of Deep Cryogenic Treatment on Residual Stress and Mechanical Behaviour of Induction Hardened En 8 Steel. *Adv. Mater. Process. Technol.* **2016**, *2*, 427–436. [CrossRef]
413. Arunkarthikeyan, K.; Balamurugan, K. Performance Improvement of Cryo Treated Insert on Turning Studies of AISI 1018 Steel Using Multi Objective Optimization. In Proceedings of the International Conference on Computational Intelligence for Smart Power System and Sustainable Energy, CISPSSE 2020, Keonjhar, India, 29–31 July 2020. [CrossRef]
414. Wigley, D.A. *The Metallurgical Structure and Mechanical Properties at Low Temperature of Nitronic 40 with Particular Reference to Its Use in the Construction of Models for Cryogenic Wind Tunnels*; National Aeronautics and Space Administration: Hampton, VA, USA, 1982.
415. Gaddam, S.; Haridas, R.S.; Sanabria, C.; Tammana, D.; Berman, D.; Mishra, R.S. Friction Stir Welding of SS 316 LN and Nitronic 50 Jacket Sections for Application in Superconducting Fusion Magnet Systems. *Mater. Des.* **2022**, *221*, 110949. [CrossRef]
416. Sastry, C.C.; Hariharan, P.; Pradeep Kumar, M.; Muthu Manickam, M.A. Experimental Investigation on Boring of HSLA ASTM A36 Steel under Dry, Wet, and Cryogenic Environments. *Mater. Manuf. Process.* **2019**, *34*, 1352–1379. [CrossRef]
417. Y Chow, J.G.; Klamut, C.J. *Properties of Cast C£-8 Stainless-Steel Weldments at Cryogenic Temperatures*; Brookhaven National Lab.: Upton, NY, USA, 1981.
418. Thornton, R.; Slatter, T.; Jones, A.H.; Lewis, R. The Effects of Cryogenic Processing on the Wear Resistance of Grey Cast Iron Brake Discs. *Wear* **2011**, *271*, 2386–2395. [CrossRef]
419. Franco Steier, V.; Kalombo Badibanga, R.; Roberto Moreira Da Silva, C.; Magalhães Nogueira, M.; Araújo, J.A. Effect of Chromium Nitride Coatings and Cryogenic Treatments on Wear and Fretting Fatigue Resistance of Aluminum. *Electr. Power Syst. Res.* **2014**, *116*, 322–329. [CrossRef]
420. Kara, F.; Çiçek, A. Multiple Regression and ANN Models for Surface Quality of Cryogenically-Treated AISI 52100 Bearing Steel Micro Machining of Ti6Al4V and Inconel 718 View Project Improvement of Machining Precesses View Project. *Artic. J. Balk. Tribol. Assoc.* **2013**, *19*, 570–584.
421. Gunes, I.; Cicek, A.; Aslantas, K.; Kara, F. Effect of Deep Cryogenic Treatment on Wear Resistance of AISI 52100 Bearing Steel. *Trans. Indian Inst. Met.* **2014**, *67*, 909–917. [CrossRef]
422. Villa, M.; Pantleon, K.; Somers, M.A.J. Enhanced Carbide Precipitation during Tempering of Sub-Zero Celsius Treated AISI 52100 Bearing Steel. In Proceedings of the Heat Treat & Surface Engineering Conference & Expo, Chennai, India, May 16–18 2013; pp. 1–7.
423. Hong, S.Y.; Ding, Y. Micro-Temperature Manipulation in Cryogenic Machining of Low Carbon Steel. *J. Mater. Process Technol.* **2001**, *116*, 22–30. [CrossRef]
424. Jamali, A.R.; Khan, W.; Chandio, A.D.; Anwer, Z.; Jokhio, M.H.; Karachi, P. Effect of Cryogenic Treatment on Mechanical Properties of AISI 4340 and AISI 4140 Steel. *J. Eng. Technol.* **2019**, *38*, 2413–7219. [CrossRef]

425. Lisiecki, A.; Ślizak, D.; Kukofka, A. Laser Cladding of Co-Based Metallic at Cryogenic Conditions. *J. Achiev. Mater. Manuf. Eng.* **2019**, *95*, 20–31. [CrossRef]
426. Keseler, H.; Westermann, I.; Kandukuri, S.Y.; Nøkleby, J.O.; Holmedal, B. Permanent Effect of a Cryogenic Spill on Fracture Properties of Structural Steels. *IOP Conf. Ser. Mater. Sci. Eng.* **2015**, *102*, 012004. [CrossRef]
427. Abdin, A.; Feyzabi, K.; Hellman, O.; Nordström, H.; Rasa, D.; Thaung Tolförs, G.; Öqvist, P.-O. *Methods to Create Compressive Stress in High Strength Steel Components*; Ångströmlaboratoriet: Uppsala, Sweden, 2018.
428. Walters, C.L.; Alvaro, A.; Maljaars, J. The Effect of Low Temperatures on the Fatigue Crack Growth of S460 Structural Steel. *Int. J. Fatigue* **2016**, *82*, 110–118. [CrossRef]
429. Wang, C.; Yi, Y.; Huang, S.; Dong, F.; He, H.; Huang, K.; Jia, Y. Experimental and Theoretical Investigation on the Forming Limit of 2024-O Aluminum Alloy Sheet at Cryogenic Temperatures. *Met. Mater. Int.* **2021**, *27*, 5199–5211. [CrossRef]
430. Fiedler, T.; Al-Sahlani, K.; Linul, P.A.; Linul, E. Mechanical Properties of A356 and ZA27 Metallic Syntactic Foams at Cryogenic Temperature. *J. Alloys Compd.* **2020**, *813*, 152181. [CrossRef]
431. Sagar, S.R.; Srikanth, K.M.; Jayasimha, R. Effect of Cryogenic Treatment and Heat Treatment on Mechanical and Tribological Properties of A356 Reinforced with SiC. *Mater. Today Proc.* **2021**, *45*, 184–190. [CrossRef]
432. Zhao, Z.; Hong, S.Y. Cooling Strategies for Cryogenic Machining from a Materials Viewpoint. *J. Mater. Eng. Perform.* **1992**, *1*, 669–678. [CrossRef]
433. Jovičević-Klug, M.; Jovičević-Klug, P.; Sever, T.; Feizpour, D.; Podgornik, B. Extraordinary Nanocrystalline Pb Whisker Growth from Bi-Mg-Pb Pools in Aluminum Alloy 6026 Moderated through Oriented Attachment. *Nanomaterials* **2021**, *11*, 1842. [CrossRef] [PubMed]
434. Jovičević-Klug, M.; Tegg, L.; Jovičević-Klug, P.; Dražić, G.; Almásy, L.; Lim, B.; Cairney, J.M.; Podgornik, B. Multiscale Modification of Aluminum Alloys with Deep Cryogenic Treatment for Advanced Properties. *J. Mater. Res. Technol.* **2022**, *21*, 3062–3073. [CrossRef]
435. Jovičević-Klug, M.; Verbovšek, T.; Jovičević-Klug, P.; Batič, B.Š.; Ambrožič, B.; Dražić, G.; Podgornik, B. Revealing the Pb Whisker Growth Mechanism from Al-Alloy Surface and Morphological Dependency on Material Stress and Growth Environment. *Materials* **2022**, *15*, 2574. [CrossRef] [PubMed]
436. Wang, X.; Fan, X.; Chen, X.; Yuan, S. Forming Limit of 6061 Aluminum Alloy Tube at Cryogenic Temperatures. *J. Mater. Process. Technol.* **2022**, *306*, 117649. [CrossRef]
437. Wang, X.; Fan, X.; Chen, X.; Yuan, S. Cryogenic Deformation Behavior of 6061 Aluminum Alloy Tube under Biaxial Tension Condition. *J. Mater. Process. Technol.* **2022**, *303*, 117532. [CrossRef]
438. Bouzada, F.; Cabeza, M.; Merino, P.; Trillo, S. Effect of Deep Cryogenic Treatment on the Microstructure of an Aerospace Aluminum Alloy. *Adv. Mat. Res.* **2012**, *445*, 965–970. [CrossRef]
439. Mohan, K.; Suresh, J.A.; Ramu, P.; Jayaganthan, R. Microstructure and Mechanical Behavior of Al 7075-T6 Subjected to Shallow Cryogenic Treatment. *J. Mater. Eng. Perform.* **2016**, *25*, 2185–2194. [CrossRef]
440. Siyi, M.; Su, R.; Wang, K.; Yang, Y.; Qu, Y.; Li, R. Effect of Deep Cryogenic Treatment on Wear and Corrosion Resistance of an Al–Zn–Mg–Cu Alloy. *Russ. J. Non-Ferr. Met.* **2021**, *62*, 89–96. [CrossRef]
441. Wei, L.; Wang, D.; Li, H.; Xie, D.; Ye, F.; Song, R.; Zheng, G.; Wu, S. Effects of Cryogenic Treatment on the Microstructure and Residual Stress of 7075 Aluminum Alloy. *Metals* **2018**, *8*, 273. [CrossRef]
442. Zhang, P.; Liu, Z.; Liu, J.; Yu, J.; Mai, Q.; Yue, X. Effect of Aging plus Cryogenic Treatment on the Machinability of 7075 Aluminum Alloy. *Vacuum* **2023**, *208*, 111692. [CrossRef]
443. Deshpande, Y.V.; Andhare, A.B.; Padole, P.M. How Cryogenic Techniques Help in Machining of Nickel Alloys? A Review. *Mach. Sci. Technol.* **2018**, *22*, 543–584. [CrossRef]
444. Baig, A.; Jaffery, S.H.I.; Khan, M.A.; Alruqi, M. Statistical Analysis of Surface Roughness, Burr Formation and Tool Wear in High Speed Micro Milling of Inconel 600 Alloy under Cryogenic, Wet and Dry Conditions. *Micromachines* **2022**, *14*, 13. [CrossRef] [PubMed]
445. Satyanarayana, K.; Krishna, B.R.; Bhargavi, M.; Vasuki, R.E.; Kiran, K.R. Taguchi Optimization in Machining Inconel 600 with WEDM Process Using Cryogenically Treated Brass Wire. *E3S Web Conf.* **2021**, *309*, 01110. [CrossRef]
446. Mandal, P.K.; Michael Saji, A.; Kurian Lalu, A.; Krishnan, A.; Nair, A.S.; Jacob, M.M. Microstructural Study and Mechanical Properties of TIG Welded Inconel 617 Superalloy. *Mater. Today Proc.* **2022**, *62*, 3561–3568. [CrossRef]
447. Akgün, M.; Demir, H. Optimization of Cutting Parameters Affecting Surface Roughness in Turning of Inconel 625 Superalloy by Cryogenically Treated Tungsten Carbide Inserts. *SN Appl. Sci.* **2021**, *3*, 277. [CrossRef]
448. Yıldırım, Ç.V. Experimental Comparison of the Performance of Nanofluids, Cryogenic and Hybrid Cooling in Turning of Inconel 625. *Tribol. Int.* **2019**, *137*, 366–378. [CrossRef]
449. Anburaj, R.; Pradeep Kumar, M. Experimental Studies on Cryogenic CO2 Face Milling of Inconel 625 Superalloy. *Mater. Manuf. Process.* **2020**, *36*, 814–826. [CrossRef]
450. Makhesana, M.A.; Patel, K.M.; Khanna, N. Analysis of Vegetable Oil-Based Nano-Lubricant Technique for Improving Machinability of Inconel 690. *J. Manuf. Process.* **2022**, *77*, 708–721. [CrossRef]
451. Jovičevič Klug, P.; Jovičević Klug, M.; Podgornik, B. Potential in Deep Cryogenic Treatment of Non-Ferrous Alloys. In Proceedings of the European Cryogenics Days 2021, Virtual Conference, 4 November 2021; Cryogenics Society of Europe: Darmstadt, Germany, 2021.

452. Palanisamy, A.; Jeyaprakash, N.; Sivabharathi, V.; Sivasankaran, S. Effects of Dry Turning Parameters of Incoloy 800H Superalloy Using Taguchi-Based Grey Relational Analysis and Modeling by Response Surface Methodology. *Proc. Inst. Mech. Eng. Part C J. Mech. Eng. Sci.* **2022**, *236*, 607–623. [CrossRef]
453. Palanisamy, A.; Selvaraj, T.; Sivasankaran, S. Optimization of Turning Parameters of Machining Incoloy 800H Superalloy Using Cryogenically Treated Multilayer CVD-Coated Tool. *Arab. J. Sci. Eng.* **2018**, *43*, 4977–4990. [CrossRef]
454. Palanisamy, A.; Selvaraj, T. Optimization of Turning Parameters for Surface Integrity Properties on Incoloy 800 h Superalloy Using Cryogenically Treated Multi-Layer Cvd Coated Tool. *Surf. Rev. Lett.* **2019**, *26*, 1850139. [CrossRef]
455. Dhananchezian, M. Study the Machinability Characteristics of Nicked Based Hastelloy C-276 under Cryogenic Cooling. *Measurement* **2019**, *136*, 694–702. [CrossRef]
456. Nas, E.; Kara, F. Optimization of EDM Machinability of Hastelloy C22 Super Alloys. *Machines* **2022**, *10*, 1131. [CrossRef]
457. Akincioğlu, S.; Gökkaya, H.; Akincioğlu, G.; Karataş, M.A. Taguchi Optimization of Surface Roughness in the Turning of Hastelloy C22 Super Alloy Using Cryogenically Treated Ceramic Inserts. *Proc. Inst. Mech. Eng. Part C J. Mech. Eng. Sci.* **2020**, *234*, 3826–3836. [CrossRef]
458. Ekambaram, P. Study of Mechanical and Metallurgical Properties of Hastelloy X at Cryogenic Condition. *J. Mater. Res. Technol.* **2019**, *8*, 6413–6419. [CrossRef]
459. Wu, Y.; Yuan, X.; Wen, X.; Jiao, M. Body-Centered Cubic High-Entropy Alloys. In *Materials Horizons: From Nature to Nanomaterials*; Springer: Singapore, 2022; pp. 3–34. [CrossRef]
460. Hu, W.; Dong, Z.; Wang, H.; Ahamad, T.; Ma, Z. Microstructure Refinement and Mechanical Properties Improvement in the W-Y_2O_3 Alloys via Optimized Freeze-Drying. *Int. J. Refract. Met. Hard Mater.* **2021**, *95*, 105453. [CrossRef]
461. Yildiz, Y.; Sundaram, M.M.; Rajurkar, K.P.; Nalbant, M. The Effects of Cold and Cryogenic Treatments on the Machinability of Beryllium-Copper Alloy in Electro Discharge Machinability. In Proceedings of the 44th CIRP Conference on Manufacturing Systems, Madison, WI, USA, 1–3 June 2011.
462. Bagherzadeh, A.; Kuram, E.; Budak, E. Experimental Evaluation of Eco-Friendly Hybrid Cooling Methods in Slot Milling of Titanium Alloy. *J. Clean. Prod.* **2021**, *289*, 125817. [CrossRef]
463. Uygur, I.; Gerengi, H.; Arslan, Y.; Kurtay, M. The Effects of Cryogenic Treatment on the Corrosion of AISI D3 Steel. *Mater. Res.* **2015**, *18*, 569–574. [CrossRef]
464. Shinde, T.; Pruncu, C.; Dhokey, N.B.; Parau, A.C.; Vladescu, A. Effect of Deep Cryogenic Treatment on Corrosion Behavior of AISI H13 Die Steel. *Materials* **2021**, *14*, 7863. [CrossRef] [PubMed]
465. Wang, Y.M.; Liang, Y.; Zhai, Y.D.; Zhang, Y.S.; Sun, H.; Liu, Z.G.; Su, G.Q. Study on the Role of Cryogenic Treatment on Corrosion and Wear Behaviors of High Manganese Austenitic Steel. *J. Mater. Res. Technol.* **2023**, *24*, 5271–5285. [CrossRef]
466. Akhbarizadeh, A.; Amini, K.; Javadpour, S. Effects of Applying an External Magnetic Field during the Deep Cryogenic Heat Treatment on the Corrosion Resistance and Wear Behavior of 1.2080 Tool Steel. *Mater. Des.* **2012**, *41*, 114–123. [CrossRef]
467. Wang, L.; Dong, C.; Cao, Y.; Liang, J.; Xiao, K.; Li, X. Co-Enhancing the Mechanical Property and Corrosion Resistance of Selective Laser Melted High-Strength Stainless Steel via Cryogenic Treatment. *J. Mater. Eng. Perform.* **2020**, *29*, 7052–7062. [CrossRef]
468. Baldissera, P.; Delprete, C. Deep Cryogenic Treatment of AISI 302 Stainless Steel: Part II—Fatigue and Corrosion. *Mater. Des.* **2010**, *31*, 4731–4737. [CrossRef]
469. Cai, Y.; Luo, Z.; Zeng, Y. Influence of Deep Cryogenic Treatment on the Microstructure and Properties of AISI304 Austenitic Stainless Steel A-TIG Weld. *Sci. Technol. Weld. Join.* **2016**, *22*, 236–243. [CrossRef]
470. He, X.; Lü, X.-Y.; Wu, Z.-W.; Li, S.-H.; Yong, Q.-L.; Liang, J.-X.; Su, J.; Zhou, L.-X.; Li, J. M23C6 Precipitation and Si Segregation Promoted by Deep Cryogenic Treatment Aggravating Pitting Corrosion of Supermartensitic Stainless Steel. *J. Iron Steel Res. Int.* **2021**, *28*, 629–640. [CrossRef]
471. Cabeza, M.; Feijoo, I.; Merino, P.; Trillo, S. Effect of the Deep Cryogenic Treatment on the Stress Corrosion Cracking Behaviour of AA 2017-T4 Aluminium Alloy. *Mater. Corros.* **2016**, *67*, 504–512. [CrossRef]
472. Diekman, F. Cold and Cryogenic Treatment of Steel. In *Steel Heat Treating Fundamentals and Processes*; ASM International: Almere, The Netherlands, 2013.